Advances in Complementary-Metal–Oxide–Semiconductor-Based Integrated Biosensor Arrays

ARTICLE *in* CHEMICAL REVIEWS · MAY 2015

Impact Factor: 46.57 · DOI: 10.1021/cr500554n · Source: PubMed

5 AUTHORS, INCLUDING:

Sunil Kumar Arya

Institute of Microelectronics

71 PUBLICATIONS **1,942** CITATIONS

CHEMICAL REVIEWS

Review

pubs.acs.org/CR

Advances in Complementary-Metal–Oxide–Semiconductor-Based Integrated Biosensor Arrays

Sunil K. Arya,* Chee Chung Wong, Yong Joon Jeon, Tushar Bansal, and Mi Kyoung Park

Institute of Microelectronics, 11 Science Park Road, Singapore Science Park II, Singapore 117685

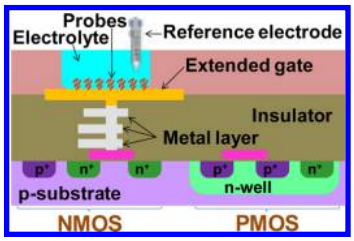

CONTENTS

1. Introduction A
2. Basics of CMOS B
2.1. CMOS Fabrication for Biosensor Arrays B
2.2. CMOS Postprocessing for Biosensor Application C
2.3. CMOS Packaging for Biosensor Application E
3. Application of CMOS as a Transducer in a Biosensor G
3.1. Electrochemical Transducers G
3.2. Optical, Piezoelectric, Magnetic, and Other Transducers Using CMOS Circuitry G
4. CMOS-Based Circuitry for Biosensor Application H
4.1. Circuits for a Potentiostat H
4.2. Circuit for Amplifiers and Signal Conditioning I
4.3. Circuits for ISFET-Based Biosensors M
4.4. Circuits for Capacitance Measurement M
4.5. Circuit for Impedance Measurement N
4.6. Circuits for Amperometric Measurement P
4.7. Circuits for RF Signal Measurement Q
4.8. Circuits for Resistance Measurement Q
4.9. Circuits for Optical and Magnetic Biosensors Q
4.10. Circuits for Implantable Biosensors R
5. Advances in CMOS-Based Biosensors V
5.1. Voltammetry-Based Biosensors X
5.2. Potentiometric/ISFET-Based Biosensors X
5.3. Amperometric Biosensors Z
5.4. Impedimetric Biosensors AA
5.5. Capacitive Biosensors AB
5.6. Piezoresistive-Stress-Based Biosensors AC
5.7. Optical Biosensors AD
5.8. Magnetic Biosensors AH
5.9. Surface-Acoustic-Wave-Based Biosensors AI
5.10. Implantable Biosensors AI
5.11. Other Biosensors AJ
6. Commercial CMOS Biosensors AK
7. Challenges and Prospects of CMOS in Biosensors AL
8. Conclusion AL
Author Information AM
Corresponding Author AM
Notes AM
Biographies AM
Acknowledgments AN
Glossary AN
References AN

1. INTRODUCTION

Biosensors are devices which facilitate specific detection of analytes and produce detectable signals correlating with the presence of a target analyte such as proteins, DNA, glucose, cholesterol, toxins, hormones, bacteria, etc. Biosensors have gained much consideration lately owing to their capability to detect the early onset of diseases by measuring multiple biomarkers and analytes from bodily fluids, including blood, saliva, urine, etc.[1] However, until now, only a handful of biosensor solutions have successfully made a transition from benchtop to portable point-of-care devices. The challenges lie not in building sensitive detectors but in integrating fluidic connections and signal processing circuitry, while keeping a small system footprint. Furthermore, for multiplex biosensor arrays, if multiplexing circuitry is not made as a part of the original design, every electrode on chip will require a contact pad, thereby increasing the footprint of the chip.[2] To solve these and other issues, biomedical researchers have come to rely on the semiconductor industry to develop high-performance, compact, and cost-effective biosensor systems.

Complementary-metal–oxide–semiconductor (CMOS) technology (used heavily in the microprocessor and semiconductor industry) has emerged as a viable option to solve some of the key issues in biosensor development and to provide large integration, small size, and compatibility with point-of-care platforms. Especially, silicon-based biosensors can be monolithically integrated with CMOS technology on a single chip, providing fast detection times, higher sensitivity, and better signal-to-noise ratios (SNRs), while reducing overall costs. Figure 1 shows the schematic of an integrated biosensor system with the sensor, sensor interface, and communication circuit and display unit.

In CMOS-driven, monolithically integrated bio/chemical sensor arrays (Figure 2), each sensor electrode can be functionalized with just one type of probe to detect one biomarker or with different probes to achieve parallel/multiplexed detection. CMOS-based biosensor arrays can operate via detection of signals from electric potential, current, capacitance, impedance, and/or light intensity.[3] With CMOS, integration of a logic circuit (analog or digital or both) can be realized on-chip, enabling control of all electrodes in an array.[4]

Received: September 30, 2014

DOI: 10.1021/cr500554n
Chem. Rev. XXXX, XXX, XXX–XXX

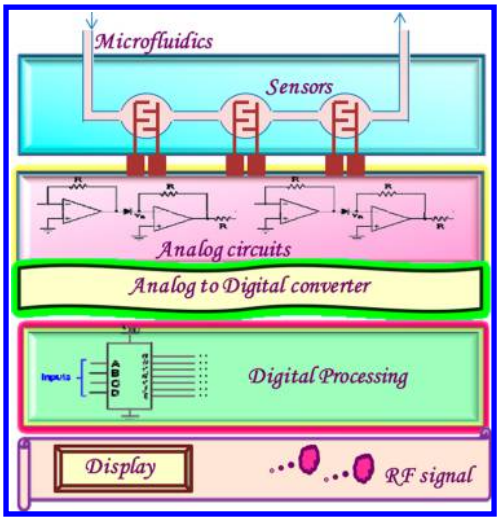

Figure 1. Schematic for an integrated biosensor unit.

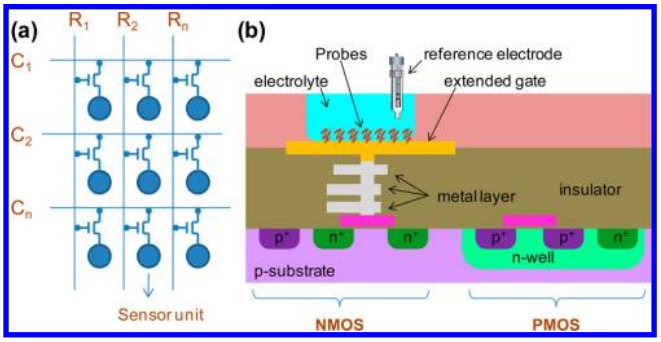

Figure 2. (a) Schematic for a CMOS-based sensor array where R and C are row and column, respectively. (b) CMOS circuit schematic with sensor. Adapted with permission from ref 3. Copyright 2013 Nakazato K.

Furthermore, on-chip circuitry for multiple detections and signal processing provide the opportunity to develop biosensor arrays.[5] Biosensor arrays fabricated using CMOS technology are smaller in device footprint and can automate multiple assays simultaneously. CMOS processes in several embedded sensing devices, e.g., in photodiodes and various transistors, etc., have been successfully applied for detection of bioluminescence, pH, biochemical reaction detection, temperature measurements, etc.[6] Since multidisciplinary teams are usually required to develop such biosensors, the primary motivation behind this review is to act as a knowledge bridge among biologists, chemists, biochemists, surface chemists, and engineers, and help them understand the underlying set of complex technical challenges, which must be solved together. This review starts with providing a general understanding of CMOS technology and its role in developing biosensor platforms. The review also covers basics of CMOS fabrication, postprocessing and packaging techniques, architecture of the most common readout circuits, and advances made in CMOS-based biosensors over the recent past. Additionally, the review also gives examples of companies/teams that have successfully solved these myriad issues and have launched commercial products in the marketplace. Finally, the review discusses some of the present and future challenges in biosensor development that must be addressed going forward.

2. BASICS OF CMOS

CMOS is described as an integrated circuit (IC) design style and process on Si substrates using groups of p-channel (PMOS) and n-channel (NMOS) metal−oxide−semiconductor field-effect transistors (MOSFETs) (Figure 2b).[1a] In "metal−oxide−semiconductor", the term "metal" represents the gate electrode over an insulator (usually oxide)/semiconductor stack. At the heart of the CMOS technology is an inverter utilizing PMOS and NMOS transistors. A CMOS inverter can essentially be seen as a digital switch. Under normal operation, gates of both PMOS and NMOS are connected to a common input signal. A low input signal closes the NMOS transistor and offers a low-resistance current path through PMOS, thereby causing the output signal to be high. A high input signal closes the PMOS and offers a low-resistance current path through NMOS, thereby causing the output signal to be low. More complex functionality (such as amplifiers and radio frequency (RF) circuits) can be built from these simple components. Commercial ICs are composed of billions of such tiny transistors (or digital switches). The CMOS process can greatly facilitate system integration for biosensor platforms.

CMOS-based devices are capable of handling complex data and to generate simplified digital output. Furthermore, design techniques and circuit architectures commonly applied in the CMOS world allow the simple formation of sensor arrays. Thus, it is possible to integrate many sensors on one die with only a few electrical connections to the outside world.[7] CMOS circuits for filters, amplifiers, signal processers, etc. can help in reducing the complexity and cost of the device.[8] In development of microarrays for high-throughput, parallel, and multiple analysis, CMOS technology allows the integration of the various sensing electrodes and detection circuitries on the same chip. CMOS technology has also shown promise in implantable devices, where devices with a small footprint with low power consumption are required to do multiple tasks of stimulation, signal recording, amplification, communication, etc.[9] Also, CMOS-based sensor systems are more flexible in modification, scalable, and of low cost when made in bulk.[10] Furthermore, for point-of-care (POC) applications, a CMOS-based electrochemical biosensor array may avoid the use of large-size equipment usually used in other platforms, such as in fluorescence-based microarrays.[11]

2.1. CMOS Fabrication for Biosensor Arrays

Various approaches and methods have been described in the literature for fabrication of CMOS-based biosensor devices (Figure 2b).[12] Fabrication of a CMOS-based biosensor array usually starts with CMOS readout circuit fabrication in foundries, followed by postprocessing and sensor fabrication. CMOS devices are mainly fabricated on a crystalline silicon wafer using p-type and n-type MOSFETs.[1a]

On a p-type Si wafer with boron doping, Yang et al. described the double-metal n-well CMOS design for fabrication of the biosensor chip (Figure 3): "In brief, NMOS and PMOS regions were defined by implanting n-type phosphorous impurity in the p-type substrate on grown field oxide. Gate was fabricated by polysilicon deposition and transistor drain and source were created by separate implantation of p^+ and n^+ in n-well and the substrate, respectively. Electrical passivation was achieved using grown gate oxide and then metal lines and tetraethyl orthosilicate (TEOS) oxide (passivation layer) were created for connecting multi-metal layers. Finally, a passivation and protecting layer of nitride was deposited."[13]

DOI: 10.1021/cr500554n
Chem. Rev. XXXX, XXX, XXX−XXX

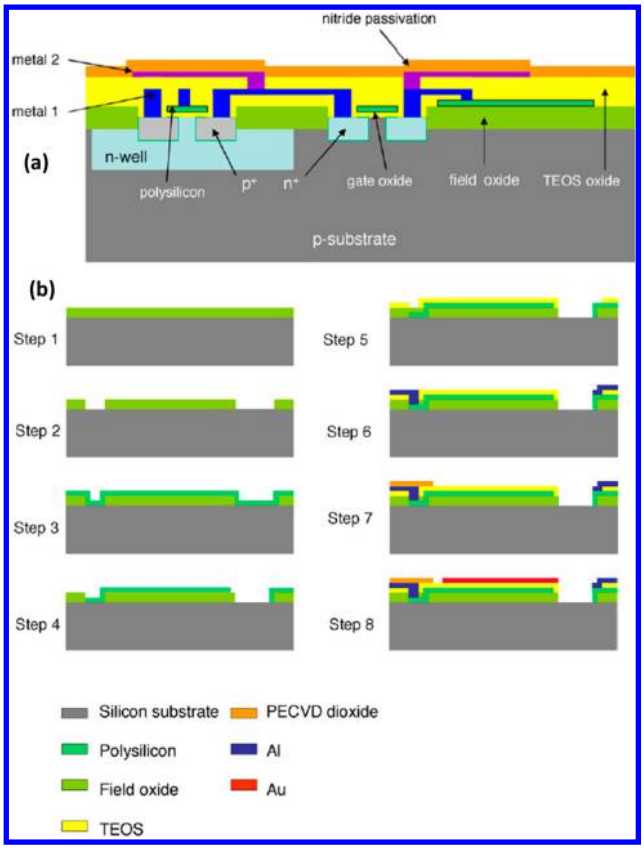

Figure 3. (a) Schematic diagram of the cross-section of a double-metal n-well CMOS process, where metal 2 is used as the immobilized layer, TEOS oxide as the top insulation layer, polysilicon as the piezoresistive layer, and field oxide as the bottom insulation layer. (b) CMOS process flow of the biosensor chip. Reprinted with permission from ref 13. Copyright 2007 Elsevier.

To improve the characteristics of the present Si-based CMOS devices, Nah et al. described the III−V CMOS electronics on silicon substrates.[14] In their study, ultrathin III−V semiconductor membranes on Si/SiO_2 were assembled via a two-step epitaxial layer transfer route. In n- and p-MOSFETs, created using 13 nm indium arsenide (InAs) and 7 nm indium gallium arsenide (InGaAs) layers, the peak effective mobilities were found to be ∼370 and ∼1190 $cm^2/(V\ s)$ for holes and electrons, respectively. Furthermore, the efficacy of III−V CMOS logic operation was demonstrated via NOT and NAND gate fabrication.[14]

2.2. CMOS Postprocessing for Biosensor Application

In CMOS-based analog circuits, mechanisms for detecting low-level currents, impedances, and voltages are very well understood. However, using the same mechanisms in a biosensor platform presents some unique challenges. One of the key challenges is in establishing ohmic contacts from the electrode bond pads of the sensor to the CMOS device. Furthermore, for proper functioning, CMOS electrodes in contact with a biological sample must be compatible, nontoxic, environmentally stable, and neutral to the desired analyte of detetction.[15] At present, however, the lack of such stable and compatible electrodes in CMOS processes is a major challenge for creating electrochemical biosensors. The only metal available in CMOS is Al, which is not stable in air and forms insulating oxide, and thus cannot be used for electrochemical testing. Therefore, coating a biocompatible and inert metal such as gold over the surface of CMOS microelectrodes is required.[16] However, conventional CMOS device fabrication processes do not allow precious metals such as gold or platinum to intrude into "clean" IC foundries. For such metals, processing is outsourced to packaging houses, where metal contamination is properly contained and is allowed. To solve the problem, it is suggested to use the configuration in which electrodes do not come in direct contact with the electrolyte or use a postprocessing technique to deposit a stable and inert metal electrode on the top metal layer.[1a,17] Thus, postprocessing on CMOS IC chips converts integrated circuit chips from semiconductor foundries into fully functional biosensors.

Postprocessing of incoming CMOS chips results in conversion of exposed metals such as Cu and Al (commonly found in wafers coming from foundries) into inert metal layers (e.g., Au, Pt), which can easily be processed further for biosensor fabrication.[18] Thus, postprocessing done to improve the performance of a biosensor usually includes (i) reduction of the distance between the chip surfaces and sensor by thinning the dielectric above the sensor and (ii) top-layer modification by gold/platinum deposition, which makes the top layer biocompatible and suitable for many chemistries used in biosensor fabrication. Postprocessing for gold layer deposition has been reported using various procedures. Photoresist spin

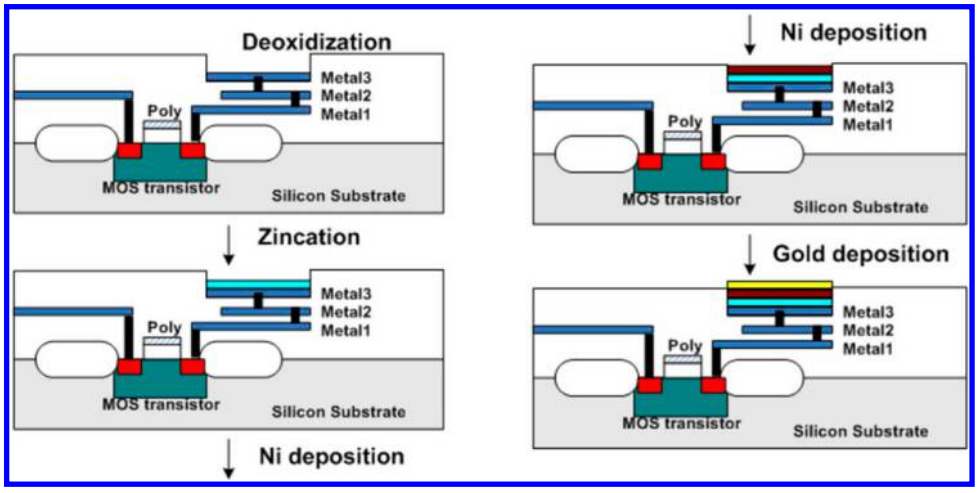

Figure 4. Electroless gold plating procedure. Reprinted with permission from ref 21b. Copyright 2009 IEEE.

DOI: 10.1021/cr500554n
Chem. Rev. XXXX, XXX, XXX−XXX

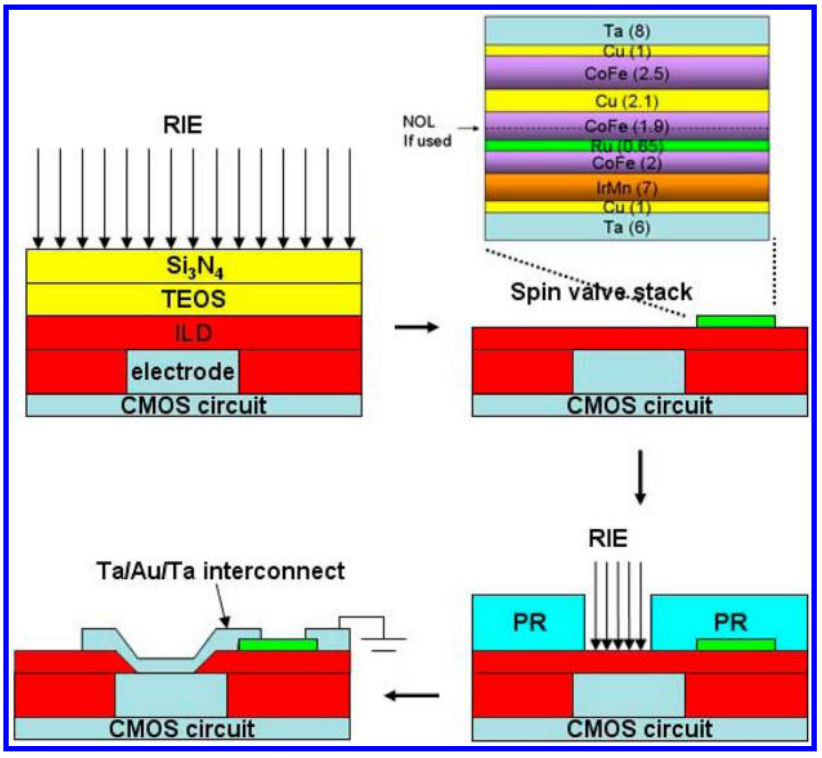

Figure 5. Micro- and nanofabrication steps for chip postprocessing. Reprinted with permission from ref 23. Copyright 2009 IEEE.

coating with liftoff followed by metal deposition is a common process for gold/platinum layer deposition on CMOS electrodes during postprocessing.[12c,19] However, the CMOS microchips become vulnerable to electrostatic discharge (ESD); hence, extra care has to be considered during postprocessing.

Another challenge in CMOS postprocessing is the removal of native aluminum oxide (Al_2O_3) on exposed aluminum sensors. Aluminum which is used for the top metal pads in CMOS fabrication is unfortunately highly reactive toward O_2 in air and oxidizes very quickly to form an inert and insulating Al_2O_3 up to a thickness of 10 nm.[15] Thus, removal of the native Al_2O_3 by chemical etching, in situ argon sputtering, etc. before deposition of a noble-metal film onto Al becomes critical in ensuring an ohmic contact between Al and the sensor layer. Besides native metal oxides, other issues for postprocessing such as process-induced electrostatic discharge and weak contamination control on the sensing electrodes also need to be considered. The phenomenon known as the "antenna effect" has to be strictly adhered to when designing the density of exposed metals.[20] Polymeric materials (such as photopatternable resist materials, polyimide, Parylene, etc.), which are usually introduced in the last stage of CMOS postprocessing to create a filter, traps, and fluidic channels alongside the biosensor, can leave behind a residue on the sensing electrodes and introduce high pixel to pixel nonuniformity, thus needing careful attention.

To deposit biocompatible Pt on Al electrodes, Heer et al. described a two-mask postprocessing procedure, where Al was blocked by Pt deposition and a passivation layer. In passivation to prevent degradation during cell culturing over around one month, a 1.6 μm thick layer of alternating oxide and nitride layers was found to be much more effective than a single 1 μm silicon nitride (Si_3N_4) passivation layer.[2] Other than this, electroless gold plating (EGP),[16,21] polymer deposition, wafer thinning, etc. have also been employed as postprocessing steps. EGP is a multistep (deoxidization, zincation, Ni deposition, and Au deposition) wet chemical process that involves consistent and uniform coating of Au onto Al electrodes (Figure 4).[21b] Using an electroless nickel immersion gold (ENIG) plating process that does not require any lithography, Manickam et al. first deposited Ni followed by a Au layer on the exposed Al surface.[21a,22]

Using 6 M 0.25 μm BiCMOS technology, Han et al. described the postprocessing of a CMOS chip for development of a magnetoresistive biosensor array chip (Figure 5). Postprocessing involved the use of a SF_6 and Ar mixture based reactive ion etch (RIE) for passivation thinning, followed by patterning of spin valves via an e-beam lithography and liftoff method.[23]

With no requirement of complex and expensive semiconductor processing equipment, Graham et al. described benchtop-based postprocessing using the Al anodization and plating technique. The process involved the formation of nanoporous alumina (aluminum oxide) by anodization in phosphoric acid followed by gold filling and Pt black plating.[8] In another study involving a microelectrode array with 11 011 Pt electrodes (7 μm diameter), Fiscella et al. performed postprocessing via electrochemical deposition of a Pt black layer onto the electrodes. For Pt black deposition, a hexachloroplatinic acid and lead acetate solution in hydrochloric acid (pH 1) was used, and a current density of 0.5 nA/μm^2 was employed.[24]

Schindler et al. described low-temperature atomic-layer-deposition-based passivation via an Al_2O_3 and hafnium oxide multilayer over an Al electrode. With a multilayer thickness of just 50 nm, the device showed "biocompatibility, a very low leakage current and stability up to 6 V".[25] In another study, Huang et al. described "aminomethyl-[2,2] paracyclophane polymer" (amino-functionalized Parylene)-based postprocessing for DNA biosensor fabrication. In their approach, chemical

DOI: 10.1021/cr500554n
Chem. Rev. XXXX, XXX, XXX−XXX

vapor deposition was used for deposition of a 0.5 μm thick layer at room temperature.[26]

Meyburg et al. described the stable device passivation method against electrolyte solutions via use of titanium silicide for all interconnects. Floating gate (FG) FET array chips with such passivation showed long-term stability and no degradation during several cleaning procedures and cell cultures. However, due to use of silicide for connections in place of Al, the chip exhibited $I-V$ characteristics similar to those of a diode and a higher noise level in p-channel FG FETs.[4]

For fabrication of CMOS surface acoustic wave (SAW) devices, Tigli et al. described postprocessing via RIE and maskless ZnO RF magnetron sputtering for interdigitated electrode definition and piezoelectric material deposition, respectively, followed by pad formation through shadow mask photolithography.[27] Hayasaka et al. described film-transfer-technology-based postprocessing of CMOS chips. In their study, a benzocyclobutene (BCB) bonding interlayer was used to transfer fabricated boron-doped diamond (BDD) on Si to an 0.18 μm CMOS wafer. In this process, the BDD microelectrodes were arrayed without damaging the CMOS circuit. Figure 6 shows the various postprocessing steps involved in the fabrication process of a CMOS-based amperometric biosensor array with BDD electrodes.[28] For open-gate-structure-based sensors, which have shown enhancement in signal transduction over floating-gate-structure-based field-effect sensors via avoiding threshold variation, Chang et al. described the two different die-level post-CMOS processes. In one, they used diluted KOH-based wet etching at 80 °C, and in the other, they used RIE-based dry etching using XeF_2 for making open-gate field-effect transistors (OGFETs). In both processes the transistor's sensing area was cleaned by removing all materials above it, which allowed interfacing of the FET with solutions via its 7 μm thin gate oxide.[29] Besides electrochemical biosensors, postprocessing is also required for optical biosensors, where visible light is used. As silicon is not transparent to visible light, postprocessing is required to allow coupling of light with integrated photodiodes. In such postprocessing, the thickness of the silicon substrate is reduced so that light can reach the integrated photodiode or photosensitive component effectively.[1a]

2.3. CMOS Packaging for Biosensor Application

In CMOS systems, signals can be recorded from the top or bottom of the sensor chip and depend on the transduction method chosen for measurement. However, before measurements can be made, suitable passivation of contact pads along with packaging of the CMOS sensor is required. Proper packaging of various components of the sensor and interfaces is crucial for the desired working of the sensor in a physiological medium. Since conventional CMOS circuits are designed to operate in the dry mode, the packaging of the CMOS chip becomes challenging for biosensors, where measurements are usually recorded in a liquid medium. For biosensors, biochips are usually connected to the real world through microfluidics. Thus, selection of the material and design of the fluidic interface becomes crucial to ensure a bubble-free and proper flow path. To handle flow of liquid reagents, electrolytes, or biological fluids into the system, the on-chip circuitry and exposed electronic connections must be sealed from such liquids. Therefore, the complete electronic and fluidic package is a major contributor to the overall cost of the biochip and deserves considerable attention. In most electronic packaging

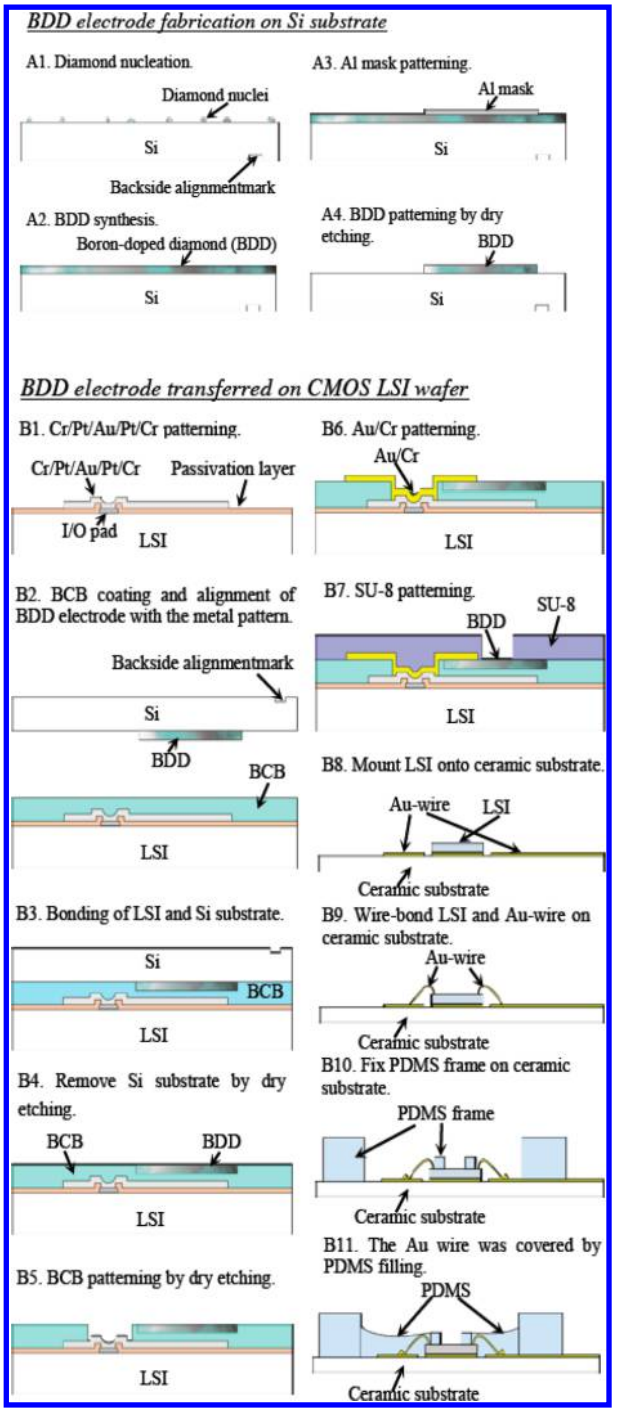

Figure 6. Fabrication process of a CMOS-based amperometric biosensor array with BDD electrodes. Reprinted with permission from ref 28. Copyright 2014 IEEE.

production lines, postprocessed wafers are diced and mounted through a die attached on standard chip carriers or printed circuit boards (PCBs), and then electrical connections are made either through wire-bonding or flip-chip technology. The key strategy in packaging biosensors is combining special material requirements for lid formation and encapsulation for safe liquid handling. Lastly, the completed device requires sterilization prior to shipment.

Various packaging approaches to protect the electrical connections and to create microfluidic arrangements have been reported using epoxy-based adhesives or poly-

DOI: 10.1021/cr500554n
Chem. Rev. XXXX, XXX, XXX−XXX

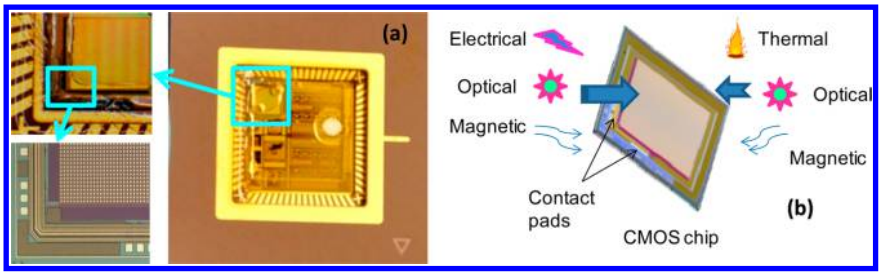

Figure 7. (a) Packaging approach for a CMOS IC in which the sensor chip and packaging base are coupled using bond wires. (b) Various pathways for applying and recording the signal from CMOS-chip-based transducers.

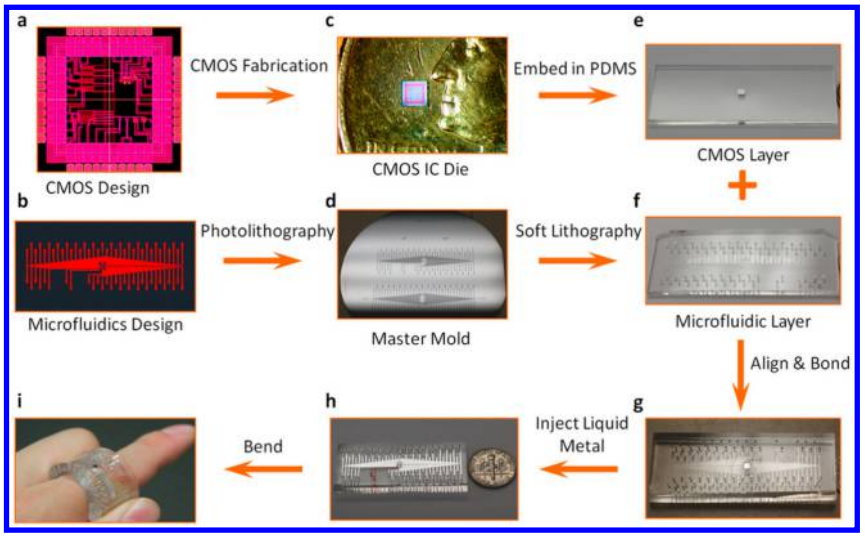

Figure 8. Schematic illustration of the fabrication and packaging procedures to produce flexible CMOS/microfluidic hybrid microsystems. Reprinted with permission from ref 35. Copyright 2013 Nature Group.

(dimethylsiloxane) (PDMS), which allows the operation of CMOS circuitry within a liquid medium.[19,30] However, in many cases controlling contamination of sensing elements via overflow of epoxy on the sensor surface becomes hard as it is done by hand. Also, in many cases, epoxy applied on the sensor chip by hand also suffers from poor adhesion, which in the presence of liquid causes leakage and failure of the device.[31] Figure 7a shows an example of a packaging approach for a CMOS IC in which the sensor chip and packaging base are coupled using bond wires, and Figure 7b shows the various pathways for applying and recording the signal from CMOS-chip-based transducers.

For packaging of signal-processing CMOS ICs and large biosensor arrays, Yang et al. described compliant interconnect and through-silicon-via (TSV) technologies. They showed that, for wafers with prefabricated sensors or a wafer whose thickness cannot be reduced, TSV technology provides a packaging solution. On the other hand, compliant interconnect technology is useful where permanent interconnections with minimal stress or reusable CMOS ICs with low-force temporary interconnections are required.[32]

Among polymers, Parylene being biocompatible, transparent, and mechanically stable has been utilized for packaging of CMOS chips. It is hydrophobic in nature and provides electrical insulation along with a chemical- and physiological-liquid-resistant environment.[31,33] In one of the studies, Brettschneider et al. described a technique to integrate a CMOS-based biosensing chip into a polymer-based microfluidic system. The packaging involved wafer-level package fabrication by embedding a silicon die into a mold compound to make a reconstituted mold wafer. Afterward, lithography-based redistribution was used to fan out the electrical interfaces. In a later stage, a laser bonding process was used to integrate the singulated sensor package into a microfluidic multilayer stack by means of a flexible hot melt foil. A CMOS biosensor was successfully packaged including protection for the nanoelectrodes on the sensing area. Use of a standard resist material allowed the adaptation of this step to a variety of different materials on the active area. For general microfluidic applications, the authors illustrated the fabrication of a flow cell which can withstand pressures of up to Δp = 780 kPa using materials with different melting temperatures and a laser bonding approach. During laser bonding, the heat entry was locally confined so that the sensing area did not experience elevated temperatures. Furthermore, low resistances were obtained for the electroplated conductor tracks, enabling applications where low losses were required.[34]

To avoid the flip-chip and wire-bonding method, Zhang et al. described an elastomer-based packaging where microfluidics and electronic circuitry were embedded in an elastomer. In their design, all liquid samples, including liquid metals, were delivered using PDMS-based microfluidic channels. A liquid gallium−indium−tin eutectic alloy through the same channels was used for making electrical interconnects to the IC chip. Their approach provided flexible packaging and seamless IC/microfluidic integration. The packaged system prepared using their approach (Figure 8) was found to be working even after bending at a curving radius of 1 cm and 15% uniaxial strain.[35]

DOI: 10.1021/cr500554n
Chem. Rev. XXXX, XXX, XXX−XXX

To achieve continuous monitoring of a biological cell's metabolic activity, Rothe et al. described the packaging scheme for a 0.35 μm process with a two-polysilicon and four-metal layer (2P4M)-based integrated CMOS chip, consisting of a large array of Pt working electrodes and various lines for current readouts (Figure 9 a): "In brief: SU-8 thin layer (10μm)

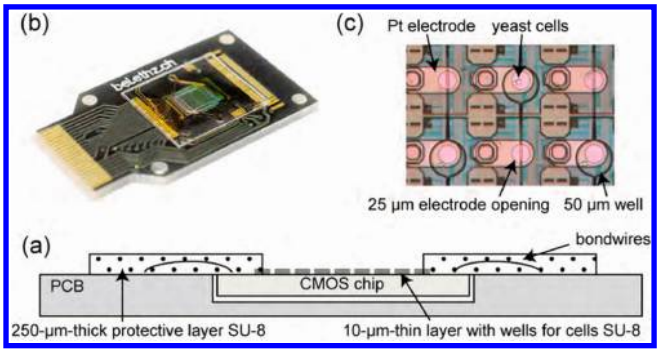

Figure 9. (a) Packaging scheme. The wells to host the cells are formed by a 10 μm thin layer of SU-8. The bond wires are protected by a 250 μm thick layer of SU-8. (b) Die embedded in a PCB, shown without the PDMS sheet. (c) Close-up of working electrodes with wells hosting yeast cells. Reprinted with permission from ref 36. Copyright 2012 IEEE.

was first applied and the wells of 20 or 50 μm diameter were patterned, followed by mounting of single dies on a PCB and wire-bonding. Further, a SU-8 layer of 250μm thickness was applied to confine the solution in array area and to protect the bondwires (Figure 9 b) and structured PDMS cover on top was utilized for electrolyte management." [36]

3. APPLICATION OF CMOS AS A TRANSDUCER IN A BIOSENSOR

The conventional microelectrode-based arrays are limited by degradation of the signal and number of interconnects, which determine the size of the array. However, CMOS-based microelectrode arrays with measurement and processing circuits address these issues and offer advantages of fewer interconnects, a smaller footprint, a low power requirement, multiplexing, and signal enhancement via in-built buffering and amplification circuits.[2,12b] Design techniques and circuit architectures commonly applied in the CMOS world allow the simple formation of sensor arrays. Thus, it is possible to integrate many sensors on one die with only a few electrical connections to the outside world.[7] The use of CMOS-based systems is thus of low cost and results in high yields and integration capabilities.[1a]

The advancement in CMOS technology and requirement of large sensor array fabrication have encouraged researchers to use CMOS-based circuits to build transducers for biosensors, especially for measuring poor biological signals with high sensitivity. In recent years CMOS technology has been utilized to design high-performance sensor transducers, which on integration with bioelectrodes and other circuits in a monolithic manner have resulted in a multiplex microsystem array for high sensitivity and quality.[37] Monolithically generated CMOS systems have shown higher resistance toward external interference and resulted in higher SNRs during independent device operation.[38] In CMOS-based electrochemical systems, passivation on top metals is removed to pattern the electrode and the multilayer circuitry makes a transducer for in-pixel biosensing.[39] A CMOS-based microluminometer described by Simpson et al. has shown advantages of a lower signal detection limit and resistance to variation due to a thermally induced leakage current.[40]

CMOS-based electrochemical transducers, where electrons and ions are charge carriers and utilize potential change, capacitance change, current change, variation in impedance, etc. to extract information from electrode−electrolyte systems, provide a very common and compatible transducer platform. CMOS technology has also been used to fabricate optical, magnetic, and mechanical transducers. Furthermore, the integration of amplifiers, signal converters, and processors in the CMOS process has improved the system cost and performance requirements.[1a]

3.1. Electrochemical Transducers

In electrochemical sensors, CMOS technology has been used to incorporate amperometric, potentiometric, and impedimetric readout circuits along with buffer, amplifier, switching, and biasing circuits and other controllers necessary for electrochemical measuring techniques.[1b,41] The CMOS process with FG FETs, characterized by metallized gates insulated by an additional dielectric, has been used as a sensor input for biosensor applications. Such a design helps in improving the strength of the gate by providing higher protection of the gate dielectric. Meyburg et al. showed the transconductance and low noise behavior of n-channel FG FETs. Furthermore, it was found that p-channel FG FET arrays showing diode-like output characteristics are better sensors for extracellular couplings.[4]

CMOS-based EIS circuitry with improved measurement speeds and a frequency-independent response time has been described by Yang et al. and for 1 mHz to 100 kHz frequency range measurement has shown a response time of less than 20 ms.[42] Also it has been shown that CMOS-based EIS transducers provide improved signal conditioning, amplification, and processing with lower noise.[22] Hassibi et al. described a CMOS-based programmable electrochemical sensor microarray with each pixel consisting of a differential electrochemical-based transducer. Such a transducer helps in suppressing ionic and biochemical interference along with leakage currents and drift, thus improving the working range and sensitivity of the system. Such a configurable sensor has great potential for affinity-based sensors requiring various electrochemical measurements.[43] A CMOS-based transducer has also been employed for real-time monitoring of admittance-based biosensors.[39]

3.2. Optical, Piezoelectric, Magnetic, and Other Transducers Using CMOS Circuitry

Doped silicon exhibiting piezoresistive effects has been employed to fabricate CMOS-based mechanical transducers.[12a] For resonant cantilever-based biosensing, biased p-channel MOS transistors have been used for piezoresistive Wheatstone bridge development and have shown an improvement in power usage and resistivity signal when compared to diffusion-based silicon resistors.[38] For RF dynamics manipulation and monitoring of protons in water during nuclear magnetic resonance, CMOS-design-based RF transceivers have also been described. In such transduction, measurement of proton dynamics alteration by the target analyte is used as the biosensing principle.[44] In CMOS-based systems, Tajalli et al. investigated the process variation effect on the noise margin, power dissipation, and delay during transducer performance.[45]

To improve the digital cytometric skills of the CMOS-based optical active pixel sensor (APS) for microscopic particle

DOI: 10.1021/cr500554n
Chem. Rev. XXXX, XXX, XXX−XXX

detection and counting in the near field, Hosseini et al. described the modified dual-APS-array scheme. Using such a scheme, they were able to detect 5−15 μm (diameter) size particles flowing at speeds up to ∼500 μm/s.[46] Patounakis et al. described a CMOS-based optical transducer for fluorescence-detection-based assays. Without needing an external reader, they were able to perform fluorescence spectroscopy in a time-gated, time-resolved manner. The array was able to detect photon densities up to 1.15×10^8 /cm^2, and had subnano-second timing resolution.[47] In a different study, Erarslan et al. reported a CMOS-based optical readout utilizing diffraction grating interferometry for a microelectromechanical system (MEMS)-based sensor array (Figure 10). In their study, a CMOS-based photodetector array was used to capture the reflected light.[48] To perform optical stimulation, imaging, and electrical recording, Nakajima et al. described a CMOS-based optogenetic transducer.[49] CMOS-based transducers for magnetic biosensors have been demonstrated by Zhang et al. and Han et al.[23,35]

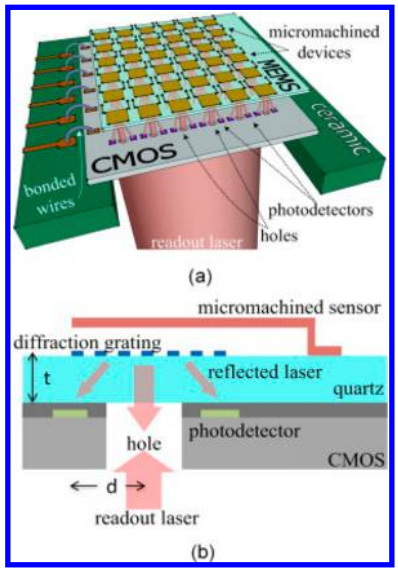

Figure 10. (a) Side view of one sensor. (b) Schematic of the integrated device. Reprinted with permission from ref 48. Copyright 2014 Elsevier.

4. CMOS-BASED CIRCUITRY FOR BIOSENSOR APPLICATION

Increasing requirements of developing an integrated biosensor array have necessitated the development of various CMOS-compatible circuitries to measure the biosensor response and convert it into a digital format. An interface circuit controls the sensor array and generates the sensor response. In sensitive electrochemical biosensor systems, it is desired to have circuits which exhibit low noise levels and support a wide range of input currents to result in higher SNRs. Furthermore, to minimize the footprint and cost of the device, it is desired to have integrated circuitry in the same chip. Studies have shown that the CMOS process can be employed to fabricate integrated microsystems for biochemical applications. Furthermore, on the basis of the requirement of a biosensor array, CMOS-based electrochemical interface circuits can be tuned to result in low noise and high sensitivity. Many such CMOS-based circuits for impedance, stress, current, etc. measurements have been described.[42,50] This section will describe the various circuits in brief, which have been implemented for various transducers and improving biosensor signals. For greater details, readers are encouraged to go through the full text of the respective reference.

4.1. Circuits for a Potentiostat

A potentiostat is one of the main instruments required for electrochemical sensing. It can be used for amperometric, potentiometric, voltammetric, etc. studies. In the CMOS-based biosensor array design, various potentiostat designs have been proposed. Using a 0.5 μm CMOS-based design, Yang et al. described an on-chip potentiostat integrated with chip surface

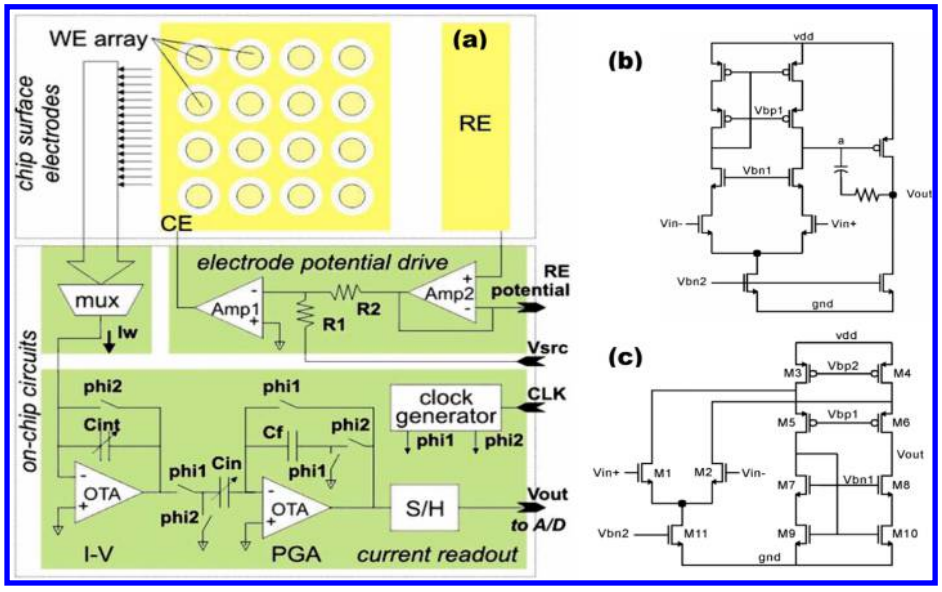

Figure 11. (a) Schematic of the surface electrode array and the on-chip potentiostat comprised of a switched capacitor amperometric readout block, an electrode potential drive block, and a current switching matrix (mux). (b) Schematic of the two-stage amplifier. (c) Schematic of the folded cascode OTA. Reprinted with permission from ref 41. Copyright 2009 IEEE.

DOI: 10.1021/cr500554n
Chem. Rev. XXXX, XXX, XXX−XXX

electrodes (Figure 11a). In their system the potential applied across the chip was set using the control signal V_{src}, and the reference electrode (RE) potential was measured using Amp2 in unity gain buffer mode. To suppress the output noise and to improve the sensitivity, they utilized a correlated double sampling (CDS) approach. Furthermore, to achieve a wide bandwidth, a high direct current (DC) gain, and a broad dynamic range, they described the use of the folded cascode structure (Figure 11c) and an operational transconductance amplifier (OTA) configuration (Figure 11b) in the current readout block. The OTA generating high gain ensured an accurate operation, while a rapid settling time enabled half clock period settling for the output signal. The simulation results for the OTA circuit showed a "24 MHz of unity gain bandwidth, 79 dB of DC gain, with settling time of 33 ns, slew rate of 49, phase margin of 60, 0.8 V to 3 V of input/output range, 107 dB (DC) of common-mode rejection ratio and a 80 dB of power supply rejection ratio". The chip with designed circuits supported various voltammetry measurements and for an array of working electrodes showed that the chip can be used for amperometric measurement over an "input range of 6 pA to 10 μA".[41]

In a separate study, Zhang et al. utilized a similar 0.5 μm CMOS-process-based low-noise interface circuit, which included an integrated potentiostat and amperometric readout amplifier for three-electrode electrochemical measurements. The results revealed that the system can handle 10 pA to 10 μA of output current with acceptable noise performance.[51] With the same configuration, Li et al. described a 0.5 μm CMOS-based "single-ended potentiostat with four-channels and amperometric readout circuit for voltammetric studies".[33] Also, in another study, Zhang et al. described a potentiostat which maintained the 0.7 V voltage difference between the working and reference electrodes.[52]

For an electrochemical biosensor featuring redox enzymes, Huang et al. reported a CMOS-based bipotentiostat comprising two readout channels for application of excitation signals and a potential control unit to support redox recycling (Figure 12). In their study, they achieved high gain and precision with operation in the "1 nA to 10 μA of dynamic range". Moreover, use of CDS in the entire readout chain helped in reducing the noise and amplifier offset.[53]

In designing a nanoelectrode microarray for biosensing, Zhang et al. described the on-chip potentiostat opamp (Figure 13) to accommodate the sensor current and to stabilize the electrolyte potential. In the potentiostat opamp circuit, transistors M29 to M32 defining the class-AB output stage helped to accommodate the electrolyte current by providing a maximized loading capability. On the other hand, use of an input stage with a complementary folded cascode configuration and comprising transistors M0 to M13 provided a big potential voltage swing with reduced input-referred noise to achieve a steady potential.[54]

To improve DNA sensing at a high pixel density, Krupa et al. suggested the use of mixed signal circuitry, which employs sensitive recording of the current over a broad range. For such a system, they designed various peripheral circuits and an array of analog-pixel-circuit-based CMOS sensor chips (Figure 14). A laptop was employed to control all signals applied and generated using the CMOS circuit.[55] In another study, Levine et al. demonstrated the dual-slope analog-to-digital converter (ADC) architecture to digitize the current in the range of 100 pA to 100 nA with sampling rates up to 5 kHz (Figure 15). It

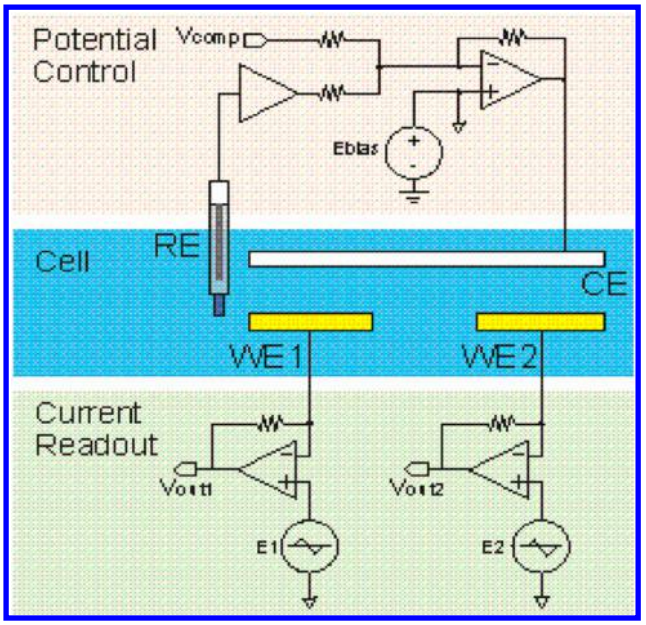

Figure 12. Architecture of the CMOS bipotentiostat with a connected counter electrode (CE), reference electrode (RE), and working electrodes (WEs). Reprinted with permission from ref 53. Copyright 2009 IEEE.

consisted of an on-chip-linear-capacitor (5 pF)-based integrating amplifier, a digital counter with control logic, and a comparator with a track and latch. Using the conservative design, they achieved better stability and low noise over a broad operating conditions range.[56]

4.2. Circuit for Amplifiers and Signal Conditioning

For parallel-cantilever-design-based sensors (Figure 16a), Yang et al. described a negative impedance converter and balance-network-based circuit for signal conditioning (Figure 16b). Using these circuits, they achieved improvement in the adjustment of the offset voltage and compensation of temperature drift for sensitive and accurate measurements.[57] For sensitive DNA sensing, Stagini et al. reported a 128-sensor array with circuitry for conditioning, multiple detection, signal conversion, and integrated measurement (Figure 17). A high-gain output stage with two differential input stages was employed for the comparator circuit, and a current mirror circuit was employed as the source of the current.[58] However; it was observed that, in the sensing circuit shown in Figure 17, there was no means to set the common-mode voltage of the I_{IN} and I_{OUT} nodes to prevent saturation of the current sources.

Hu et al. described a capacitive feedback transimpedance amplifier (TIA) topology (Figure 18) to be interfaced with an analog neural circuit and a biosensor array. The system was designed in 0.18 μm CMOS 1P6M technology, and a very high transimpedance gain with low power and low noise was achieved. The improvement in design flexibility for gain bandwidth trade-off was observed with their device, and they were able to circumvent design-related concerns coming from on-chip resistors. The system with such a configuration achieved a "trans-impedance gain of 100MΩ with bandwidth of 1 MHz, Peak to Peak voltage swing of 1 V, phase shift of less than 10° between 0.2−130 kHz, input referred current noise of 158fA/rt(Hz) at biosensors sampling frequency, while consuming power of 132μW from a 1.8 V source".[59]

DOI: 10.1021/cr500554n
Chem. Rev. XXXX, XXX, XXX−XXX

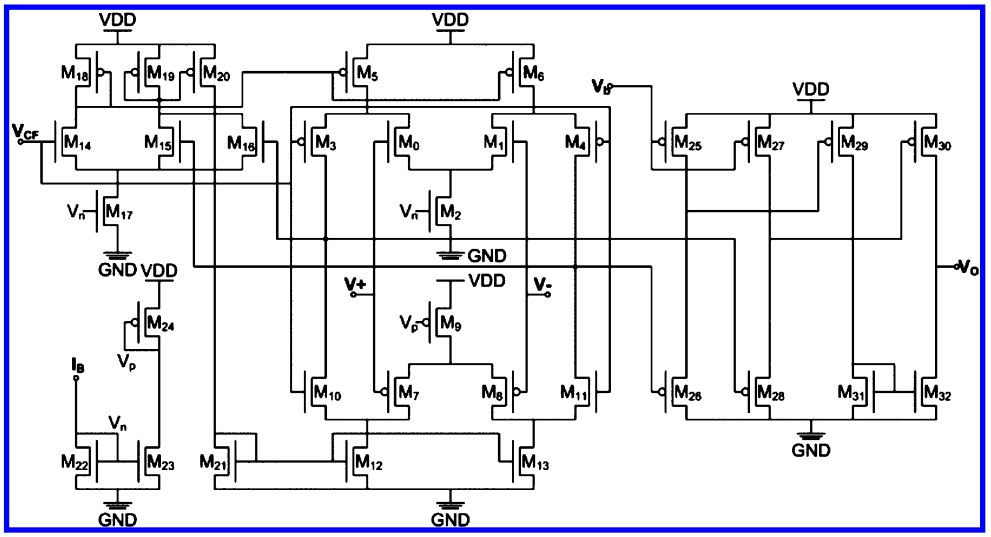

Figure 13. Schematic of the potentiostat opamp. Reprinted with permission from ref 54. Copyright 2011 IEEE.

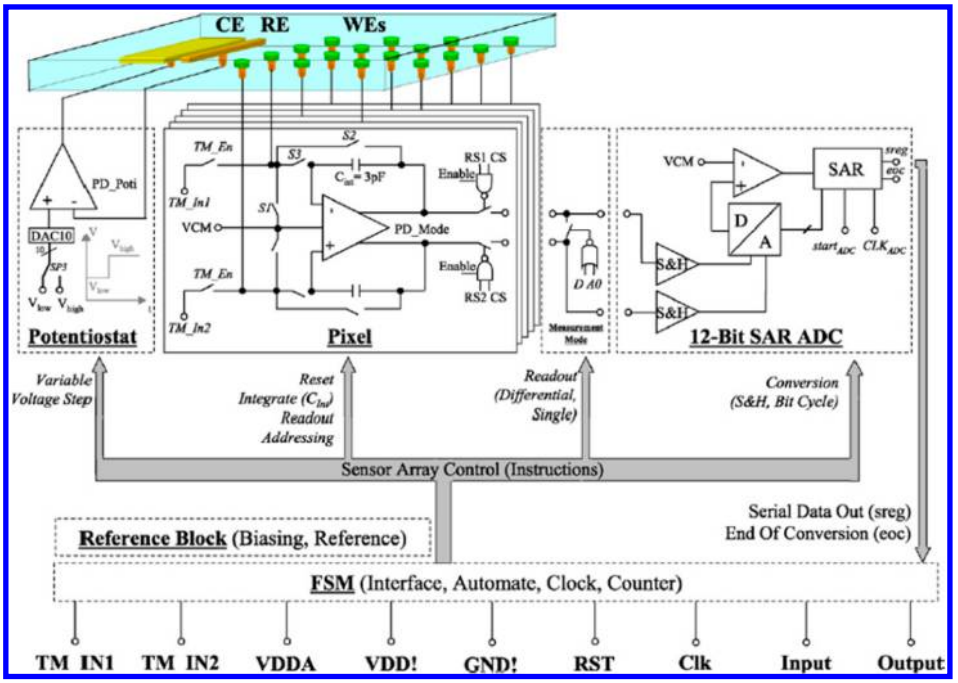

Figure 14. Block diagram of the sensor chip platform. Reprinted with permission from ref 55. Copyright 2010 Elsevier.

Hassibi et al. described the required circuitry of an 0.18 μm CMOS-based microarray for electrochemical sensing. Figure 19a shows the programmable sensor topology, where nine switches in each pixel control the functionality of the sensor. For suppression of low-frequency noise, they described the "Op-amp gain-boosted topology with switched biasing" (Figure 19b). Furthermore, using a configurable design, they showed the configuration for impedance spectroscopy, differential current measurements, and differential ISFETs.[43]

For CMOS-based biosensor array (128 × 128 electrodes) fabrication to record neural activity from outside the cell, Eversmann et al. utilized a combination of various CMOS-based circuits. Figure 20 shows all subcircuits of the complete signal path with the circuit for detection, which utilized the "sensor-MOSFET mismatch-compensated current-mode technique" for measurement.[60] In our analysis for the circuit diagram shown in Figure 20a, there might be large parasitic capacitance development on a row signal line due to the large number of connected pixels in it.

For continuous monitoring of a biological cell's metabolic activity, Rothe et al. described an integrated CMOS chip comprised of a Pt-based working electrode array (1024 eletrode) and 64 channels for current reading. In their chip, current was measured using two types of Σ−Δ ADCs. The first-order Σ−Δ converter (Figure 21) with a simple design that consumes low power and area provided "integration of double-layer capacitance (C_{dl})", while two switched-capacitor integrators in a second-order Σ−Δ converter (Figure 22) resulted in a higher bandwidth and resolution. The results reveal that linearity and resolution better than 11 and 12 bits can be achieved using first-order Σ−Δ and second-order Σ−Δ converters, respectively.[36]

Zhang et al. described the preamplifier buffer (Figure 23) and gain-stage amplifier (Figure 24) circuits in a 0.5 μm, 2P3M

DOI: 10.1021/cr500554n
Chem. Rev. XXXX, XXX, XXX−XXX

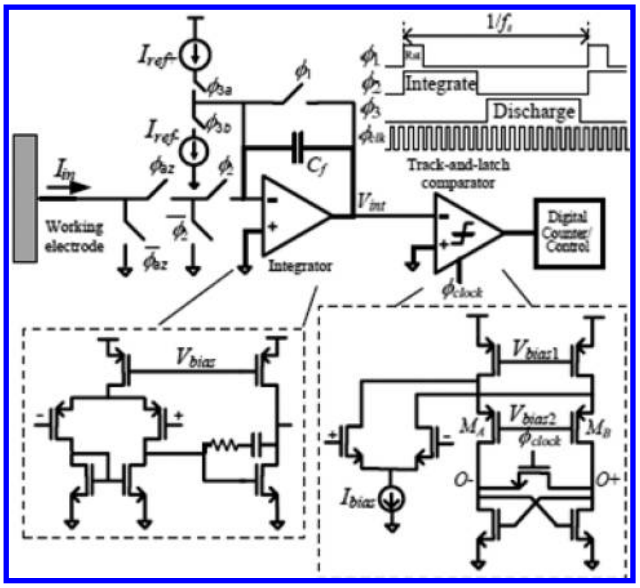

Figure 15. Dual-slope ADC and internal circuitry at each sensing site. Reprinted with permission from ref 56. Copyright 2007 IEEE.

CMOS-process-based biosensing system to record in vitro extracellular neural signals via a 24-channel mixed signal with improved parameters of gain, noise, and power usage. The circuit noise performance was improved using preamplifier buffers, which generated "higher drive capability" with "lower output impedance" required in next-stage neural signal amplification. On the other hand, the gain-stage amplifier provided considerable gain to the buffered signal and converted the signal of a few "hundred μV to a couple of volts". In their work they utilize "20dB closed-loop gain through resistive feedback" for the preamplifier buffer and "OTA with a capacitive feedback configuration" for the two-stage amplifier. The results for their system revealed satisfactory neural signal SNRs with frequencies within 100 Hz to 10 kHz and amplitudes in the 600 μV to 2 mV range.[61]

An analog front-end (AFE) circuit in teh 0.35 μm CMOS process with lower power consumption and "selectable on-chip dual AC/DC-coupled paths" was described by Lie et al. In AFE

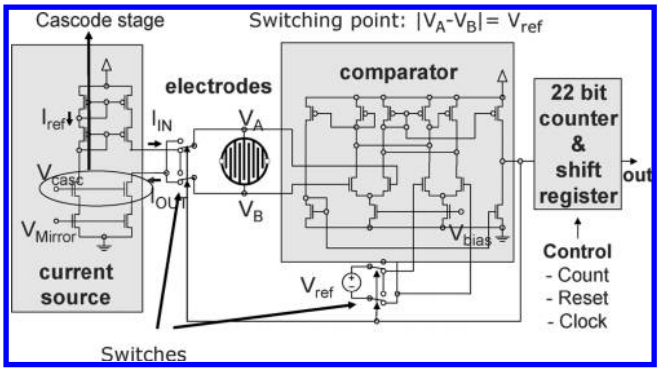

Figure 17. Schematic of the circuit associated with each sensing element. Reprinted with permission from ref 58. Copyright 2006 IEEE.

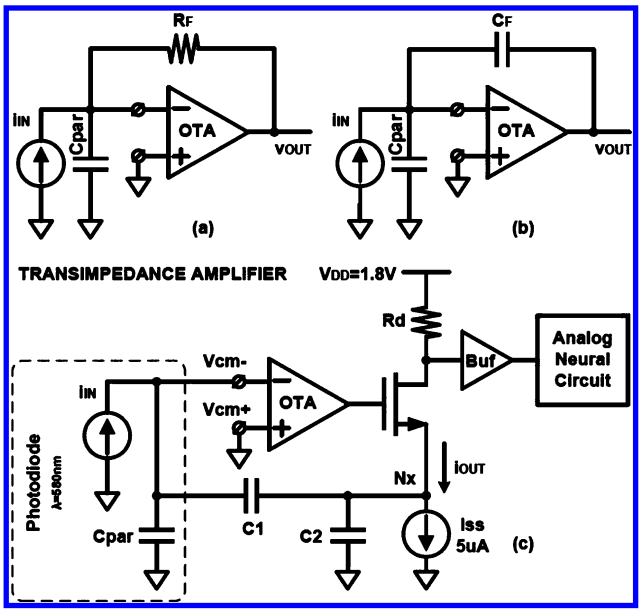

Figure 18. (a) Resistive feedback TIA. (b) Capacitive feedback TIA. (c) Schematic of the proposed TIA design with the improved capacitive feedback single-ended topology. Reprinted with permission from ref 59. Copyright 2010 IEEE.

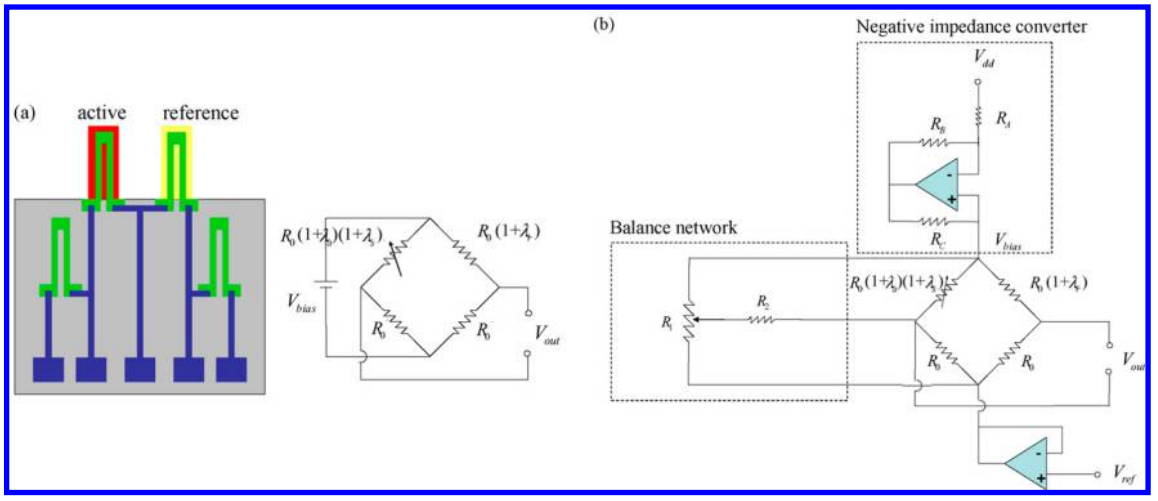

Figure 16. (a) Parallel microcantilever design in a bridge circuit: an active cantilever, a reference cantilever, and two fixed resistors (R_0). (b) Signal conditioning circuit composed of the balance network and the negative impedance converter. Reprinted with permission from ref 57. Copyright 2008 Elsevier.

DOI: 10.1021/cr500554n
Chem. Rev. XXXX, XXX, XXX−XXX

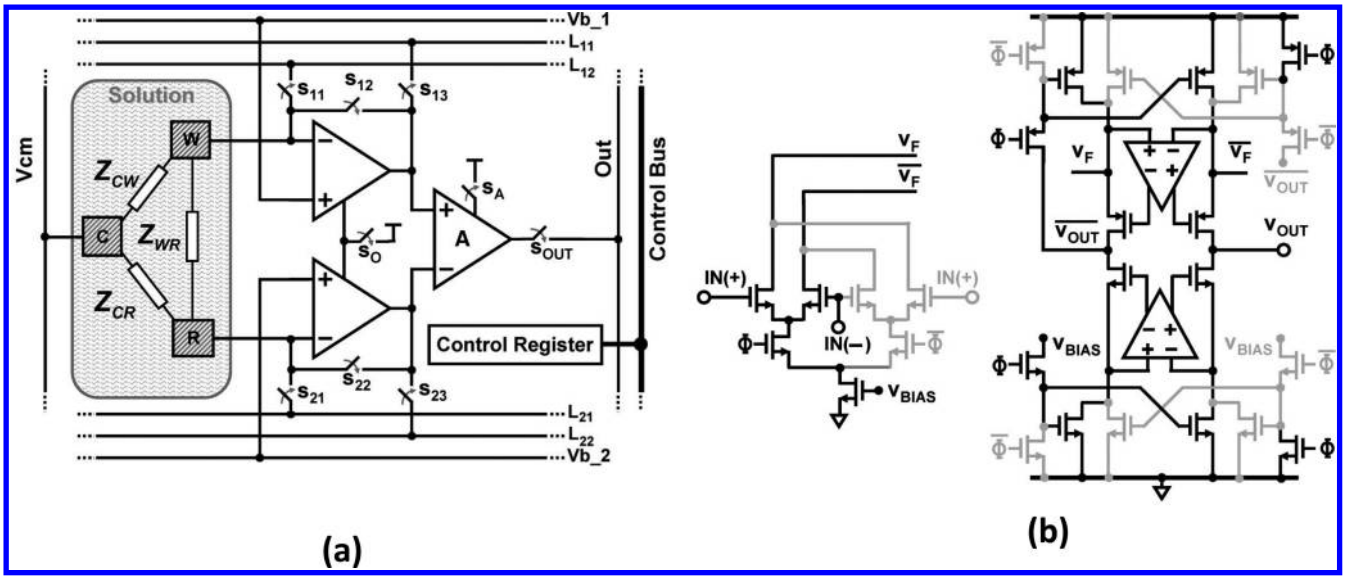

Figure 19. (a) Topology of the configurable sensor. (b) Opamp gain-boosted topology with switched biasing for low-frequency noise suppression. The gray paths indicate the alternative paths required for switched biasing. Φ and $\bar{\Phi}$ are the switching signals. Reprinted with permission from ref 43. Copyright 2006 IEEE.

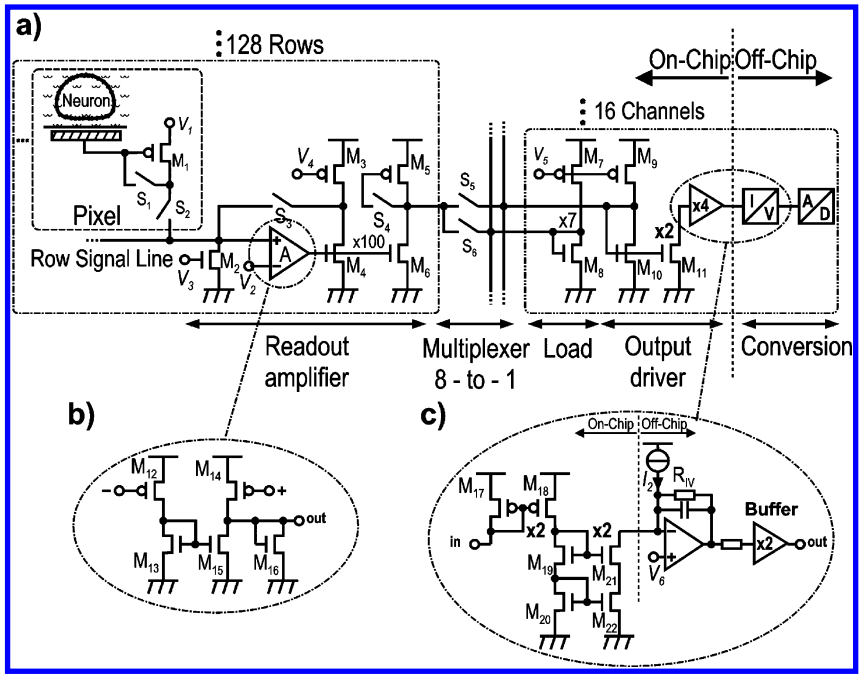

Figure 20. (a) Circuit diagram of the complete signal path with details in (b) and (c). (b) Quasi-differential stage in the readout amplifier. (c) Output driver and *I*/*V* conversion. Reprinted with permission from ref 60. Copyright 2003 IEEE.

a "DC-coupled instrumentation amplifier (INA)" was implemented using a resistor-feedback-network-controlled differential difference amplifier (DDA). In three-stage DDA (Figure 25), the required high gain was provided by the first and second stages and the resistor-feedback network was operated by the source follower third stage. During large offset voltage, saturation of the channels was prevented via use of programmable INA gain.[62] The results revealed that, without external buffer, the AFE circuit consumed only "2.37 μA/channel with an input referred noise of ∼40 μVrms in range of 1 Hz to 1 kHz". Also for QRS peak detection, it properly displayed the waveforms of electrocardiogram and electrogram.

In another study, Ballini et al. described 0.35 μm CMOS-technology (2P4M)-based readout channels with a configurable gain and bandwidth (Figure 26). With closed-loop topologies in three stages, they achieved uniformity in gain for all channels without requiring any calibration. In stage 1, low-frequency drifts of the electrode potential during alternating current (AC) coupling were prevented via use of 1.4 pF input capacitors. In the second stage, antialiasing filtering and a limiting bandwidth were achieved using resistive-feedback-controlled DDA. In the third stage, thermal noise suppression and cutoff frequency control were achieved via use of an area-efficient multirate SC circuit. With such a combination of stages, each channel occupied 0.036 mm^2 and consumed 53.4 μW. In their system, a

DOI: 10.1021/cr500554n
Chem. Rev. XXXX, XXX, XXX−XXX

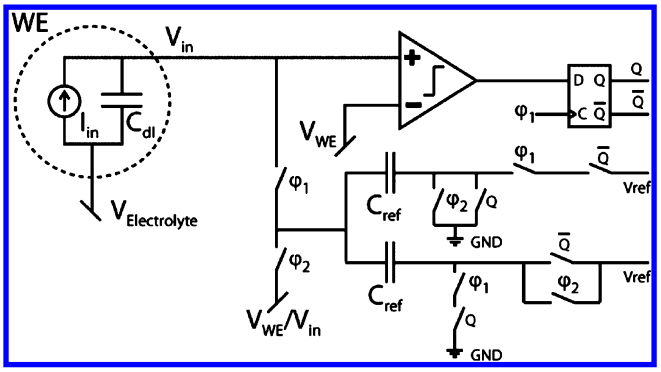

Figure 21. First-order Σ−Δ converter scheme. Reprinted with permission from ref 36. Copyright 2012 IEEE.

total power consumption of 75 mW was observed and linearity of 9 bits with a 100 μA output current range was achieved.[63]

4.3. Circuits for ISFET-Based Biosensors

For ISFET-based sensors, a source-drain follower circuit employed with an extended-gate electrode configuration (Figure 27a) has been proposed and found to consume low power.[3,64] Due to infinite input impedance for AC and DC signals, the source-drain follower does not influence the sensing system. Furthermore, in the voltage follower mode of this circuit, the device parameters, such as environmental temperature conditions and threshold voltage, do not influence its output voltage.[3] Figure 27b shows a schematic diagram of the source-drain follower circuit proposed by Kagohashi et al. for the development of integrated extended-gate ISFET arrays (16 × 16 and 32 × 32) using the 1.2 μm CMOS process (Semiconductor Technology, Japan). Using a Si_3N_4 film as the sensor, they achieved an average pH sensitivity of 41 mV/pH, with a standard deviation of 1.5−3.4 mV. However, looking at the given source-drain follower circuit, it seems that it will take a long time to reach its final value because the positive feedback comprised of NMOS current mirrors N_1, N_{11}, N_2, and N_{12} and PMOS current mirrors P_1, P_2, P_3, and P_4, hinders V_x and V_y from converging to a common voltage level.[64] In another report, Im et al. described the current readout circuit, comprising a single-slope 10 bit ADC and current integrator for "dielectric modulated field effect transistor (DMFET) arrays" fabricated as a biosensor cartridge.[65]

4.4. Circuits for Capacitance Measurement

To measure small electrode capacitance in interdigitated (IDT) microelectrodes, Lu et al. described a "self-oscillating readout circuit" using the CMOS process to generate an electrode−analyte capacitance-dependent digital pulse stream (Figure 28). In their circuit, an electrode−analyte capacitor was charged via a fixed but adjustable (1−16 μA) current source. Using this circuit, the system was found to reduce the parasitic effect and to enhance the sensing resolution.[66]

To measure variation in the sensor's capacitance as oscillation frequency output, Yang et al. described an oscillator circuit (Figure 29). In their circuit, the glucose sensor capacitance, resistances, load capacitance, and inverters were represented using C_{sensor}, R_1 and R_2, C_1, and Inv's 1−5, respectively. Simulation results for the described circuit showed that, for an increase of 15−50 pF in sensor capacitance, the oscillation frequency decreases from 25.49 to 8.13 MHz. In experimental glucose sensing, absorption of glucose by glucose oxidase resulted in a change in sensor capacitance, thus causing a change of oscillation frequency. For glucose concentrations of 5 and 10 mM, the sensor showed oscillation frequencies of 17.27 and 23.71 MHz, respectively.[67]

In another study, Yusof et al. utilized a 1.2 μm, 2P2M CMOS technology for describing the circuit for charge-based capacitance measurement (CBCM) (Figure 30). To confirm that current at any given time is conducted through either of the two switches (S1, S2), two nonoverlapping clock pulses were incorporated in the circuit. During DNA sensing via this circuit, a capacitance decrease of 20% was observed for the hybridization event.[17c] For the circuit shown in Figure 30, it seems that the charge integration capacitor C_i in the fully differential capacitive gain amplifier might not be in the best orientation to form a negative feedback loop through each input to the corresponding output path, which can ensure a stable operation of the circuit.

It is observed that, in recording the extracellular potential via a multichannel, parasitic capacitance on contact usually interferes with sensing of the potential. As signal levels of interest in neural signal applications are quite low (50−500 μV), on-chip buffering is required for obtaining low output

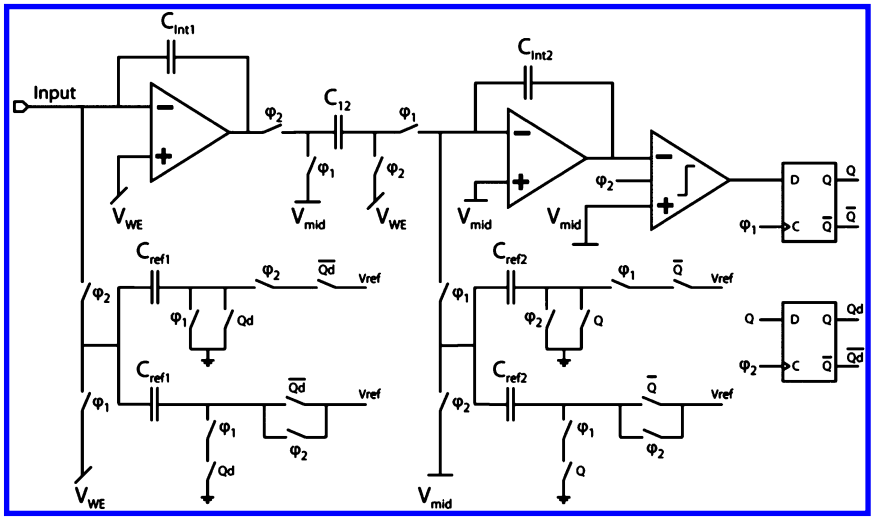

Figure 22. Second-order Σ−Δ converter scheme. Reprinted with permission from ref 36. Copyright 2012 IEEE.

DOI: 10.1021/cr500554n
Chem. Rev. XXXX, XXX, XXX−XXX

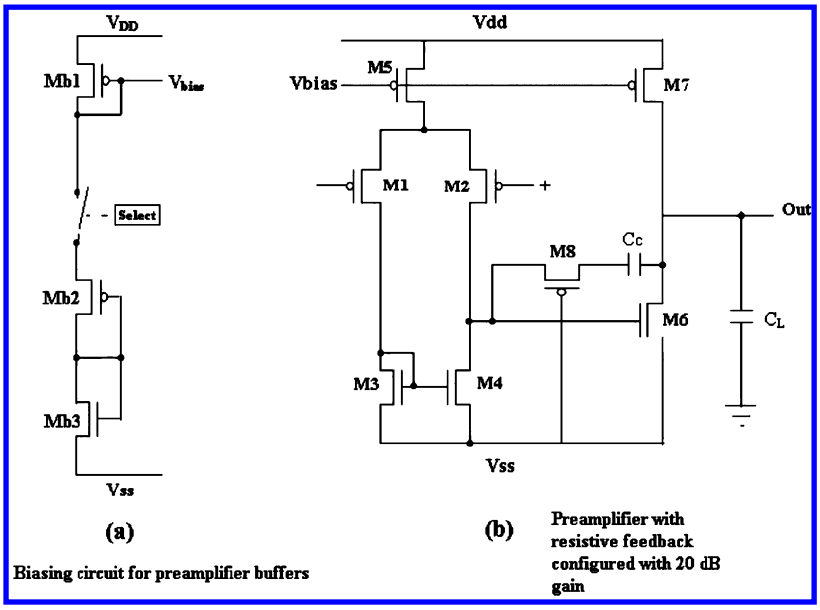

Figure 23. Schematics of the preamplifiers. Reprinted with permission from ref 61. Copyright 2009 IEEE.

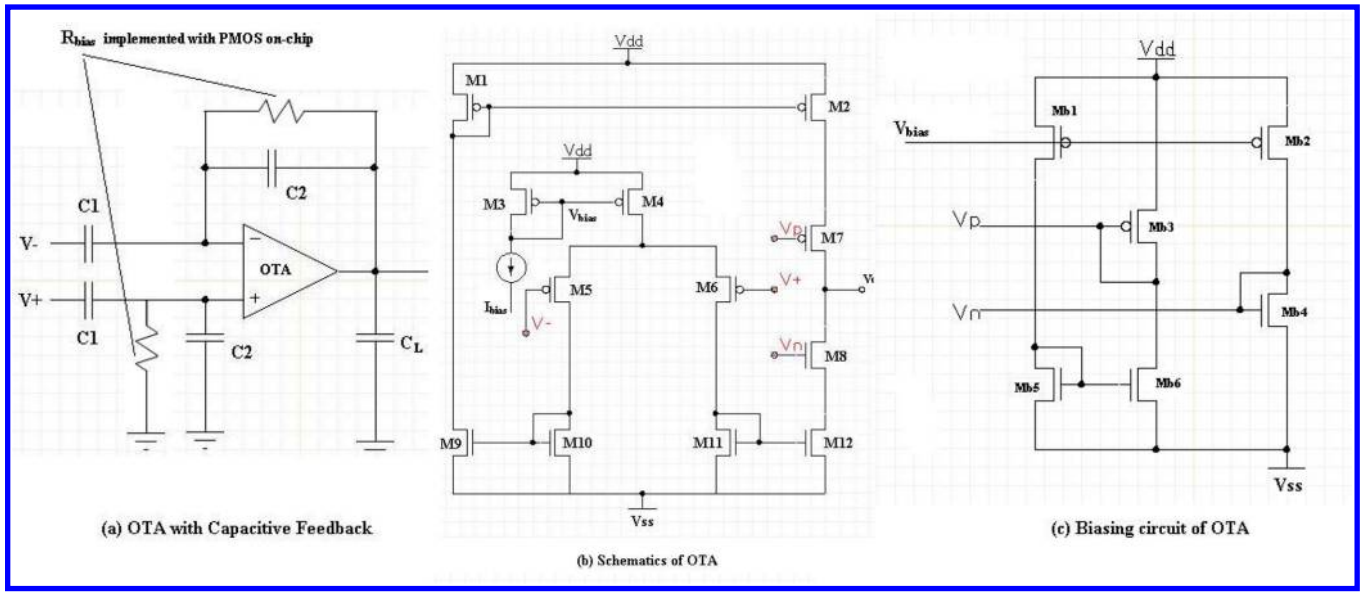

Figure 24. Schematics of the OTA-based high-gain amplifier. Reprinted with permission from ref 61. Copyright 2009 IEEE.

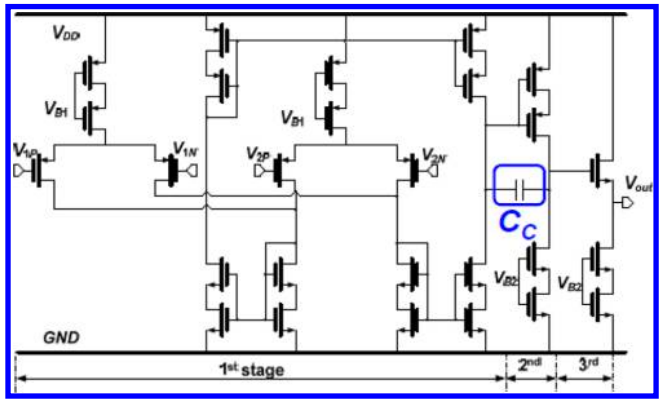

Figure 25. Schematic of the proposed differential difference amplifier (miller cap C_c shown and highlighted here). Reprinted with permission from ref 62. Copyright 2013 Lie, D. Y. C.

impedance levels and high drive capability. For such applications Zhang et al. described a unity gain buffer circuit in the 1.5 μm, 2P2M CMOS technology (Figure 31) to lower the charge injection for the MOS transistor. The chip with their circuit resulted in a reasonable SNR for neural signals with frequencies in the 20−2000 Hz range and amplitudes in the 50−500 μV range.[68]

4.5. Circuit for Impedance Measurement

Yufera et al. presented a 0.35 μm CMOS-technology-based closed-loop circuit for impedance measurements. The system consisted of a "rectifier, instrumentation and error amplifiers, and a current oscillator with configurable output current amplitude" (Figure 32). The circuit provided "alternate current excited systems" which were able to operate and measure at the same time. The rectifier was utilized for detection of the full wave peak, and the system generated independent and individually optimizable phase and magnitude signals that can

DOI: 10.1021/cr500554n
Chem. Rev. XXXX, XXX, XXX−XXX

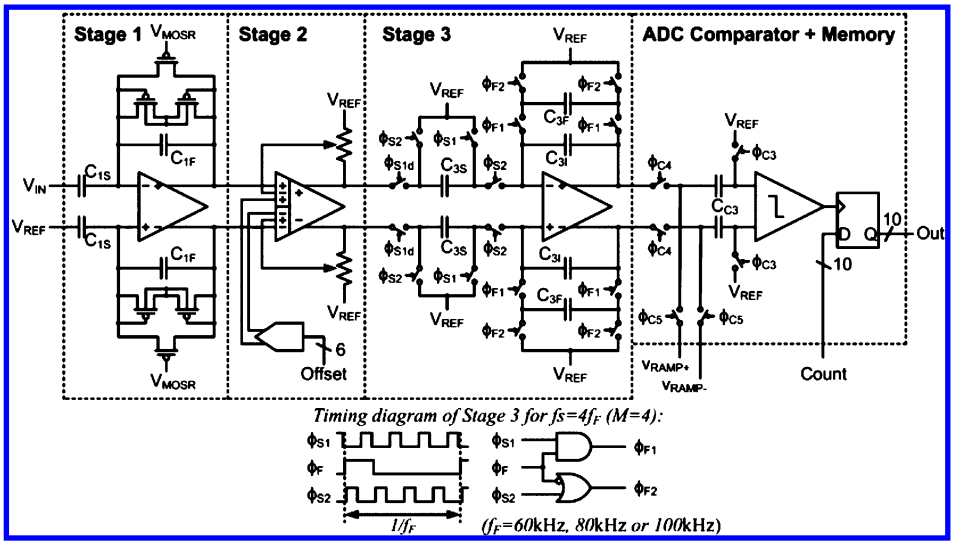

Figure 26. Schematic of the readout chain, with a timing diagram for the third stage. Reprinted with permission from ref 63. Copyright 2013 IEEE.

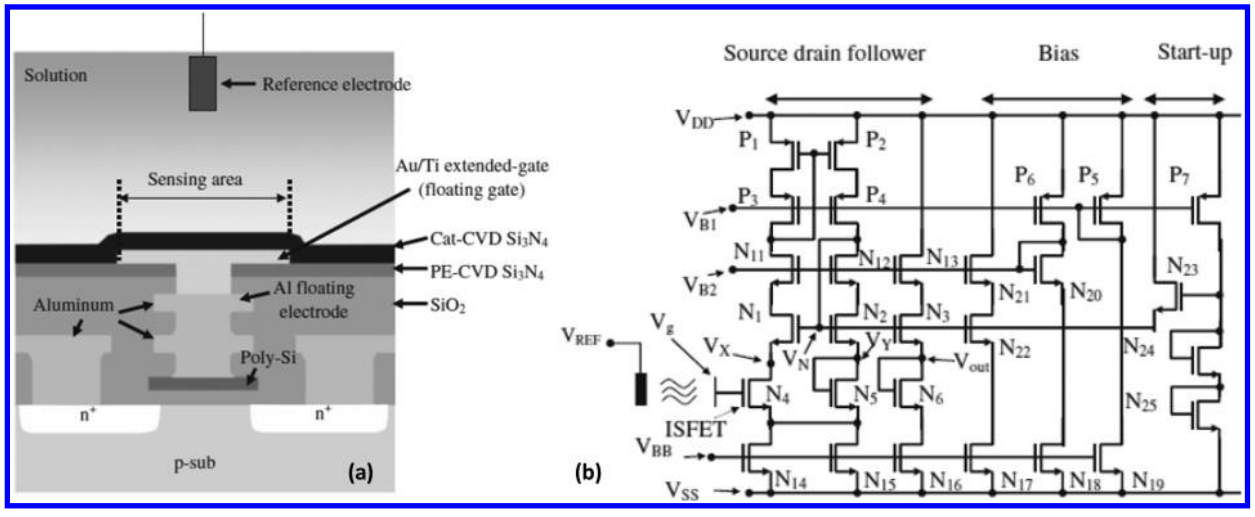

Figure 27. (a) Cross-sectional view of an extended-gate ISFET with catalytic chemical vapor deposition Si_3N_4. (b) Schematic diagram of the source-drain follower circuit. Reprinted with permission from ref 64. Copyright 2010 The Japan Society of Applied Physics.

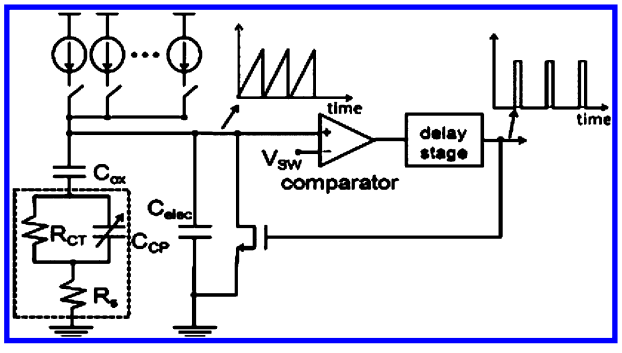

Figure 28. Schematic of the capacitive readout circuit. Reprinted with permission from ref 66. Copyright 2010 Elsevier.

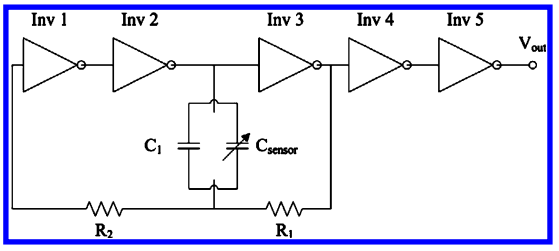

Figure 29. Oscillator circuit for the glucose sensor. Reprinted with permission from ref 67. Copyright 2012 Elsevier.

be used for any kind of resistive and capacitive load. However, in our view it is worth verifying this impedance measurement system by IC fabrication and measurement.[69]

To extract sensor impedance information, Yang et al. described a 0.5 μm CMOS-based low-power lock-in impedance-to-digital converter (IDC) circuit (Figure 33). The response current of the sensor was analyzed by IDC, and its frequency-dependent admittance with *real* and *imaginary* parts was calculated. In their system, hardware efficiency was maximized by resource sharing between "bidirectional counter/shifter and multiplying integrator for impedance measurement and digitization". The circuit was found to be working for "frequency, up to 10 kHz" and input current in the "78 fA to 100 nA" range. Power consumption for the circuit was found to be low and showed an acceptable response for a gramicidin-ion-channel-based biosensor.[70] The disadvantage of this lock-in IDC is that it cannot cover a typical

DOI: 10.1021/cr500554n
Chem. Rev. XXXX, XXX, XXX−XXX

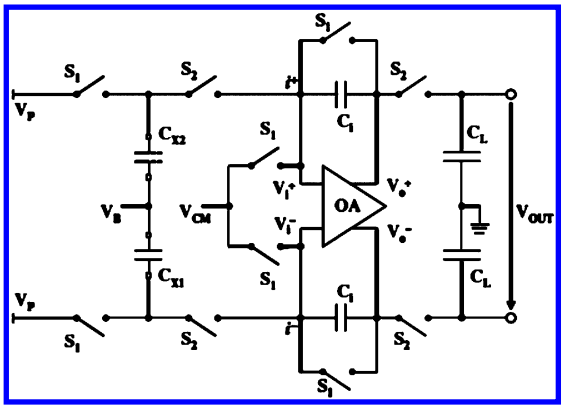

Figure 30. Schematic of a fully differential capacitance sensor. Reprinted with permission from ref 17c. Copyright 2010 The Japan Society of Applied Physics.

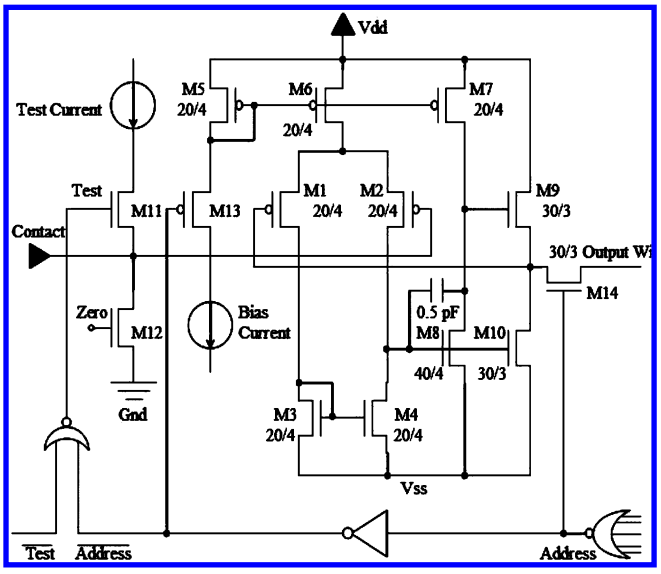

Figure 31. Schematic of the unity gain buffer. Reprinted with permission from ref 68. Copyright 2005 IEEE.

EIS frequency range up to several megahertz, mainly due to the phase error in its zero crossing detection.

For DNA and protein sensing via the EIS method in the biosensor array, Manickam et al. described a CMOS-based circuit with low-noise TIA (bias 50 μA), which provided

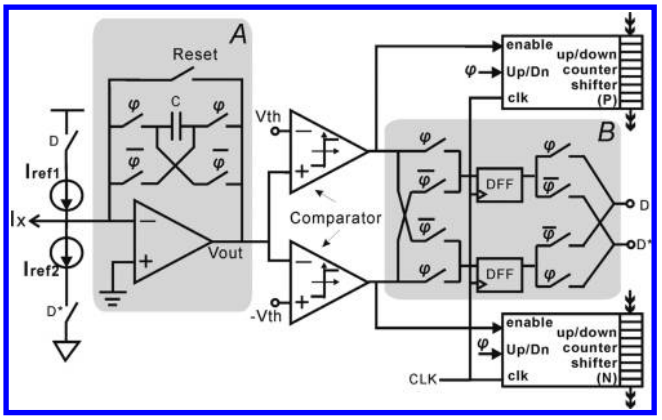

Figure 33. Principal schematic of the lock-in IDC circuit. Reprinted with permission from ref 70a. Copyright 2009 IEEE.

amplification and kept the impedance node lower at the contact point of the sensing electrode.[21a,22,39] Other than bias circuits, Figure 34 shows the entire pixel circuit diagram, where use of a differential amplifier resulted in gain boost with lower input impedance. Possible faradic processes between the sensing and reference electrodes were also kept in control by setting the DC voltage between these electrodes using a differential amplifier. In a single-ended positive input system, a steady DC reference voltage "for negative input of differential mixer" was generated using a low-noise TIA replica circuit with a bias of 5 μA. With the described circuit, they achieved a limit of detection (LOD) of around 10^5 molecules.[21a] In our opinion, the EIS system shown in Figure 34 adopted a direct conversion-to-DC topology, but it does not have a DC offset cancellation means, which will lead to large errors in the impedance measurement. Even though the authors suggested measurement of the DC offset for the desired pixel prior to the impedance measurement, the DC offset may vary during the measurement.

4.6. Circuits for Amperometric Measurement

The usually observed variations in potential during switching from one electrode to another via directly connected switches in amperometric measurement for a multiple-microelectrode system has presented another challenge. To suppress such variation in electrode potential due to switching, Hasegawa et al. described a current buffer circuit between the electrode and the switches (Figure 35). The results indicate that the circuit consumed low power and helped in reducing the switching effect.[1b]

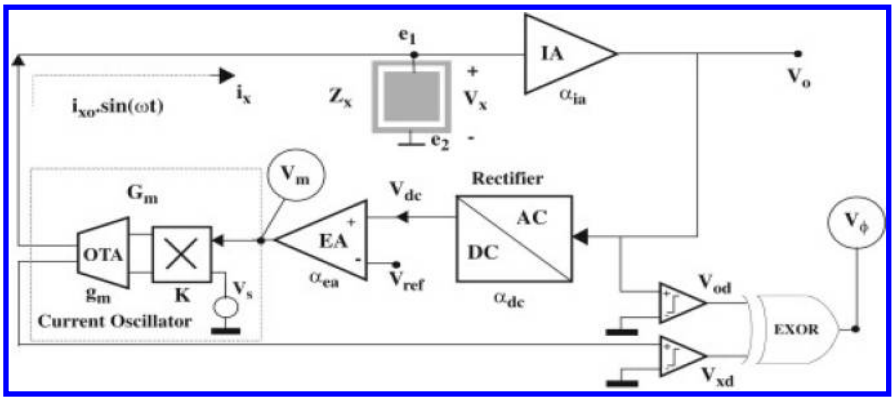

Figure 32. Proposed circuit blocks for impedance sensing. The magnitude and phase are obtained from signals V_m and V_Φ, respectively. Reprinted with permission from ref 69. Copyright 2010 Elsevier.

DOI: 10.1021/cr500554n
Chem. Rev. XXXX, XXX, XXX−XXX

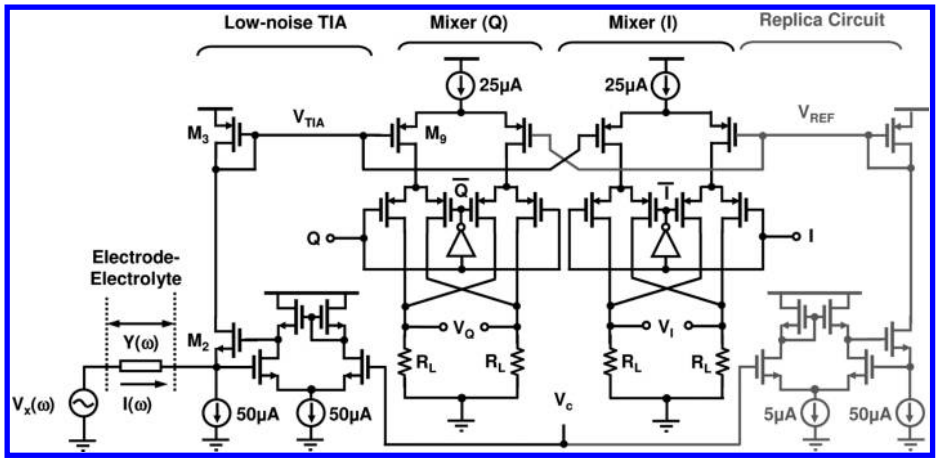

Figure 34. Circuit topology of the pixel. Reprinted with permission from ref 39. Copyright 2010 IEEE.

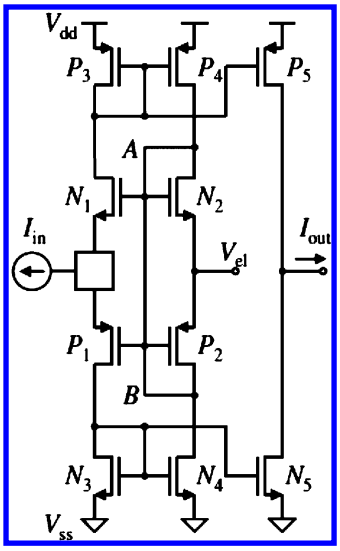

Figure 35. Schematic diagram of the current buffer circuit. Reprinted with permission from ref 1b. Copyright 2011 The Japan Society of Applied Physics.

Zhang et al. developed an integrated 64 pixel (with each pixel of 600 nm size) CMOS-based microarray (Figure 36) for biosensor applications. For reducing complexity in the pixel design, they described a "decoding scheme of memories"-based circuit where the "current amplifiers and potentiostat opamp" were shared. In the microarray system, they activated the desired electrodes via use of a "pre-decoding and pixel decoding based two-stage approach" and achieved low noise and high sensitivity for a nanoelectrode, by using the ultra-low-current amplifier (ULCA) (Figure 37). ULCA results in amplification of the measured current from the sensor before it is sent to the off-chip system. Furthermore, on-chip potentiostat opamp utilized a "negative feedback mechanism" to monitor the potential precisely and to deliver current to the electrolyte. The results for the circuit revealed that it can generate "19.9 dB of current gain with bandwidth of 3 dB, 15 kHz" Furthermore, it can provide "sensing sensitivity of 37.6pA, dynamic range of 141 dB, and 0.46 mA of driving capability".[54]

4.7. Circuits for RF Signal Measurement

For biosensing application, Sun et al. reported a circuit for a CMOS-based RF transceiver. Using an "image rejection algorithm in the digital domain" and adding the Hilbert transformer output, they achieved lower image noise (Figure 38).[44]

4.8. Circuits for Resistance Measurement

In development of a piezoresistive wireless CMOS hepatitis B virus (HBV) DNA system on chip (SoC), Huang et al. described a readout circuit with oscillator-based self-calibration (Figure 39A). The circuit consists of a "frequency mixer, frequency-to-digital converter (FDC), (÷4) divider, sensor integrated oscillator (OSC), and digital circuits". In the circuit the operation frequency was down-converted via a mixer, and the three RC-delay stages of OSC helped in linear conversion of the resistance change of the piezoresistor into an OSC frequency (f_{sensor}) shift. Figure 39B shows a schematic diagram of the SoC for wireless detection of DNA. The system consists of "microcantilever based DNA sensors, programmable microcontroller unit (MCU), readout circuit with self-calibration, voltage regulator, and an on−off keying (OOK) wireless transmitter/receiver (TX/RX)". The OOK receiver was used to demodulate the received external wireless command and transfer it to the on-chip MCU, where biosensing signals from DNA sensors were then converted to digital form, packaged using the MCU in RS232 format, and conveyed to the outside monitor using an OOK TX.[71]

4.9. Circuits for Optical and Magnetic Biosensors

Lechuga et al. described an APS-based CMOS array (128 × 16) for the position-sensing detector (PSD) (Figure 40). The system contained array electrodes and circuits for analog signal processing, output buffers, and a system control. To maximize the isolation of the photocurrent in each pixel, a "p-diff−n-well photodiode structure" was used, and conversion of optical power to current was achieved. Furthermore, the CDS circuit, which records the sample signal just after activation of the reset signal and at the finale of the integration interval, was employed to reduce the noise in the APS system (Figure 40).[72]

To interface an on-chip blue light-emitting diode (LED) array to neuronal tissue for "optical stimulation, imaging and electrical recording", Nakajima et al. described the 0.35 μm CMOS-process-based circuitry for an optogenetic device. Figure 41 shows the system schematic and circuit for selection and driving of the LED. The micro-LEDs in the system were addressed using a "7-bit decoder and built-in line scanner". The device in the decoder state resulted in localized excitation of proteins and in the scanning state resulted in "uniform illumination with excitation light" required for recording a

DOI: 10.1021/cr500554n
Chem. Rev. XXXX, XXX, XXX−XXX

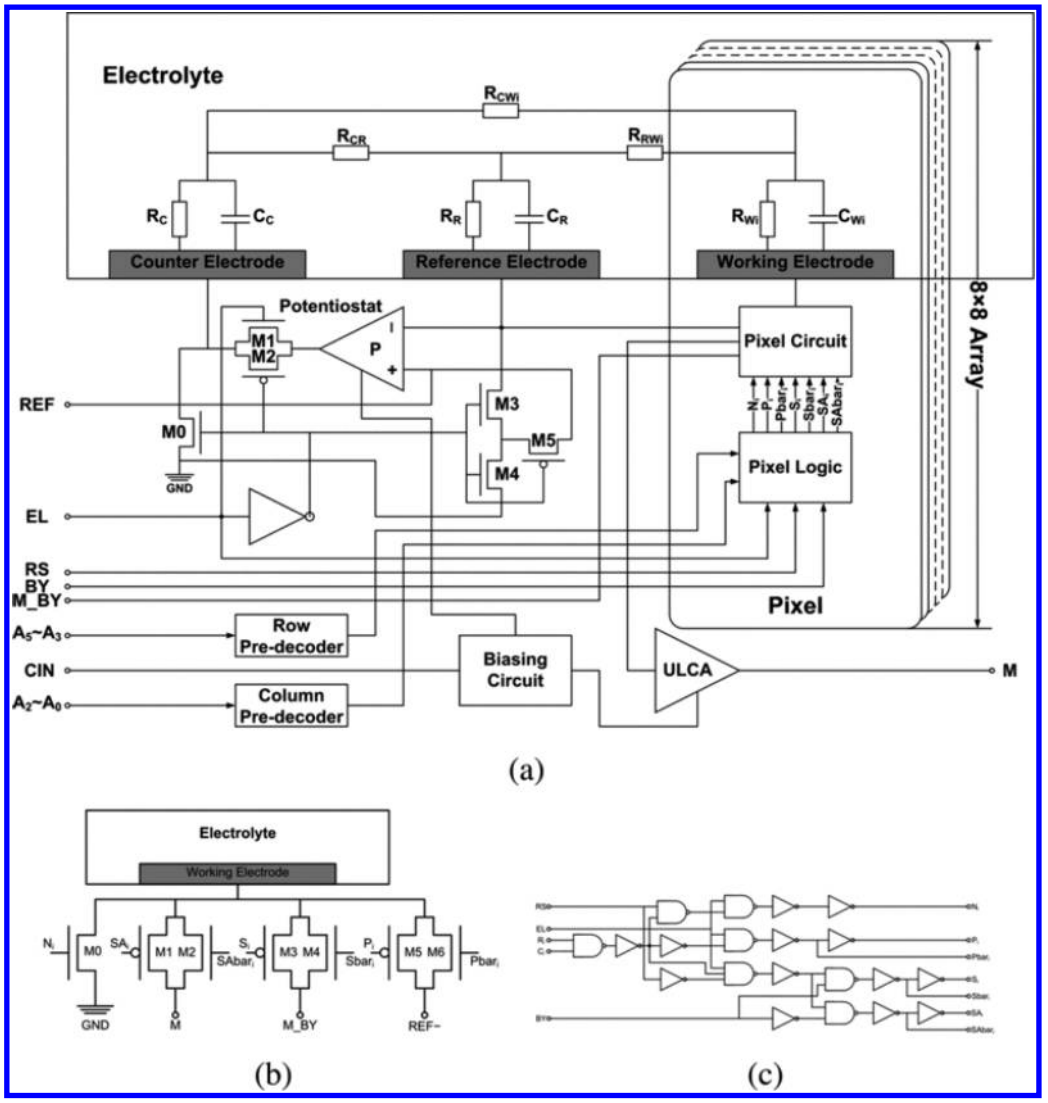

Figure 36. (a) Circuit architecture of the proposed biosensor microarray. (b) Schematic of the pixel circuit. (c) Schematic of the pixel logic. Reprinted with permission from ref 54. Copyright 2011 IEEE.

fluorescence image. The authors also described the use of a flexible polyimide substrate for mounting of the chip using epoxy resin, where connections between the chip and flexible printed circuit were made using Al bonding wires. The mechanical strength of the bonding wires was provided via use of reinforcement with ultraviolet-curable resin.[49] Han et al. described the CMOS-based magnetic biochip system with spin valve structures to record the giant magnetoresistive (GMR) effect (Figure 42). In an array of 1008 GMR biosensors, they utilized "frequency division multiplexing (FDM) and time division multiplexing (TDM) techniques" to increase the throughput and to decrease the time required for signal reading from an individual pixel. The readout channel illustrated in Figure 43 utilized a single master clock of 42 kHz and generated carrier frequencies of "3-kHz, 4.2-kHz, 5.25-kHz and 7-kHz," for the mixers. Furthermore, to maximize the dynamic range of the system, the authors also incorporated a "programmable gain amplifier (PGA) with gains of 1, 10, or 100".[23]

Zhang et al. described a 0.5 μm CMOS-technology-based magnetic field-effect transistor (MAGFET) readout circuit for magnetic sensing via the split-drain Hall effect (Figure 44). In such a system, exposure of the MAGFET to a magnetic field results in current deflection, causing Hall-effect-based imbalance in the two drain currents. The authors showed that use of a differential MAGFET improves the sensitivity of the sensor.[35] In another study on "on-chip LC resonance frequency-shift"-based magnetic biosensing, Wang et al. described the 45 nm CMOS-process-based 16-cell sensor array and utilized a CDC noise cancellation scheme to achieve high sensitivity. Figure 45 illustrates the quad-core sensor cell schematic, where each LC tank acts as an individual sensing site. In their design, the LC tank was coupled with the complementary active core using NMOS/PMOS switch pairs, and the common-mode frequency-drift effect was minimized by using the system in the differential sensing mode configuration, where three of the sensing sites were utilized as active sensors and the fourth one was used as a reference sensor.[73]

4.10. Circuits for Implantable Biosensors

For implantable biosensor applications, Zhang et al. described a 0.35 μm CMOS-process-based circuit for sensor readout that occupies 0.66 mm^2 of area and consumes low power (400 μW). The circuit utilized the current signal from the biosensor and generated an "amplitude shift keying (ASK) signal" that can be

DOI: 10.1021/cr500554n
Chem. Rev. XXXX, XXX, XXX−XXX

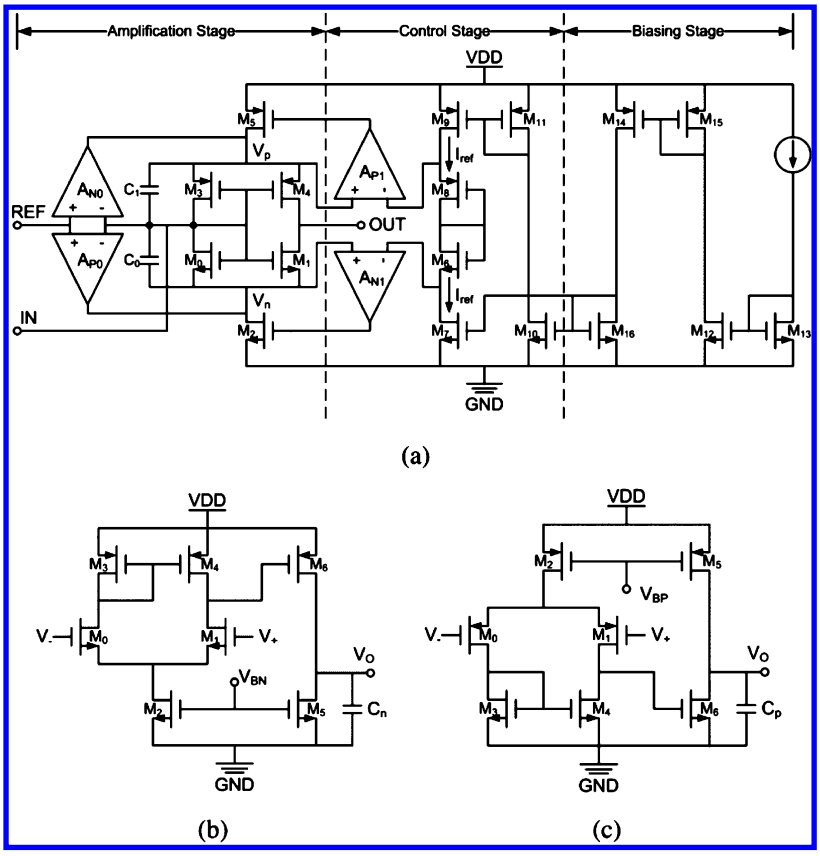

Figure 37. (a) Schematic of the proposed ULCA. (b) Auxiliary n-type opamp. (c) Auxiliary p-type opamp. Reprinted with permission from ref 54. Copyright 2011 IEEE.

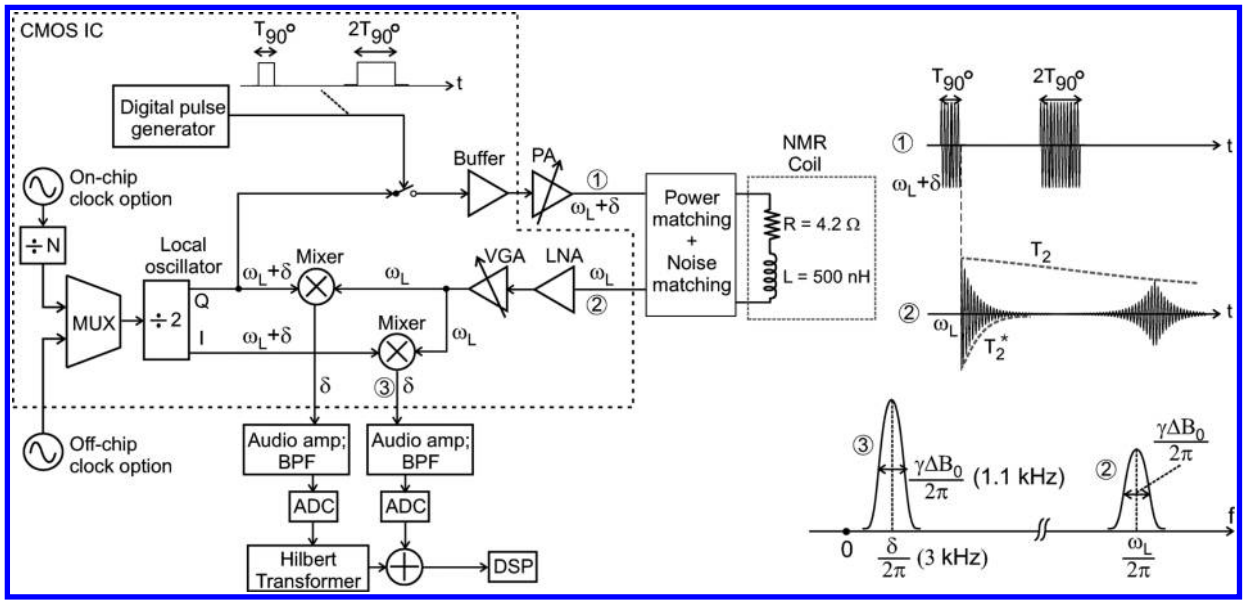

Figure 38. Architecture of the NMR RF transceiver IC. Reprinted with permission from ref 44. Copyright 2009 IEEE.

used as the input signal for commercial radios. The results of the signal processing circuit shown in Figure 46 were found to be similar to the simulation results.[52] In another study of an implantable biosensor, Hasan et al. proposed a low-voltage high-resolution CMOS comparator circuit (Figure 47) for "pre-amplification of single ended sampled-data", which counter-balances the differential input offset. For easier integration in the biosensor chip, the circuit was made using just 38 MOSFETs and 3 capacitors and found to occupy less than 1 mm^2 of area. Furthermore, higher voltage gain and output impedance were achieved using long-channel-device-based inverter amplifiers, while dummy pass gates were used along the signal path to minimize charge injection and charge absorption issues. For the comparator, the static micropower consumption was found to be lower than 10 μW when used with a 0.5 V supply voltage.[74]

DOI: 10.1021/cr500554n
Chem. Rev. XXXX, XXX, XXX−XXX

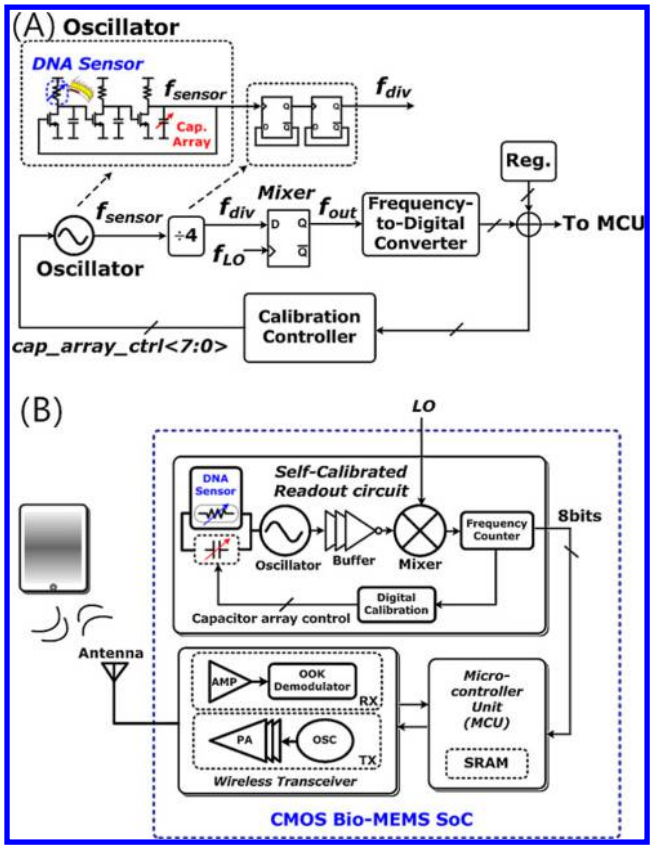

Figure 39. (A) Simplified architecture of the developed oscillator-based self-calibrated readout circuit. (B) System block diagram of the developed wireless CMOS HBV DNA SoC. Reprinted with permission from ref 71. Copyright 2013 Elsevier.

For an implantable biosensor application, radio frequency identification (RFID) transponders have also been employed as they can be used for easy communication and have been shown to work using passive power. To develop a passive RFID transponder of 13.56 MHz-based design in the 0.18 μm CMOS process, Dirini et al. described the "RF to DC voltage multiplier rectifier circuit" for harvesting the power required for it to work (Figure 48). Power-harvesting (Figure 48) and communication circuits (Figure 49) were made using "a three stage dual output full wave voltage multiplier rectifier followed by a voltage limiter" and "current starved ring oscillator", respectively. Using these circuits and the current-starved inverter in the demodulator (Figure 51), power consumption was minimized and the maximum part was kept for biosensor operation. Other than these, the authors also described the envelope detector circuit to monitor the gap in the received RF signal (Figure 50). The HSPICE simulation results also indicated the power consumption was less than 12% (6.5 μW) by design. Furthermore, a 1.4 V differential high supply voltage swing for biosensor operation was achieved using the full wave topology for the rectifier.[75]

In another study of low-voltage systems, powered by an RF link, for implantable devices to monitor physiological systems, Crepaldi et al. described the linear voltage regulator (LVR) circuit (Figure 52) along with the voltage reference circuit (Figure 53), sampler circuit (Figure 54), and others using 0.35 μm CMOS technology from the Taiwan Semiconductor Manufacturing Co. (TSMC). In their design, use of a "source follower stage" provided stability to the LVR system and use of a "cross gate rectifier structure" resulted in suppression of the threshold voltage drop for switching transistors.[76]

For closed-loop glucose monitoring via an implantable biosensing system, Paglinawa et al. described 2P4M 0.35 μm CMOS (3.3/5 V) from a TSMC-based system comprising a "wide-current-range potentiostat" (Figure 55a) and an

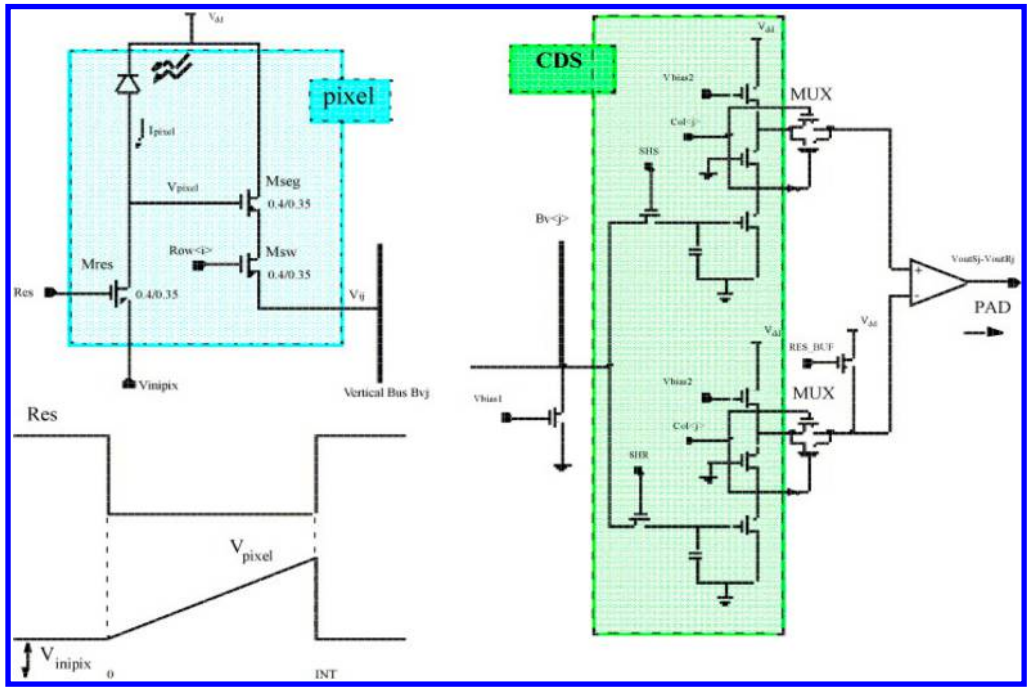

Figure 40. (a) Circuit schematic for the APS of row *i* and column *j*. (b) Transient of voltage V_{pixel} while the photocurrent is being integrated during the INT interval. (c) CDS circuit schematic of the *j* column, MUX, and buffers. The voltage vector $V_j = V_{outSj} - V_{outRj}$ is obtained. Reprinted with permission from ref 72. Copyright 2006 Elsevier.

DOI: 10.1021/cr500554n
Chem. Rev. XXXX, XXX, XXX−XXX

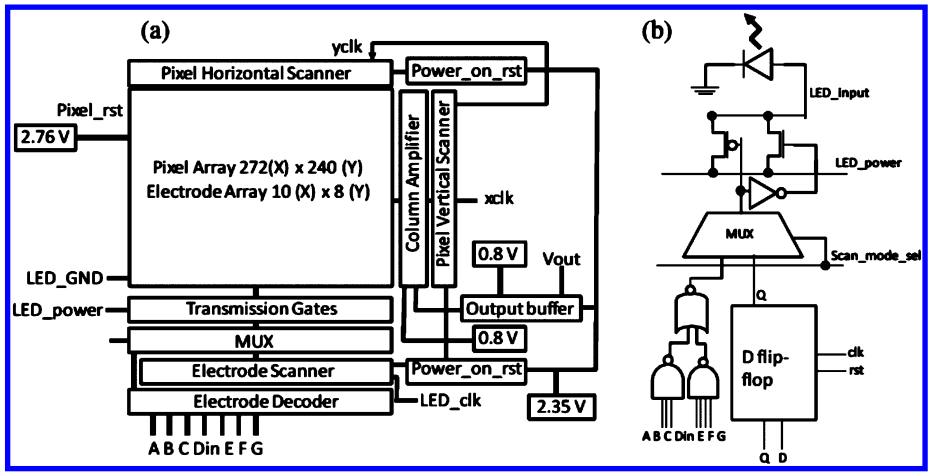

Figure 41. (a) Chip diagram of the four-wire image sensor and (b) LED selection and driver circuits. Reprinted with permission from ref 49. Copyright 2012 Optical Society of America.

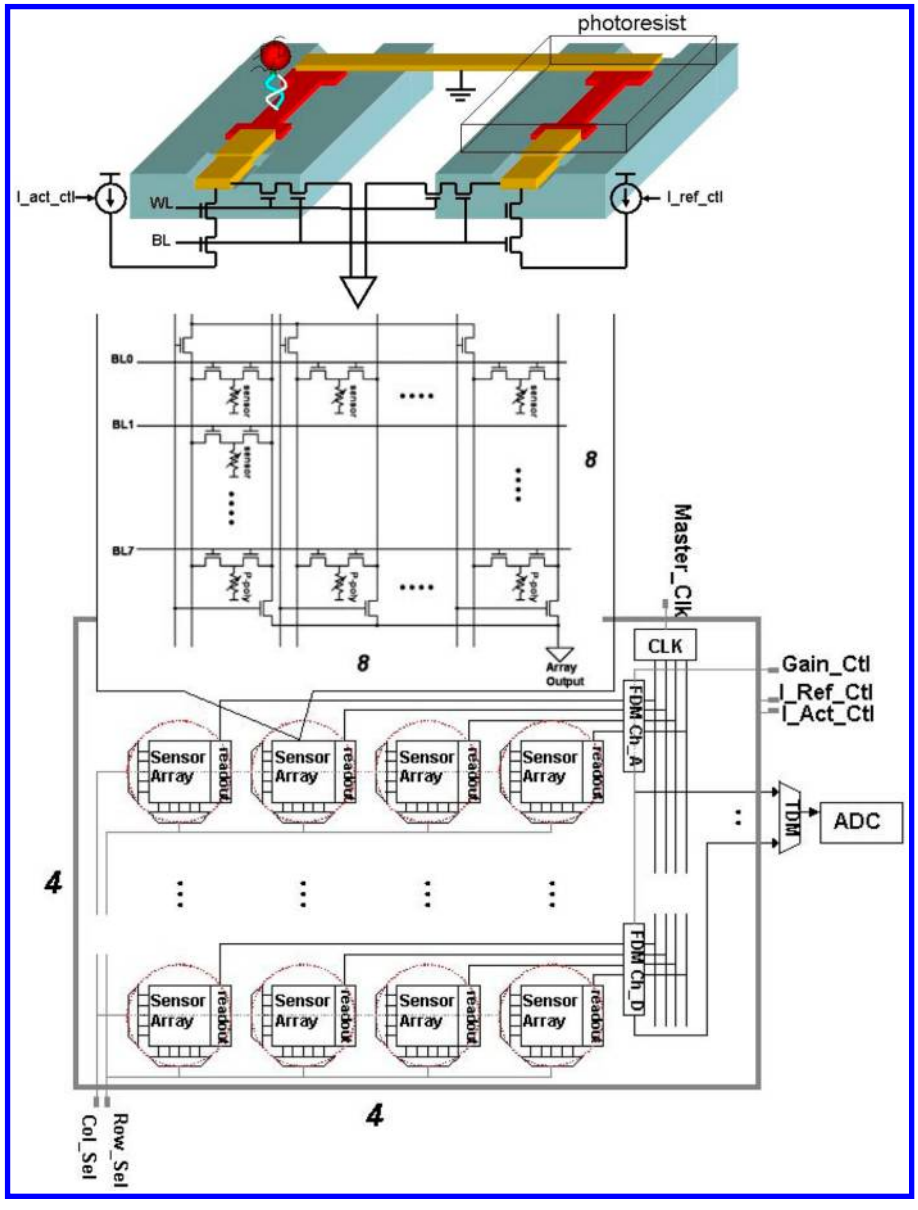

Figure 42. Magnetoresistive biosensor array chip architecture. Reprinted with permission from ref 23. Copyright 2006 IEEE.

DOI: 10.1021/cr500554n
Chem. Rev. XXXX, XXX, XXX−XXX

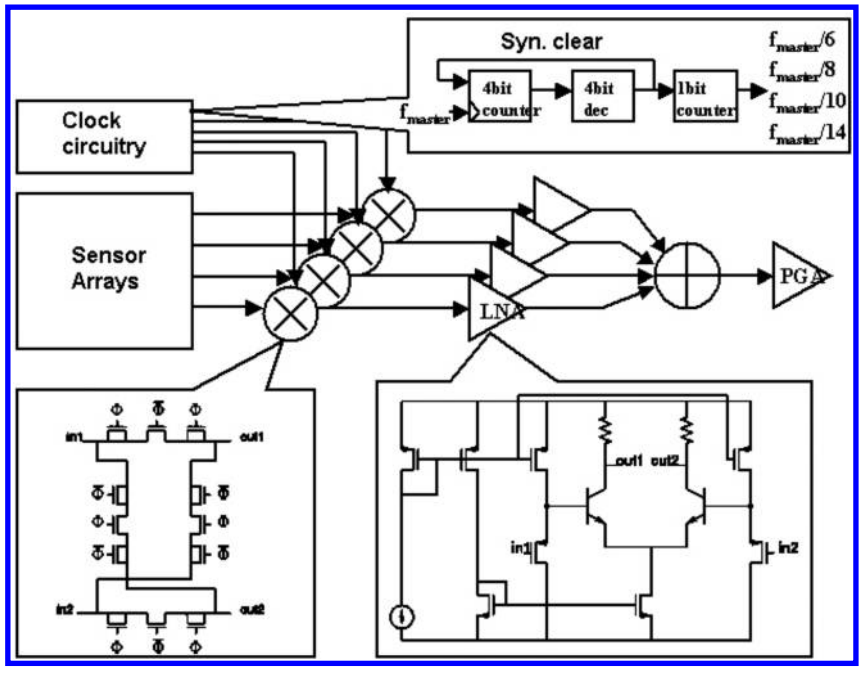

Figure 43. Schematic drawing of the readout channels, with an expanded view of the mixer and low-noise amplifier. Reprinted with permission from ref 23. Copyright 2006 IEEE.

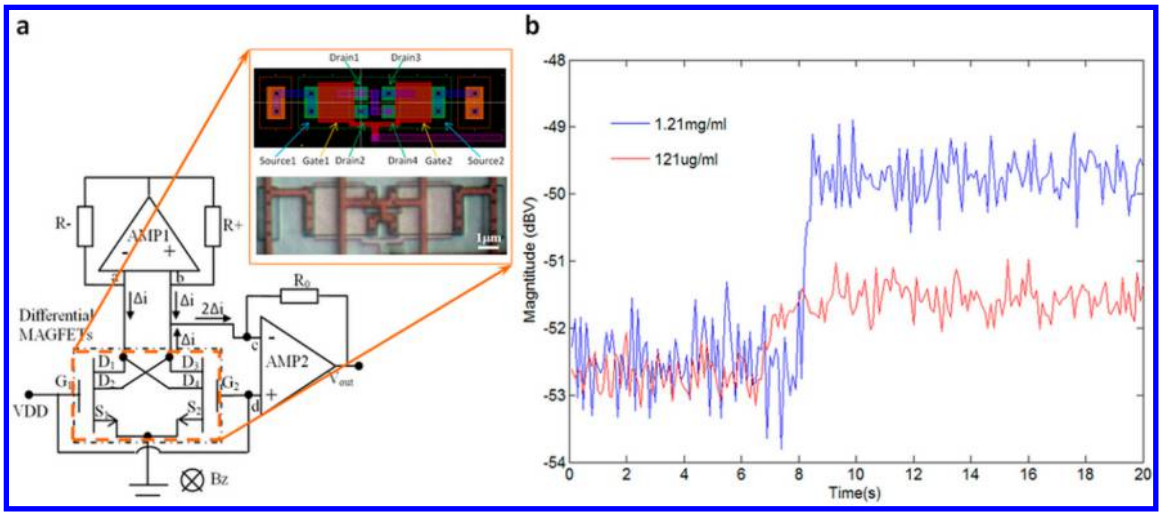

Figure 44. Detection of magnetic nanoparticles in water with a packaged CMOS MAGFET/microfluidic hybrid microsystem. (a) CMOS MAGFET readout circuit. The inset shows the design layout and optical micrograph of the MAGFET. Scale bar 1 mm. (b) Detection of magnetite nanoparticles in water using the packaged CMOS/microfluidic hybrid microsystem. Reprinted with permission from ref 35. Copyright 2013 Nature Group.

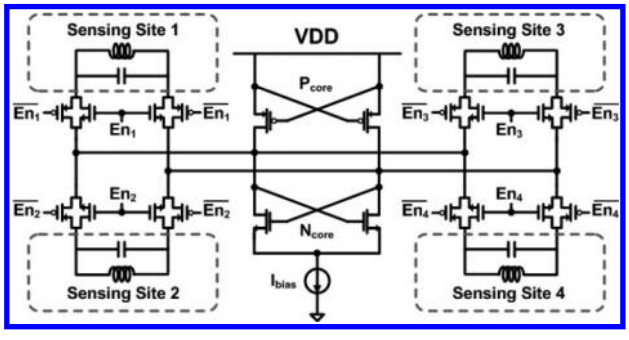

Figure 45. Quad-core sensor schematic. Reprinted with permission from ref 73. Copyright 2010 IEEE.

"integrated core circuit of drug driver for drug administration" (Figure 55b). Addition of a low-input impedance circuit in the potentiostat circuit design resulted in improvement of the current-sensing range and stability. On detecting the excess glucose level via a readout sensor, the drug driver circuit transmitted a signal to deliver the drug and set the programmer timer to control the drug delivery driver and oscillator activities. The proposed system was found to be operational in the "50 pA to 50 μA current range with a power usage of 390 to 745 μW".[77]

5. ADVANCES IN CMOS-BASED BIOSENSORS

To expand the scope and utility of biosensors, various circuits and designs based on the CMOS process have been described in the literature and have shown great promise for the future.

DOI: 10.1021/cr500554n
Chem. Rev. XXXX, XXX, XXX−XXX

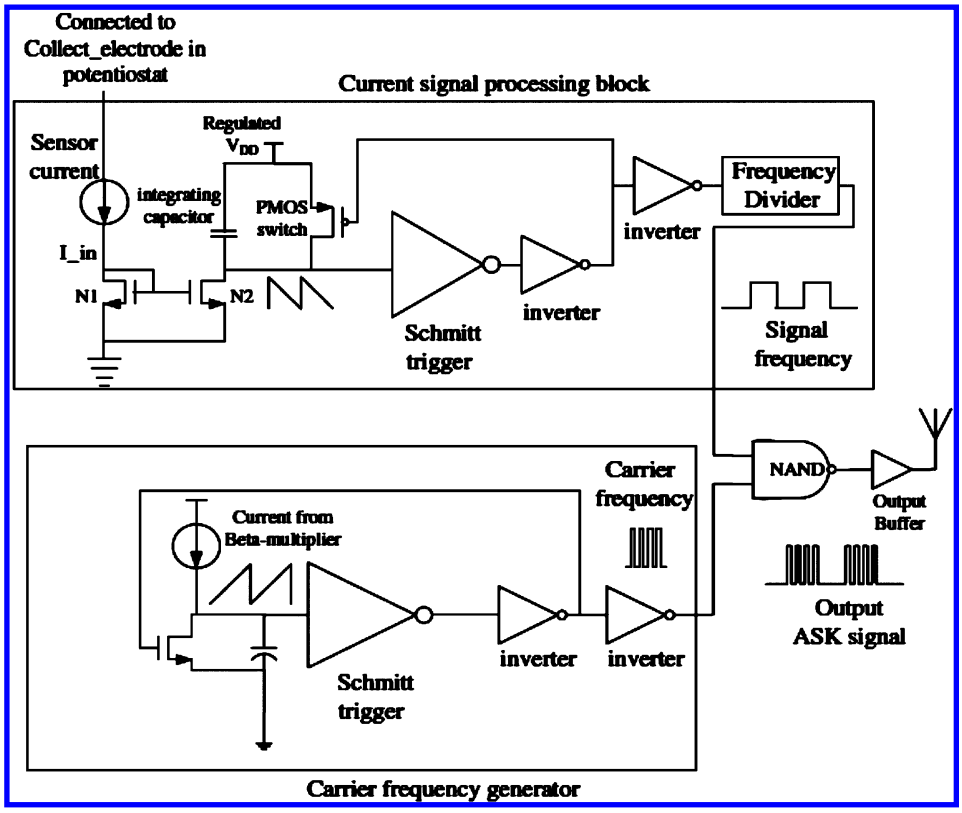

Figure 46. Block diagram for the signal processing circuit. Reprinted with permission from ref 52. Copyright 2007 IOPscience.

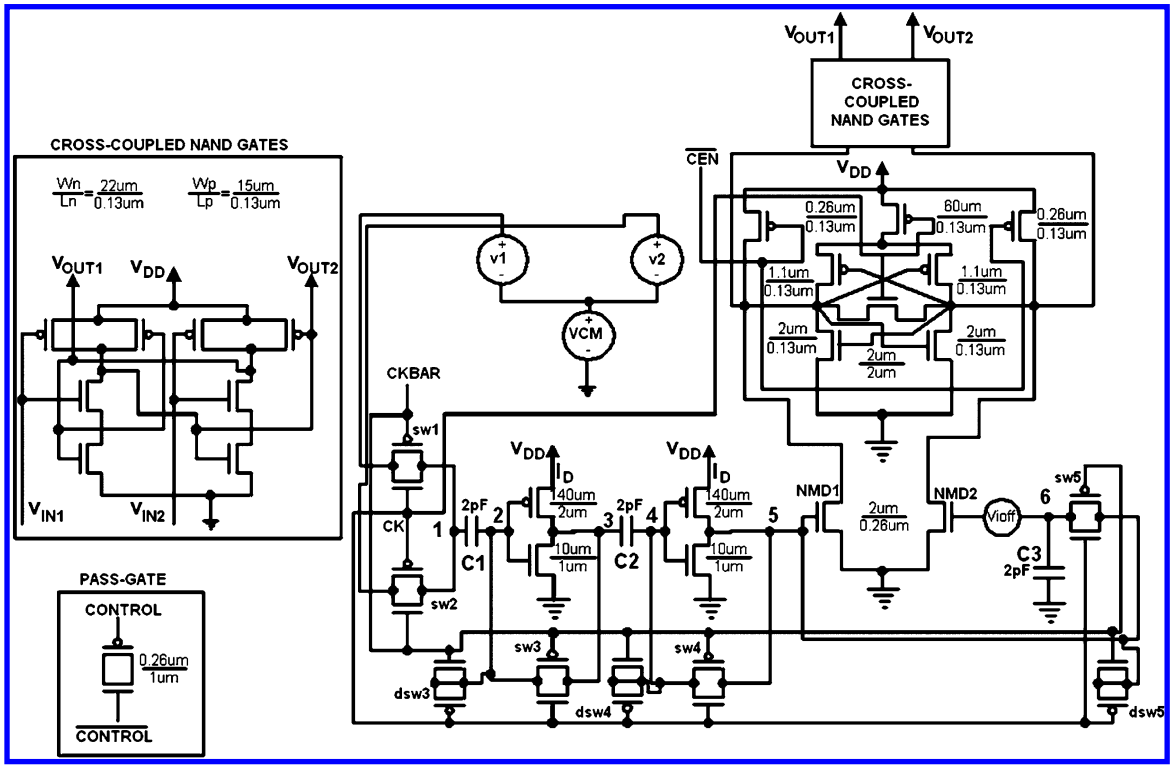

Figure 47. Complete CMOS circuit diagram of the proposed sampled data offset-compensated low-voltage comparator. Reprinted with permission from ref 74. Copyright 2008 Springer.

Commonly, in CMOS-based biosensors, the top layer of the CMOS chip is utilized as the matrix required for sensing measurements. In such a design with integrated detectors, each pixel may have an embedded transducer and readout circuit.[1a] Recently, different CMOS integrated biosensors with transduction based on capacitance, impedance, amperometry, voltammetry, FET/potentiometry, stress, etc. have been

DOI: 10.1021/cr500554n
Chem. Rev. XXXX, XXX, XXX−XXX

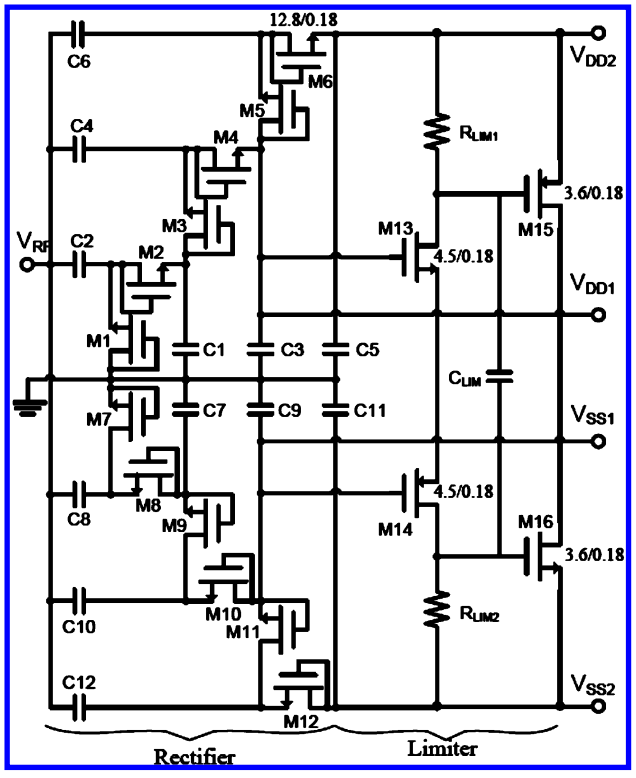

Figure 48. Power-harvesting circuitry (M1−M12 are identical; body connection in all transistors is not shown for simplicity). Reprinted with permission from ref 75. Copyright 2011 IEEE.

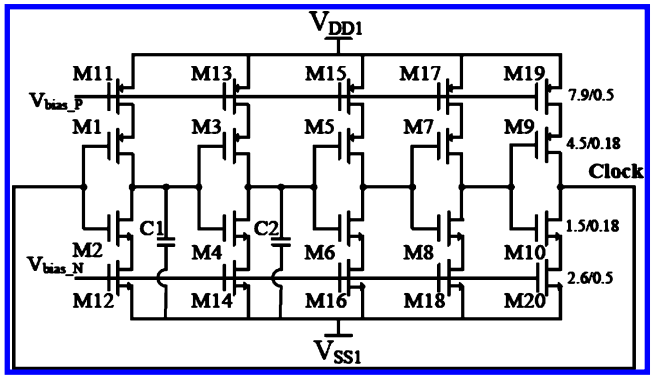

Figure 49. Current-starved ring oscillator (all stages are identical). Reprinted with permission from ref 75. Copyright 2011 IEEE.

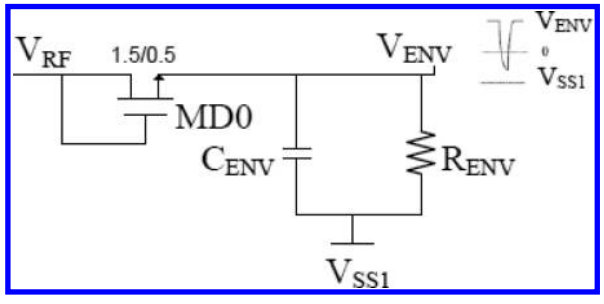

Figure 50. Envelope detector circuit showing the V_{ENV} waveform. Reprinted with permission from ref 75. Copyright 2011 IEEE.

reported.[6a,16,78] The following sections will analyze various transducer-based CMOS biosensors described in the literature.

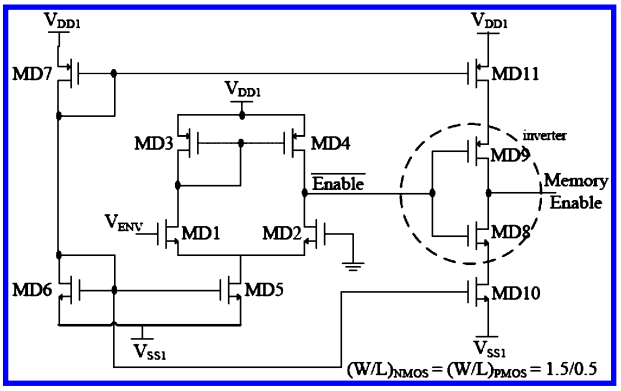

Figure 51. Design of the current-starved inverter and comparator used in the communication circuitry (identical for both blocks). Transistors MD1−MD5 form the comparator, while transistors MD8 and MD9 form the inverter. MD6 and MD7 are diode-connected transistors that maintain a constant current and use it to control the current in the inverter using the current-limiting transistors MD10 and MD11. Reprinted with permission from ref 75. Copyright 2011 IEEE.

5.1. Voltammetry-Based Biosensors

Using an IDT electrode array with an integrated bipotentiostat, Huang et al. described the fabrication of a redox enzyme modified 0.5 μm CMOS-based fructose biosensor. Redox recycling during cyclic voltammetry (CV) measurements for a fructose concentration of 200 mM resulted in enhancement of the electrochemically magnified current by 27%. CMOS-bipotentiostat-based chronoamperometry results for fructose measurement in the 50−400 mM concentration range were found to be similar to the results obtained using a commercial bipotentiostat.[53] Schienle et al. showed that in an extended 6 n-well 0.5 μm CMOS-based DNA detection chip with 128 electrodes and a digital readout system, output signals provide a robust data transmission within the array. The sensor circuit detects via an electrochemical redox cycling process and allows sampling of data from all sites simultaneously. The results exhibited a dynamic range spread over five decades with a homogeneous sensor array response.[12c] Yang et al. described the development of a 0.5 μm CMOS-based electrochemical biosensor array, with an on-chip potentiostat. The linear relationship observed in the CV response and analyte concentrations verified the system functionality. For a secondary alcohol dehydrogenase enzyme modified electrode, the results revealed good linearity between the observed current and 2-propanol concentrations (Figure 56).[41]

For multiplexed sensing, Levine et al. described a 0.25 μm CMOS-technology-based 4 × 4 electrochemical sensor array. CV measurement results verified the utility of the sensor array for biodiagnostic applications. Furthermore, DNA hybridization detection in real time was achieved using "ferrocene-conjugated DNA targets".[11,79] In another study, Krupa et al. described a 0.35 μm CMOS-technology-based fully integrated system on-chip DNA sensor using chronocoulometric measurement (Figure 57). In automatic working mode, recording of electrochemical signals for DNA detection on all 384 sensors was achieved in multiple milliseconds.[55]

5.2. Potentiometric/ISFET-Based Biosensors

Using the 1.2 μm 2P2M CMOS process, Anan et al. described a "redox-potential sensors array using extended-gate FET's" (32 × 32). High sensitivity for each extended-gate electrode was achieved via use of an 11-ferrocenylundecane-1-thiol (11-FUT)

DOI: 10.1021/cr500554n
Chem. Rev. XXXX, XXX, XXX−XXX

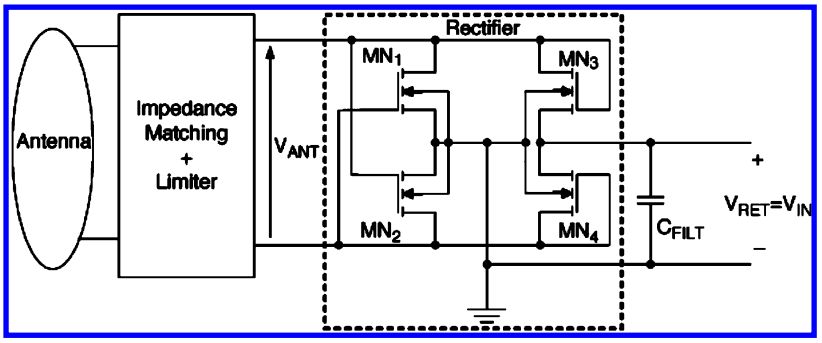

Figure 52. LVR front-end interface. Reprinted with permission from ref 76. Copyright 2012 IEEE.

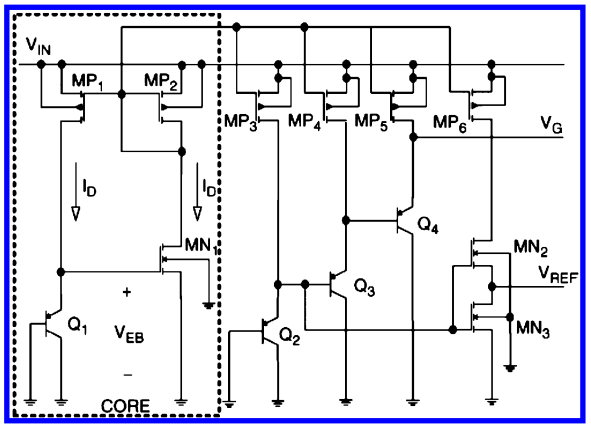

Figure 53. Proposed voltage reference circuit. Reprinted with permission from ref 76. Copyright 2012 IEEE.

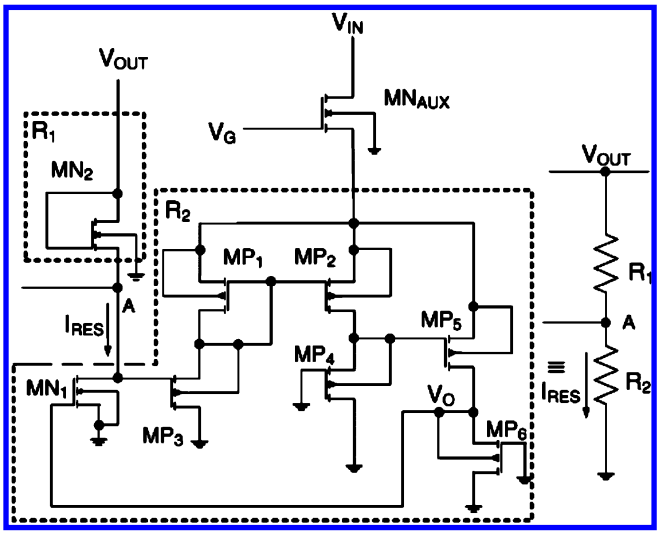

Figure 54. Sampler circuit. Reprinted with permission from ref 76. Copyright 2012 IEEE.

modified gold electrode and source-drain follower circuit. For glucose estimation via enzyme-catalyzed redox reaction (Figure 58), their sensor exhibited a sensitivity of −59.5 mV/decade in the 0.1−2 mM range, and it successfully detected glucose from 100.1 to 264.3 mg/dL in human serum samples.[80] Using the 0.35 μm CMOS technology, Chang et al. described an OGFET-based system for ion concentrations, electrophysiological signals, and desired target biomolecule detection. In their design, the active region of the transistors was defined reliably via an exposed gate obtained from stacks of sacrificial metal layers.[81] In another study, Debusschere et al. described the CMOS-based "cell-cartridge with integrated microcontroller based electronics system" for monitoring of "action potential (AP) activity within the cell-cartridges". The results of cardiomyocyte syncytia studies revealed different AP activities toward control medium flow and biochemical agent flow.[12b]

Maruyama et al. demonstrated the fabrication of a charge-transfer-technique-based label-free and fully electronic 32 × 32 DNA image sensor using the 1P1M CMOS technology (Figure 59). The improved sensitivity and SNR were achieved by using charge accumulation via a repeating charge transfer procedure. For 22 base long DNA molecules, the study reveals 76.4 ± 16.5 mV of output voltages after immobilization and 64.5 ± 15.7 mV after hybridization with an LOD of 2.7×10^7 cm^{-2} molecules.[82] Barbaro et al. reported a 0.8 μm CMOS-process-based integrated field-effect device with each sensor consisting of a "floating-gate MOS transistor, counter electrode (control-capacitor), and exposed site for DNA binding". Hybridization was monitored via recording teh drain-current change for the transistor caused by the electric charge of the hybridizing DNA molecules.[83]

Using the 0.35 μm, 2P4M CMOS technology, Xue et al. described the development of a potentiometric immunosensor for simultaneous detection of hemoglobin and HbA1c using a "micro extended gate electrode array chip" and integrated FET sensor. Studies revealed the highest sensitivity for the sensor fabricated by immobilizing antibodies on nanogold wrapped with mixed SAMs.[84] In another study, Lee et al. reported a 0.35 μm CMOS-technology-based label-free DNA biosensor that utilizes the method of direct charge accumulation to estimate the surface potential on oligonucleotide modified electrodes. The use of a differential architecture with the oversampling effect of charge accumulation resulted in improved SNR. For H5N1 avian influenza virus, the sensor exhibited high specificity with an LOD of 100 pM.[85] For on-chip cell culture monitoring, Welch et al. described the fabrication of a 0.5 μm, 2P3M CMOS-process-based chip and its integration with microfluidics using a Pyralux-based flexible PCB. The chip utilizes an ISFET and its readout circuit to monitor the pH of the solution, while the impedance change of the IDT electrodes in the top metal layer was used for cellular attachment and proliferation monitoring.[86]

Pancrazio et al. described a CMOS-based microelectrode array (MEA) device consisting of "16 instrumentation amplifiers with a gain of 50" for extracellular recording. Platinum black coating on electrodes was employed to lower the electrical insulation and microelectrode impedance. Furthermore, the extracellular microelectrode was used either as a stimulator or a sensor via use of a cross-point array. For "rat

DOI: 10.1021/cr500554n
Chem. Rev. XXXX, XXX, XXX−XXX

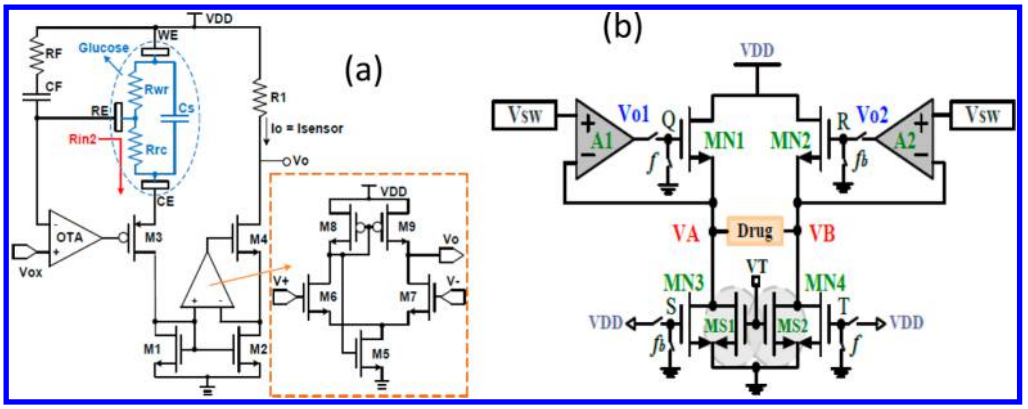

Figure 55. (a) Readout-2 (proposed wide-current-range potentiostat). (b) Core circuit of the drug driver. Reprinted with permission from ref 77. Copyright 2011 Taiwanese Society of Biomedical Engineering.

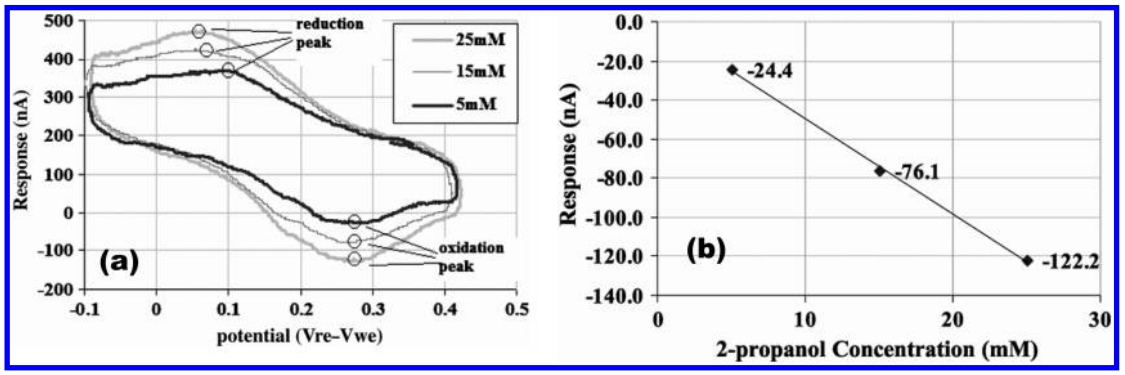

Figure 56. (a) CV plot of the MPA-TBO-PEI-NADP$^+$-2°-ADH-functionalized electrode in the presence of different concentrations of 2-propanol. (b) Measured peak electrocatalytic current at various 2-propanol concentrations. Reprinted with permission from ref 41. Copyright 2009 IEEE.

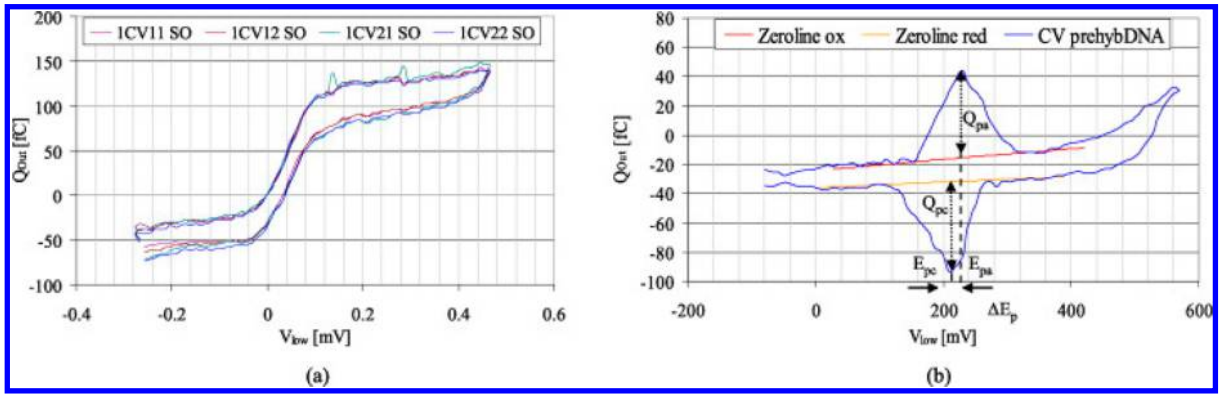

Figure 57. CV plot: (a) four cleaned Au WEs with no probes immobilized, immersed in buffer solution with 10 μM ferrocene; (b) one immobilized WE (probe with prehybridized ferrocene-labeled oligonucleotides) immersed in buffer solution without target DNA. Reprinted with permission from ref 55. Copyright 2008 Elsevier.

spinal cord neurons and chick cardiac myocytes", extracellular recordings via their system resulted in peak-to-peak biopotentials of 100−400 and 0.9−2.1 mV magnitude, respectively. However, the system was found to require a high voltage of 62.5 V with 105 mW of power consumption. Thus, a more power efficient system is required for realistic biosensor application.[87] In another report on extracellular bidirectional communication with electrogenic cells, Frey et al. described a 0.6 μm 2P3M CMOS-process-based MEA. The array comprises "11,011 metal electrodes with separate recording and stimulation electronics for each electrode" (Figure 60). The greater flexibility in electrode selection and implementation of a low-noise amplifier outside the array was achieved by use of a reconfigurable switch matrix.[88] In another such study, Hafizovic et al. described a CMOS-based monolithic microsystem featuring a 128 Pt MEA chip. In their study the biocompatibility of the sensor chip and its package along with its ability to measure signals after a longer period of culturing was verified via results obtained from signals recorded after 3 days from in vitro primary neonatal rat cardiomyocytes and after 56 days from in vitro neuronal cultures (Figure 61).[89]

5.3. Amperometric Biosensors

Cheng et al. presented a 0.35 μm 2P4M CMOS-based DNA detection biochip with an integrated circuit for current amplification and heating. For the working electrodes, they

DOI: 10.1021/cr500554n
Chem. Rev. XXXX, XXX, XXX−XXX

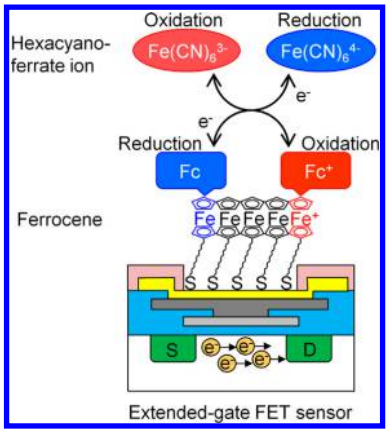

Figure 58. Redox reaction between hexacyanoferrate ions and ferrocene molecules immobilized on the gold electrode of an extended-gate FET sensor. Reprinted with permission from ref 80. Copyright 2013 Elsevier.

utilized electrodes with a nanogap of 350 nm and achieved around 10^3-fold enhancement in the current signal with the gold nanoparticle (AuNP) multilayer strategy (Figure 62). With multilayer AuNPs, the current signal was amplified to the milliampere level using cascode current mirrors so that it can easily be read by a commercial volt−ohm−milliammeter. The results revealed the ability of the sensor to distinguish the signals even from a single mutation with the lowest detectable concentration of 0.1 nM for target DNA.[90] In another study, Kim et al. described an electrochemical biosensor array in CMOS design with an in-built potentiostat to study neurotransmitter release via on-chip amperometric measurement. To reduce the readout time, they utilized an output time division multiplexing approach. The system was found to work very well even after 3 days of on-chip cell culture in an incubator and recorded the amperometric signal for all 100 electrodes simultaneously. The results indicated current resolution in the picoampere range with very short time resolution (500 μs), and the system was found to possess a sensitivity of ~6000 molecules when applied to the study of secretion events from chromaffin cells.[91]

Hayasaka et al. reported an 0.18 μm CMOS-based 20 × 20 amperometric biosensor array consisting of BDD microelectrodes. The wide potential window of the BDD electrode on a fully integrated device allowed the detection of histamine and dopamine, and allowed a 2-D image to be taken in real time for diffusion of histamine in solution.[28] In another study, Rothe et al. described the biological cell's metabolic activity monitoring using a 0.35 μm, 2P4M CMOS-based chip with 1024 Pt working electrodes. They utilized the device for fabrication of the glucose biosensor, and the results revealed an LOD of 1.1 μM with a 2.1 pA/μM sensitivity (Figure 63).[36]

5.4. Impedimetric Biosensors

For estimation of creatinine using a molecularly imprinted polymer-coated ISFET sensor, Tsai et al. designed a CMOS-BioMEMS-based platform. The experimental results on such a platform with an integrated readout circuit showed good reliability and indicated that the electrode gap influences the sensor response more than its length, with the sensor being found to have a shorter time response for a reduced gap between electrodes.[37] Manickam et al. presented a CMOS-based fully integrated 10 × 10 EIS biosensor array for DNA detection in real time and without labeling via EIS measurement. The device worked reliably over a wide frequency range and was able to measure impedance within 5 orders of magnitude.[21a,22] Chai et al. designed a CMOS chip in MEA format for impedance measurement of an on-chip cultured cell layer.[16] To stimulate and record the activity simultaneously from electrogenic cells, Heer et al. reported a 2P3M, 0.6 μm CMOS-process-based MEA. The results of the study indicated multiplex capability and improved SNR via use of an on-chip signal filter and ADC. The system was verified by recording signals from electrogenic cells from embryonic chicken cardiomyocytes (Figure 64).[2] In an other study, Ma et al. described a 0.35 μm CMOS-technology-based 16312 sensor array for DNA detection in solution via impedance recording. For measurement, they utilized the fringing field capacitance effect for planar electrodes in solution and found good correlation with target DNA concentrations. Furthermore, it was found that the device can identify the size of the DNA fragments in the polymerase chain reaction (PCR) product (Figure 65). Most importantly, the chip was found reusable, with no denaturation of the analyzed biological samples.[92]

In our group, a label-free EIS-based 96 × 96 MEA was designed using 0.18 μm CMOS technology and utilized for MCF-7 (breast cancer) cell counting and testing (Figure 66). The results revealed that the presence of a cell on the elelctrode causes an average increase of 20% in EIS signal at around 200 kHz (Figure 67). Furthermore, cells were mapped with over 90% accuracy and with single-cell resolution.[19,30]

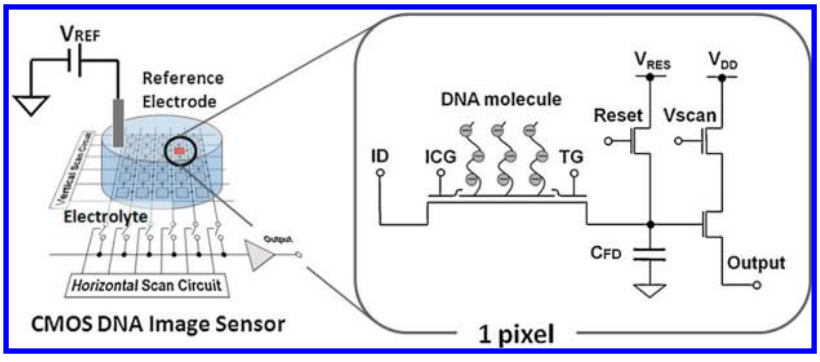

Figure 59. Concept of the CMOS DNA image sensor. The system consists of an electrolyte, a reference electrode, and a sensor. The surface potential changes induced by DNA molecules are detected as a two-dimensional image. Reprinted with permission from ref 82. Copyright 2009 Elsevier.

DOI: 10.1021/cr500554n
Chem. Rev. XXXX, XXX, XXX−XXX

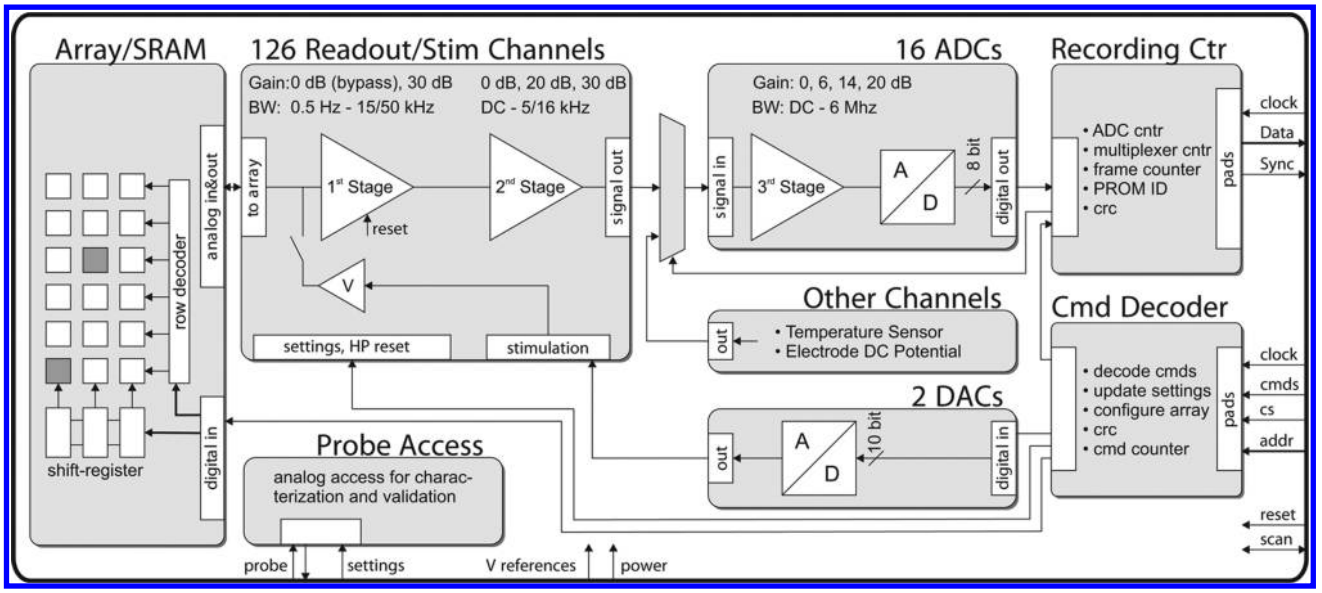

Figure 60. Block diagram of the chip architecture and the on-chip electronics. Reprinted with permission from ref 88. Copyright 2010 IEEE.

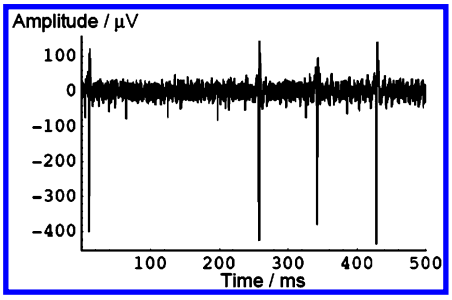

Figure 61. Action potential recorded from a spontaneously firing neuronal culture after 56 days in vitro. Reprinted with permission from ref 89. Copyright 2006 IEEE.

5.5. Capacitive Biosensors

Lu et al. presented a 2P4M 0.35 μm CMOS-based 5 × 5 array for development of a highly sensitive sensor for dopamine detection via capacitive measurement. For sensor development, they used a third Al layer as the electrode and intermetal SiO_2 on it for binding of biomolecules. The capacitance variation recorded in the form of an output frequency resulted by immobilization of 4-carboxyphenylboronic acid, and capture of DA molecules was measured via a designed readout circuit in the CMOS (Figure 68). The change in capacitance for DA is found to be higher than for the controls even at 0.1 fM and to be selective against tyramine.[66] Stagni et al. demonstrated 6 n-well 0.5 μm CMOS-technology-based microfabricated capacitors in chip for two-electrode capacitive measurements for DNA sensing. The results for DNA hybridization of the target revealed a significant change in capacitance.[17a,58] Lee et al. described a 0.35 μm 2P4M CMOS-process-based DNA biosensor which measures charge-transfer resistance and capacitance variation produced by the hybridization event. To attain high sensitivity with a stable response and no external variable influence, they utilized a triangular wave voltage input-based impedance extraction approach. The results for 1 μM target DNA indicated 31.5% and 68.6% changes in capacitance and resistance, respectively.[10] In another study, the authors

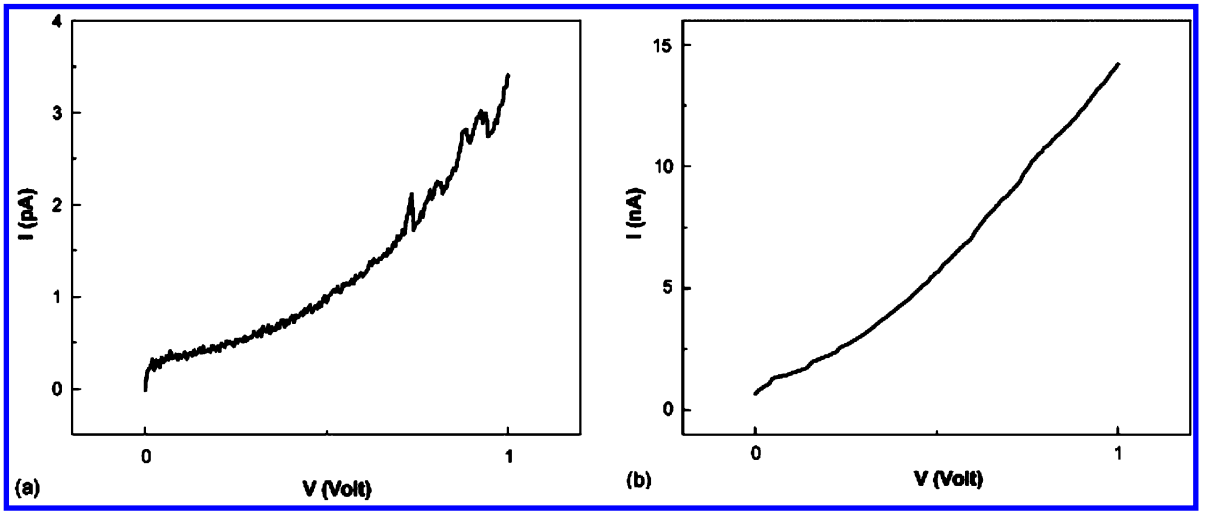

Figure 62. *I*–*V* characteristic curves of self-assembly-layered AuNPs over a 350 nm nanogap without current amplification at a target DNA concentration of 10 nM: (a) monolayer and (b) multilayer. Reprinted with permission from ref 90. Copyright 2007 Elsevier.

DOI: 10.1021/cr500554n
Chem. Rev. XXXX, XXX, XXX–XXX

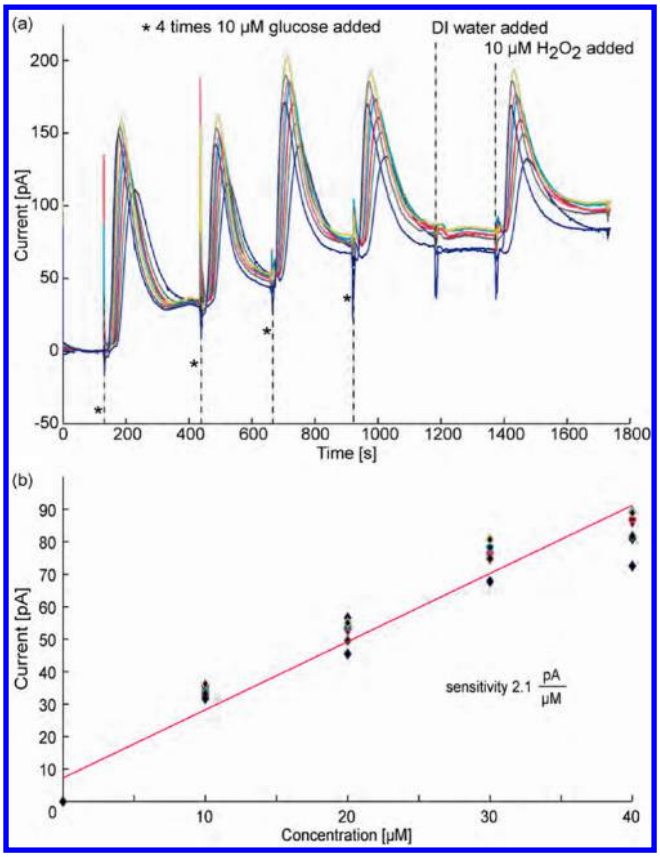

Figure 63. (a) Glucose calibration measurement of eight channels. (b) Sensitivity curve. Reprinted with permission from ref 36. Copyright 2012 IEEE.

described a DNA biosensor with a working range of 5 nM to 1 μM and an LOD of 5 nM. Also for 1 μM target DNA, the biosensor showed a 22.38% change in capacitance.[93]

Yusof et al. described a 1.2 μm, 2P2M CMOS-technology-based DNA biosensor. Designed circuits for "differential capacitance-to-voltage conversion" and C_{dl} measurement were used for DNA detection. The hybridization event resulted in a 20% capacitance change during impedance measurement.[17c] In another study, a 2P4M 0.35 μm CMOS-based sensor for capacitance change measurement was presented by Lai et al. for detection of avian influenza virus (AIV) via nonfaradic impedance measurement. The results showed that monolithic sensor integration resulted in lowering of the parasitic capacitance effect while improving the SNR. Furthermore, the signal coupling efficiency was found to be better by use of submicrometer microelectrodes with an IDT design. The results revealed a $-13.2 \pm 2.1\%$ lowering of capacitance for hybridization of target DNA in the 1−10 fM concentration range.[94] Using the 0.35 μm CMOS BioMEMS process, Yang et al. proposed a capacitive-type (IDT electrodes with a sensitive gold layer in the gaps) glucose biosensor. The system contains an in-built oscillator circuit to convert the capacitance change to a frequency response. The experimental results measuring the variation in the capacitance with the glucose level during its absorption revealed a sensitivity of 1.48 MHz/mM (Figure 69).[67]

To characterize the cell adhesion strength and cell health, Prakash et al. described a 0.5 μm, 2P3M CMOS-process-based capacitive sensor using the charge-sharing principle to investigate the interaction between living cells and the substrate (Figure 70). The system worked reliably for in vitro cell viability monitoring over the long term and was found to exhibit a resolution of 135 aF for capacitance measurement and 3 nm for the empirical distance.[95]

Chang et al. described a CMOS-process-based capacitive sensing array with in-built 8 × 8 microcoils with IDT electrodes in the center of every coil (Figure 71). On-chip magnetic actuation was utilized for moving magnetic microbeads to the sensing area, and by using capacitance-to-frequency readout, detection of streptavidin-coated microbead with single bead resolution was achieved (Figure 72). The results indicated −5.3 and −0.2 fF changes in capacitance for the target and control samples.[5]

5.6. Piezoresistive-Stress-Based Biosensors

Lechuga et al. developed a 20-micromechanical-cantilever-array-based microsystem with a signal-conditioning and acquisition circuit in a CMOS. To convert power into current, they utilized a p-diff−n-well photodiode configuration and isolated the maximum possible photocurrent in each pixel. The system showed a sensitive DNA capture event via recording cantilever deflection with resolution in the subnanometer range.[72] In another study using the 0.35 μm 2P4M CMOS process, Huang et al. described a piezoresistive-type-micro-cantilever-based SoC for HBV DNA detection in real time without labeling. The experimental results showed DNA detection in the 1 pM to 10 nM range and an LOD of 1 pM with a distinguishable signal for complementary, noncomplementary, and single-mismatch sequences (Figure 73).[71]

Using the 2P4M CMOS technology (Figure 74), Yang et al. described a microsensor with a bridge-microcantilever design. Improvement in sensitivity and isolation of the thermal effect were achieved by using a transmitter to connect a biomodified cantilever to the sensing cantilever. Such a configuration resulted in localization of biaxial surface strain limited to the

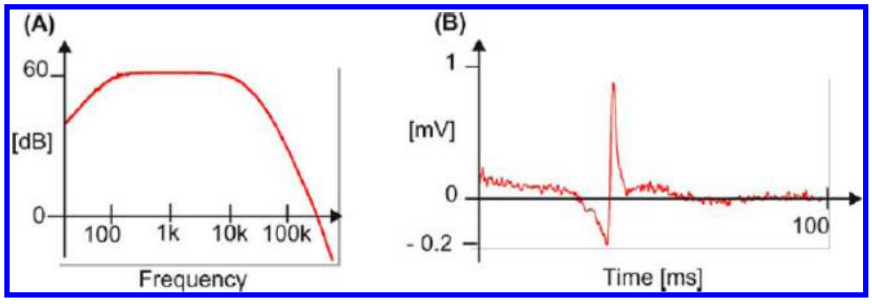

Figure 64. (A) Transfer function of the bandpass filter. (B) Typical spike from embryonic chicken cardiomyocytes where high frequencies were cut off at 3 kHz. Reprinted with permission from ref 2. Copyright 2004 Elsevier.

DOI: 10.1021/cr500554n
Chem. Rev. XXXX, XXX, XXX−XXX

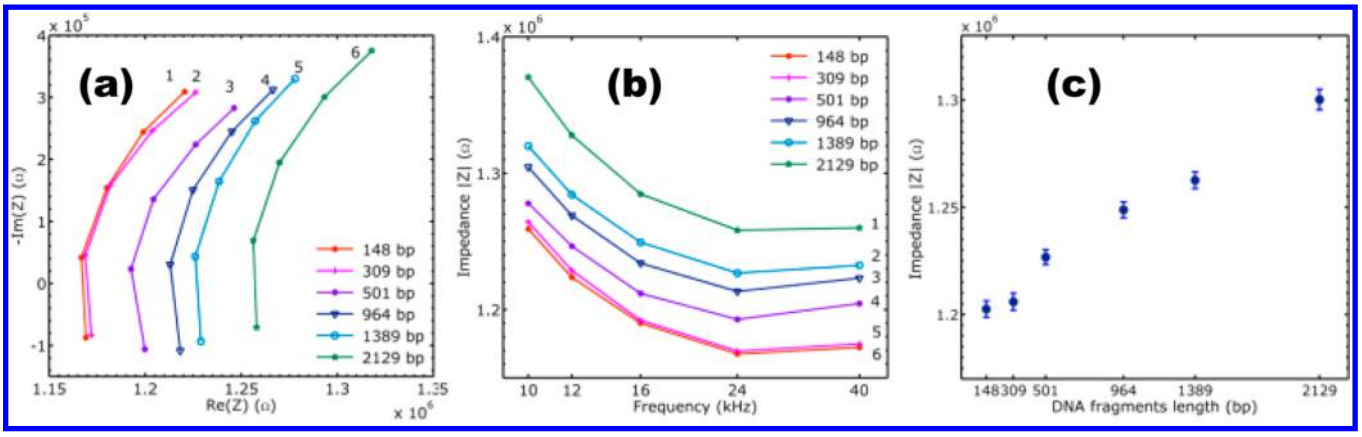

Figure 65. Impedance measurements for PCR products: (a) Cole−Cole plot showing that the impedance of each sample was dependent on the fragment length. (b) Sample impedance versus the stimulus frequency. (c) Measured impedance versus DNA length in base pairs at 10 kHz. Reprinted with permission from ref 92. Copyright 2013 Nature Group.

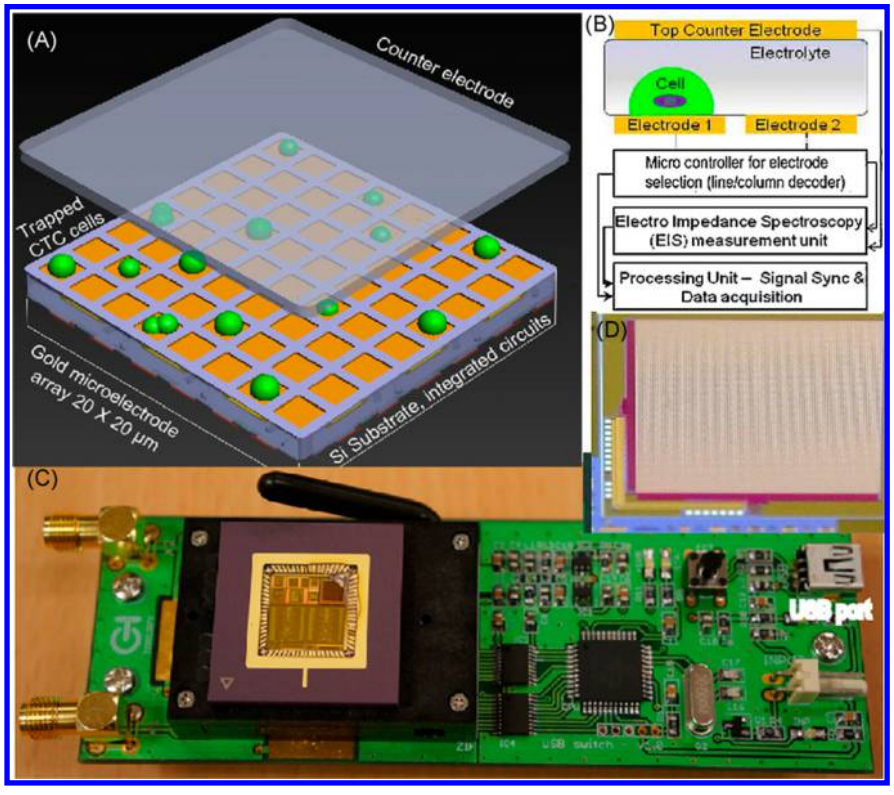

Figure 66. CMOS-based sensor array for cell counting. (A) Schematic of the microelectrode arrays for cell detection. (B) Illustration of the sensor layout and the addressing scheme employed in the CMOS sensor chip. (C) CMOS chip packaged with a switching PCB. (D) Microphotograph of more than 9000 electrodes in a single chip. Reprinted with permission from ref 30. Copyright 2012 Elsevier.

bound cantilever and helped in keeping the piezoresistive stress of the detecting cantilever as uniaxial for improved in situ sensing. Furthermore, such a configuration allowed constant batch fabrication with an on-chip circuit for signal processing.[96] In other studies, they described the development of micro-cantilever-based DNA sensors in CMOS design.[13,57] Furthermore, in their study of resistivity changes in the piezoresistor during the DNA binding event, the response time of the microcantilever was found to be less than 1 s with an equilibrium time of a few minutes. For a self-sensing CMOS biosensor system, the results revealed an LOD of around 1 μM with surface stress sensitivity of 3.5×10^{-5} m/N.[12a]

5.7. Optical Biosensors

For investigating selected retinal ganglion cell (RGC) populations to understand the principal behind the retinal circuit process in encoding visual scenes, Fiscella et al. utilized a CMOS-based array of 11 011 Pt microelectrodes (7 μm diameter) and performed stimulation and detection. Provoking the response and recording synchronous AP from various types of RGCs during light stimulation were achieved by use of switch matrix circuitry built under the electrode array with the dynamically configurable microelectronics of their system. Their system allowed stimulation and recording simultaneously from multiple and overlapping RGCs without any light-induced artifacts. For every RGC, activity was recorded on 14 ± 7

DOI: 10.1021/cr500554n
Chem. Rev. XXXX, XXX, XXX−XXX

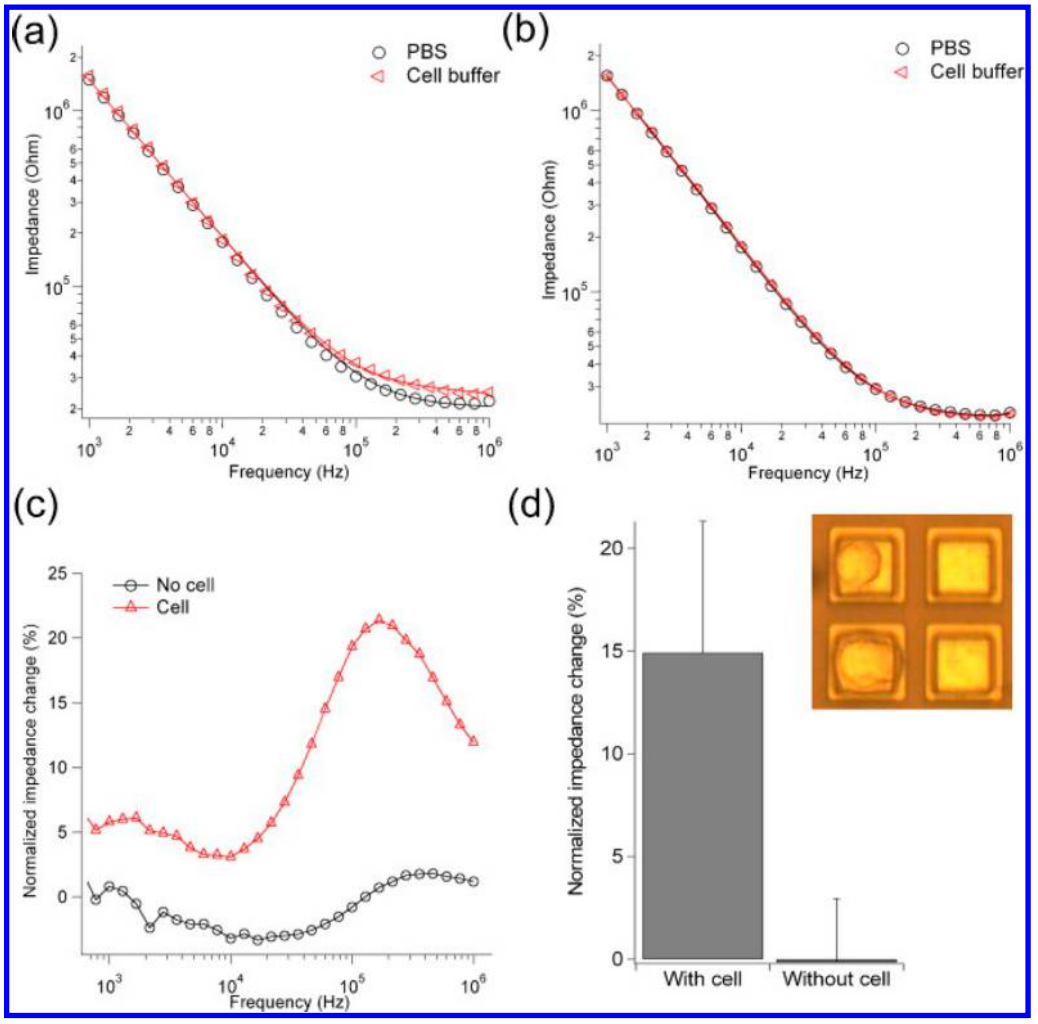

Figure 67. Impedance spectroscopy of the electrode (a) with the cell attached in the cell buffer and (b) without the cell attached in the cell buffer. (c) Percentage of normalized impedance change as a function of the measured frequency. (d) Statistical normalized impedance changes with the presence and absence of the cell on the microelectrode (n = 45 over three chips with the cell, and n = 47 over three chips without the cell). The inset shows the optical image of microelectrodes with the presence of cells (left column) and absence of cells (right column). Reprinted with permission from ref 19. Copyright 2013 Elsevier.

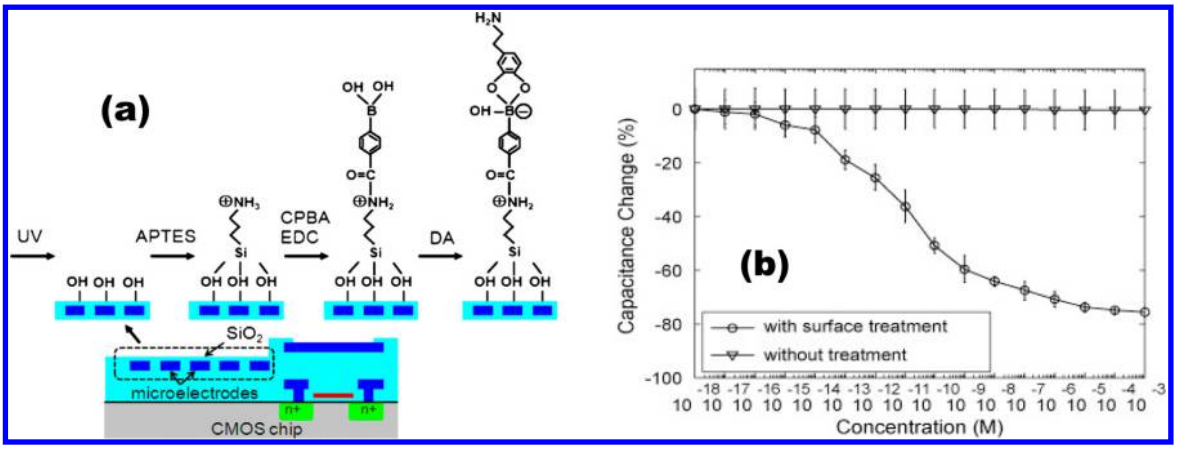

Figure 68. (a) Schematic for capacitive detection of the neurotransmitter dopamine by utilizing submicrometer interdigitated microelectrodes on a CMOS chip. (b) Percentage capacitance changes with respect to DA concentrations. Reprinted with permission from ref 66. Copyright 2010 Elsevier.

electrodes with high SNRs, and the achieved spatial resolution of the electrical activity signal for RGCs significantly assisted spike sorting.[24]

Song et al. demonstrated the CMOS-based sensor chip application in recognizing bacteria with single bacterial resolution via immunoassay coupled to laser-induced fluo-

DOI: 10.1021/cr500554n
Chem. Rev. XXXX, XXX, XXX−XXX

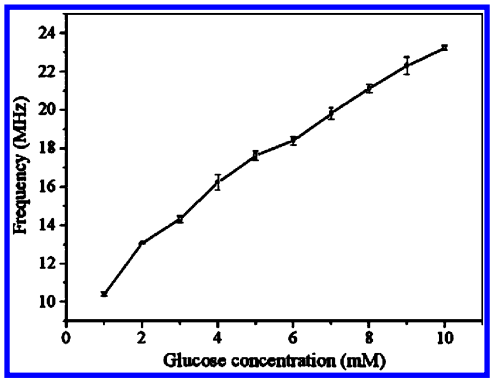

Figure 69. Measured results of the oscillation frequency for the glucose sensor. Reprinted with permission from ref 67. Copyright 2012 Elsevier.

rescence detection. High sensitivity in *Bacillus globigii* spore detection was achieved by use of enzymatic amplification following immune complex formation on a CMOS-based platform (Figure 75).[97] In another study, Ji et al. utilized the 0.5 μm CMOS technology for designing an array of APS-based image sensors along with the required circuits for readout and generating logic and control signals. The system worked as a contact imager for successful imaging of microbeads (16 μm) present on the chip surface. Furthermore, the packaged chip was found able to image on-chip cultured cells.[98]

Yan et al. described a CMOS-based biosensor utilizing a silicon photonic waveguide for multiplex detection without labeling. The system utilizes measurement of the change in local refractive index on the waveguide's upper surface during capturing events for sensing. For adsorption of bovine serum albumin with a thickness of less than 3 nm, a sensitivity of around 20%/nm photocurrent modulation was achieved with a planar-optical-waveguide-based biosensor system.[99] A CMOS-based photosensing chip modified with "horseradish peroxidase (HRP) or glucose oxidase-HRP" was utilized by Ho et al. for detection of H_2O_2 and/or glucose. Enzymes were encapsulated in highly transparent Ormosil, and HRP-catalyzed luminol luminescence was used for H_2O_2 and glucose detection in real time. The system required only 10 μL of solution and exhibited linearity in the 0.05−20 and 0.5−20 mM ranges for H_2O_2 and glucose, respectively (Figure 76).[100] To investigate the effect of irradiating human blood on the differential activity of genes from leucocytes, Huang et al. described the use of a CMOS microarray. In their design, a photocurrent impulse response time of around 800 ps was accomplished by lowering the "slow diffusive component of the photocurrent signal" by use of a fingered differential photodiode (PD) (Figure 77). Furthermore, filter-free and time-gated fluorescence with a sensitivity of 100 pM was realized using quantum dots as fluorescence labels.[26]

Simpson et al. demonstrated an integrated 0.5 μm CMOS-based microluminometer for whole cell bioluminescence detection. In their design, detector noise and wide-band white noise were minimized using a photodetector with a distributed electrode configuration and signal processing via a current-to-frequency converter, and luminescence recording was achieved from as low as 4×10^5 cells/mL.[40] Bolton et al. utilized the CMOS microluminometer with an in-built "bioluminescent bioreporter integrated circuit" for bioluminescence detection. Using a room temperature CMOS photodiode (1.47 mm^2), they were able to record detectable signal up to 0.15 fA with 1510 s of integration time. Furthermore, the microluminometer was able to record luminescence from as few as 5000 bacterial cells.[101] Eltoukhy et al. described an 0.18 μm CMOS-process-based bioluminescence detection system with 8 × 16 pixels. The system showed a capability of sensing emission rates lower than 10^6 lux over an integration time of 30 s at room temperature.[102] In another study to detect *Salmonella typhimurium*, a food-borne pathogen, via a lens-free CMOS image sensor (CIS), Jeon et al. developed an immunosensor by integrating a chemiluminometric ELISA-on-a-chip (EOC) and were able to sense the bacterium up to 4.22×10^3 CFU/mL. Furthermore, a 67-fold improvement in LOD was realized by pairing the sensor with immunomagnetic separation.[103]

For fluorescence-based detection, Shepard et al. has patented an active CMOS biosensor device (US7738086B2) that can be

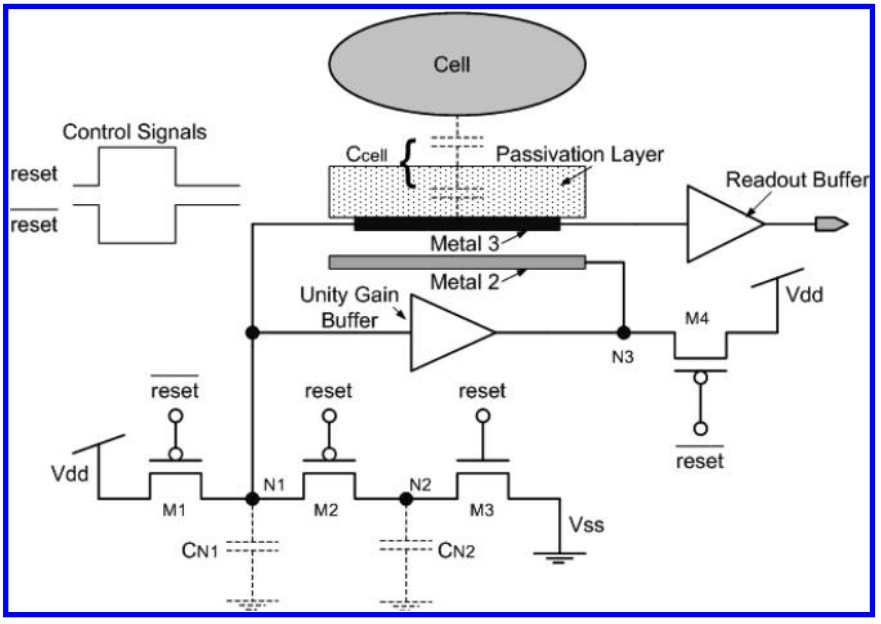

Figure 70. Capacitance sensor for cell proximity detection. Reprinted with permission from ref 95a. Copyright 2005 IEEE.

DOI: 10.1021/cr500554n
Chem. Rev. XXXX, XXX, XXX−XXX

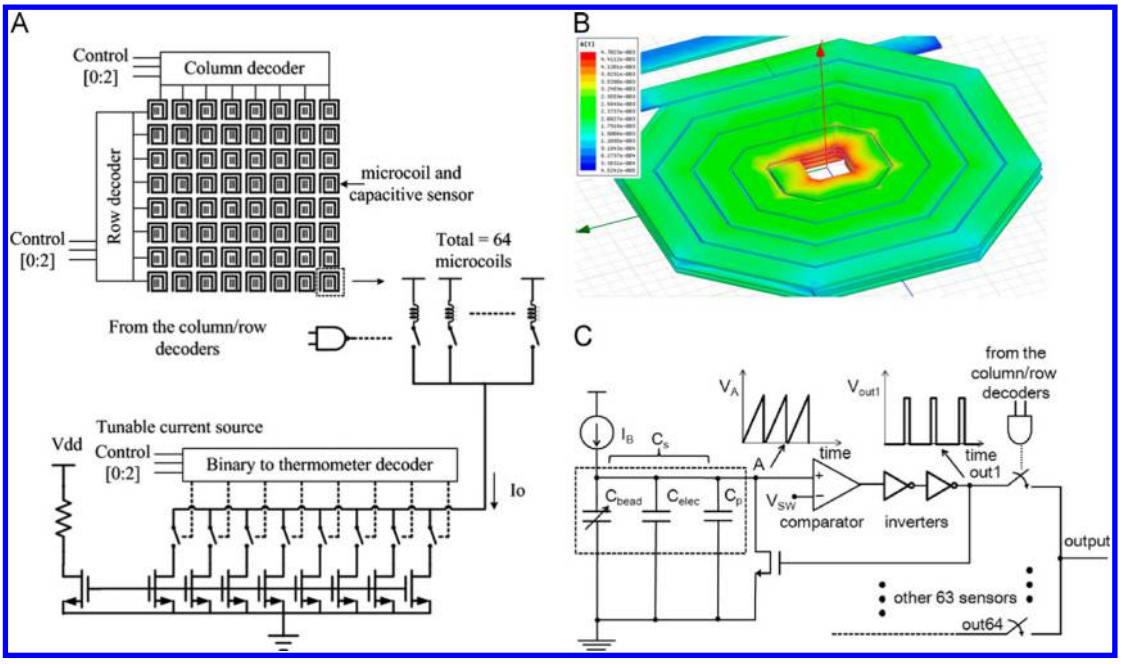

Figure 71. (a) Schematic of the CMOS micromanipulation and biosensing array. The tunable current source for driving microcoils is also illustrated. (b) Finite-element simulation of magnetic fields of the type-B microcoil. (c) Schematic of the capacitive sensing circuit. Reprinted with permission from ref 5. Copyright 2013 Elsevier.

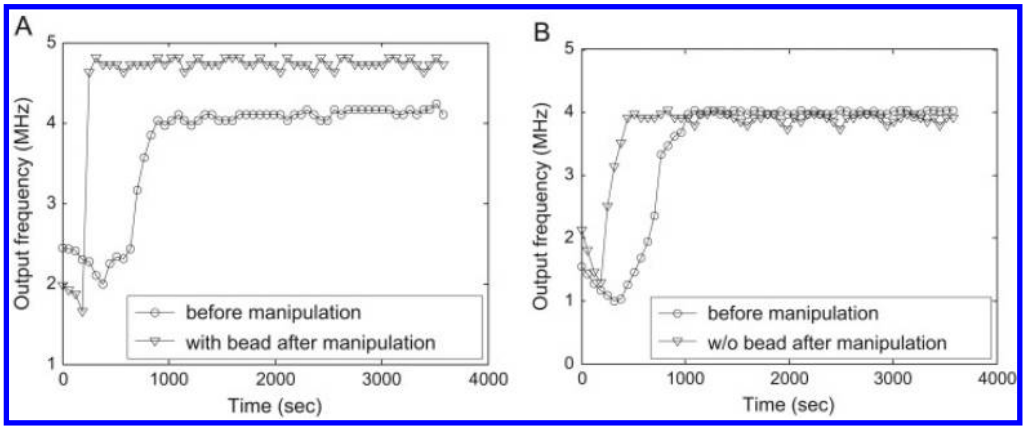

Figure 72. Measured output frequencies of capacitive sensors before and after magnetic manipulation: (A) one of the sensors with a captured microbead and (B) one of the sensors without a microbead. Reprinted with permission from ref 5. Copyright 2013 Elsevier.

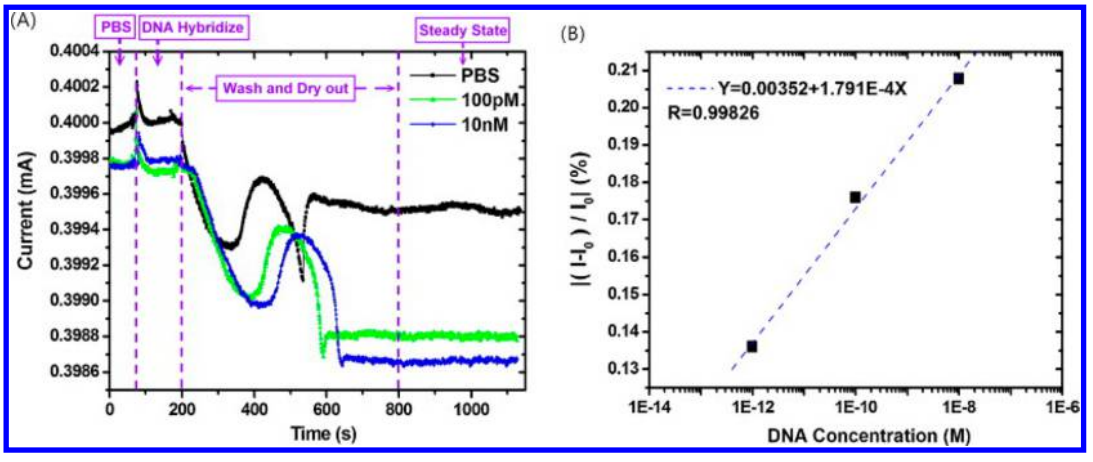

Figure 73. (A) Temporal response of current variation for a sensitivity test with different concentrations of all-matched target DNA. (B) Experimental result of a type II sensitivity test with different concentrations of all-matched target DNA. Reprinted with permission from ref 71. Copyright 2013 Elsevier.

DOI: 10.1021/cr500554n
Chem. Rev. XXXX, XXX, XXX−XXX

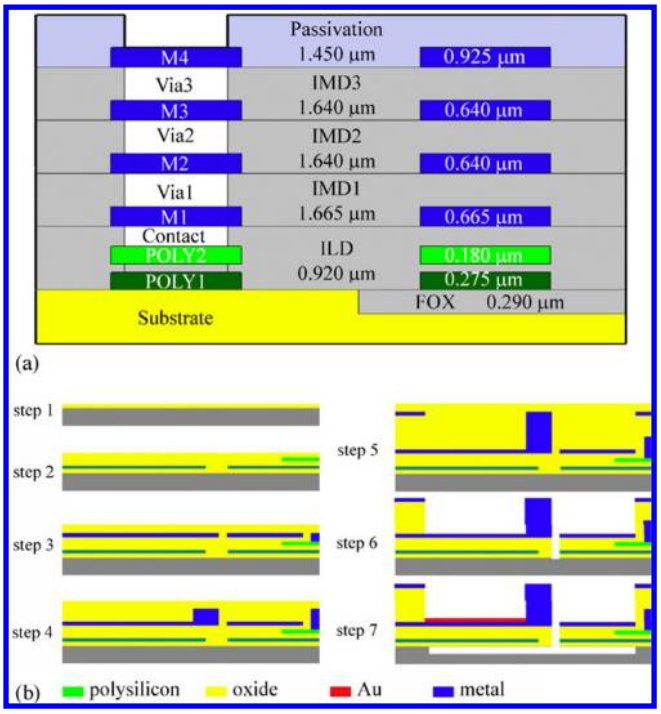

Figure 74. Schematic diagram of (a) the cross-section view of the standard 2P4M CMOS process and (b) the fabrication process flow of the bridge-microcantilever design: (1) field oxide (FOX) deposition on silicon, (2) POLY1 and POLY2 deposition with oxide in between, (3) M1 layer deposition for etching stop and contact to connect POLY2, (4) M2 layer deposition for the transmitter, (5) M2 to M4 layer deposition for the transmitter, (6) postprocess etching for structure contour definition, and (7) Au deposition by lift-off and silicon substrate etching for structure release. Reprinted with permission from ref 96. Copyright 2010 Elsevier.

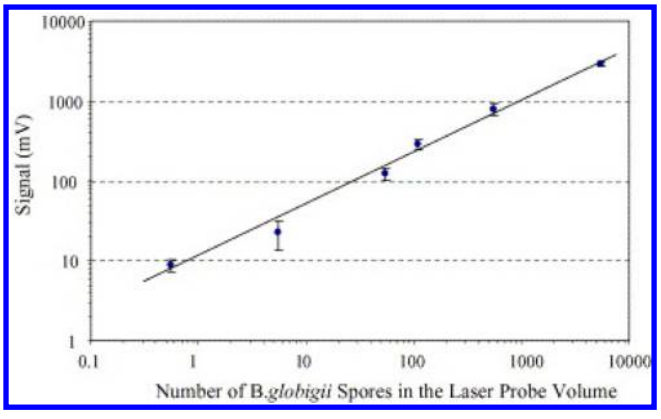

Figure 75. Quantitative determination of *B. globigii* spores. Fluorescence intensities were obtained as a result of the enzymatic reaction between the immunocomplexes and enzyme substrates. Reprinted with permission from ref 97. Copyright 2005 Elsevier.

employed to record fluorescence spectroscopy in a time-gated and time-resolved manner. The binding event of fluorophore-loaded analytes with the biomolecule modified sensor surface was used for sensing, and the fluorescence intensities of the fluorophore at different times were recorded using photodiodes with other circuitry in the device. These measurements were then averaged to generate a representation of the transient fluorescent decay response unique to the fluorophores.[104] For screening of whitening agents, Chang et al. described the 0.35 μm CMOS technology from a TSMC-based CMOS optoelectronic biosensor (Figure 78) comprising a green LED, a slide for performing the biochemical reactions, and a CMOS phototransistor, which perform sensing using the principle of absorption photometry. The results for melanin assay using 10 μL of sample revealed the detection ability of the device up to a density of 5×10^4 cells/mL.[105] Recently, Tokuda et al. reviewed the CMOS-based multifunctional image sensor for biosensing application. They reviewed the CMOS image sensors with combined optical and electric multifunctions and showed that, for such a sensor, a realistic light-sensing architecture is possible only with the APS design, which is mainly utilized in present-day CMOS image sensors. They also proposed a CMOS-based "on-chip biosensor comprising inbuilt on-chip light-emitter array".[106]

5.8. Magnetic Biosensors

A CMOS-based design methodology using Hall effects has been reported for on-chip magnetic bead label detection.[107] Aytur et al. described a 0.25 μm 1P5M BiCMOS-process-based array of Hall sensors to detect anti-Hu IgG antibody. In their assay magnetic beads functioned as the assay signal, and the sensitivity of the sensors was improved using electrical and magnetic modulation.[107a] Wang et al. patented a CMOS-based magnetic biosensor array which utilizes frequency shift for sensing and achieved sensitivity of a single bead without using an external magnet (US8378669B2).[108] For detecting magnetic particles in a sample using this device, a sensor cell having a differential sensor pair acts as an active sensor and responds to an oscillator frequency change due to one or more magnetic particles situated within a sample volume in the absence of an externally applied magnetic field.[108] On the basis of this patent, they described a 45 nm CMOS-process-based sensor array with 16 cells for "on-chip LC resonance frequency-shift"-based magnetic biosensing. To enhance the sensor performance via improving gain uniformity, while preventing location-dependent transducer gain degradation, they used a "bowl-shape stacked coil together with floating shimming metal"-based inductor. For sensing, the inductor was used to produce a magnetic field, which polarizes magnetic particles near the sensor, thus increasing the total magnetic field. Such an increase in the magnetic field causes a downshift in the oscillation frequency via an effective increase of inductance and is used as the sensing principle (Figure 79). The results reveal a dynamic range of around 85.4 dB with an 18 kHz shift in frequency per particle and linearity up to 409 beads.[73] In another study on a CMOS-based magnetic sensor using frequency shift as the sensing principle, Pai et al. developed a sensor for nucleic acid and antigen detection using a single-use open-well cartridge. The recording time and sensor noise were minimized using the "magnetic freezing" approach. Detection of interferon-g (IFN-g) protein and a DNA oligomer with 31 base pairs was accomplished down to 1 and 100 pM, respectively, in an amplification-free manner at room temperature (Figure 80).[109]

Han et al. described a CMOS-based high-density GMR sensor array with >1000 sensors for DNA hybridization detection. For DNA detection, ss-DNA was immobilized over the surface of GMR sensors, and the variation in the resistance of the sensor due to magnetic nanoparticles captured by hybridized DNA was used to measure the generated electrical signals via on-die circuitry. The results were found satisfactory, and the sensor was able to selectively capture oligonucleotides of unknown sequence.[23]

DOI: 10.1021/cr500554n
Chem. Rev. XXXX, XXX, XXX−XXX

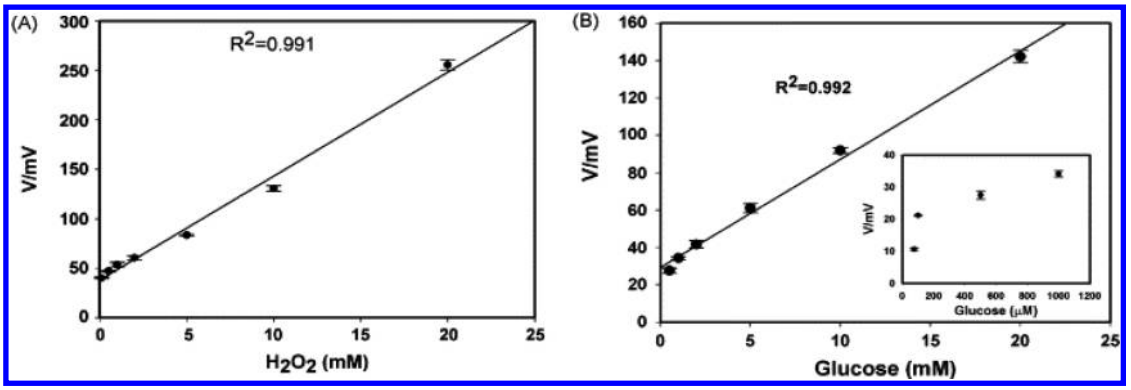

Figure 76. Calibration graphs of the miniature optical (A) H_2O_2 and (B) glucose biosensors. The inset graph shows the photocurrents of the glucose optical biosensor with glucose concentration between 75 μM and 1 mM. Reprinted with permission from ref 100. Copyright 2007 Elsevier.

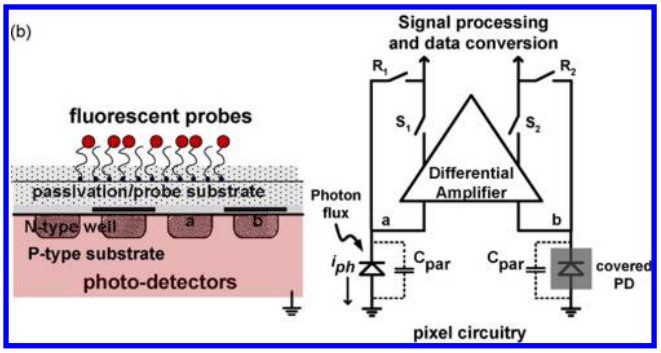

Figure 77. Cross-sectional view of a time-gated, integrated fluorescence bioassay and pixel circuit block diagram showing common-mode rejection of the differential PD, fast time-gating, and noise suppression through active reset. The photodiode geometry is fingered to improve its impulse response. Reprinted with permission from ref 26. Copyright 2011 Elsevier.

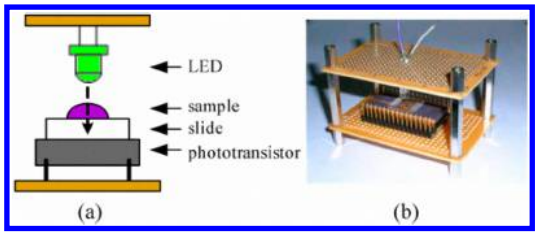

Figure 78. Miniature biosensor: (a) illustrated diagram and (b) photograph. Reprinted with permission from ref 105. Copyright 2009 IEEE.

5.9. Surface-Acoustic-Wave-Based Biosensors

Using the 1.5 μm 2P2M CMOS technology, Tigli et al. developed a surface-acoustic-wave (SAW)-based biosensor using ZnO as the piezoelectric material. In their system temperature was adjusted using implanted heater elements, while edge reflections were removed and triple transit interference was minimized using "compensation and acoustic absorbers". The sensor exhibited insertion loss of −4.83 dB, while achieving a minimum reflection and maximum transmission at 392.5 MHz.[17b] The authors also described an SAW biosensor in 0.5 μm 2P3M CMOS technology for detecting the breast cancer biomarker mammoglobin (hMAM) and accomplished frequency and mass sensitivity of 8.704 pg/Hz and 2810.25 m^2/ kg, respectively, via measuring the center frequency shifts. The sensor was found to be selective against bovine serum albumin (Figure 81).[27] Nirschl et al. reported the development of CMOS-based film bulk acoustic resonators (FBARs). The system showed success in detecting DNA in buffer and diluted serum samples and was found to be capable of detecting different DNA sequences from 1:100 diluted human serum without significant nonspecific binding.[110]

5.10. Implantable Biosensors

Implantable biosensor systems are required for reliable monitoring of physiological parameters. However, the main requirement of such devices is a low-power, low-noise system. As batteries are large in size, passive powering systems are required for implantable devices. Ohta et al. developed CMOS-based devices for retinal prosthesis and brain implants. They discussed the details of these in a recent review, where they mentioned that such CMOS-based devices comprise in-built circuits for stimulation of living cells and provide high performance and adaptable functionality for biosignal detection.[111] Anwar et al. has patented one of the CMOS-based wireless implantable biosensors for detection and measurement of analytes within the human body.[112] Poustinchi et al. described an 0.18 μm CMOS-process-based neurochemical sensing system for implantable neural prosthetica using a low-power and low-noise immune circuit. Higher selectivity with improved temporal resolution was accomplished via combined use of fast-scan cyclic voltammetry and amperometry. The result revealed the dopamine- and serotonin-sensing capability of the sensor in the micromolar range, while power consumption of 120.85 μW was found for the microsystem with improved noise resistance due to the applied averaging operation.[113]

For enhanced molecular imaging in freely moving subjects, O'Sullivan et al. reported a biosensor system based on a miniaturized "vertical-cavity surface-emitting laser (VCSEL)". The biosensor with a 1 cm^3 and 0.7 g size and mass shows the capability to detect "fluorophore and tumor-targeted molecular probes" accurately for 2 weeks in animals when implanted. Autofluorescence-controlled sensitivity was accomplished using a CMOS-based in-built readout circuit that converts the fluorescence signal into a digital form.[114] Using the hybrid 0.18 μm, 1P6M CMOS process for a "433 MHz ASK RF transmitter and receiver" and the 0.35 μm 2P4M CMOS process for the data converter, Chiu et al. described an implantable needle-type biosensor for glucose and cholesterol monitoring. Glucose oxidase and cholesterol oxidase were immobilized using a polypyrrole matrix and in-built circuit for RF wireless signaling, and +3.3 V-based TIA with dissipation of <10 mW was utilized for in vivo continuous monitoring. The

DOI: 10.1021/cr500554n
Chem. Rev. XXXX, XXX, XXX−XXX

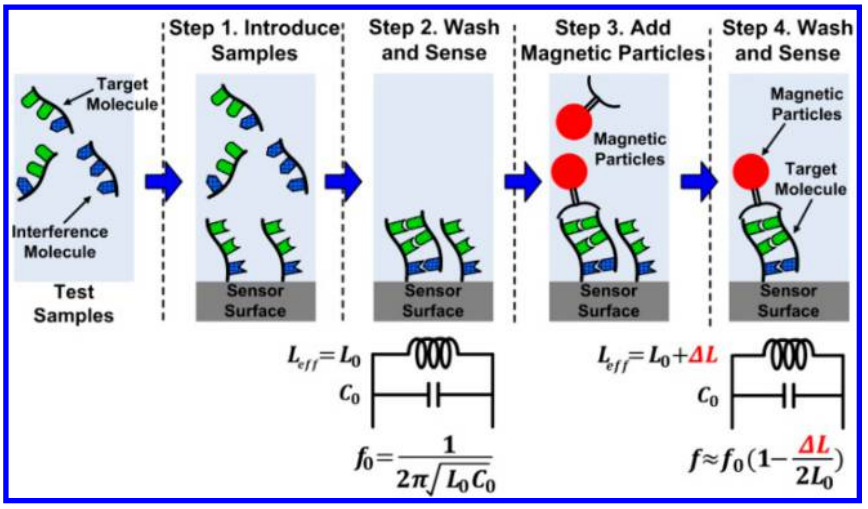

Figure 79. Frequency-shift magnetic sensing scheme. Reprinted with permission from ref 73. Copyright 2010 IEEE.

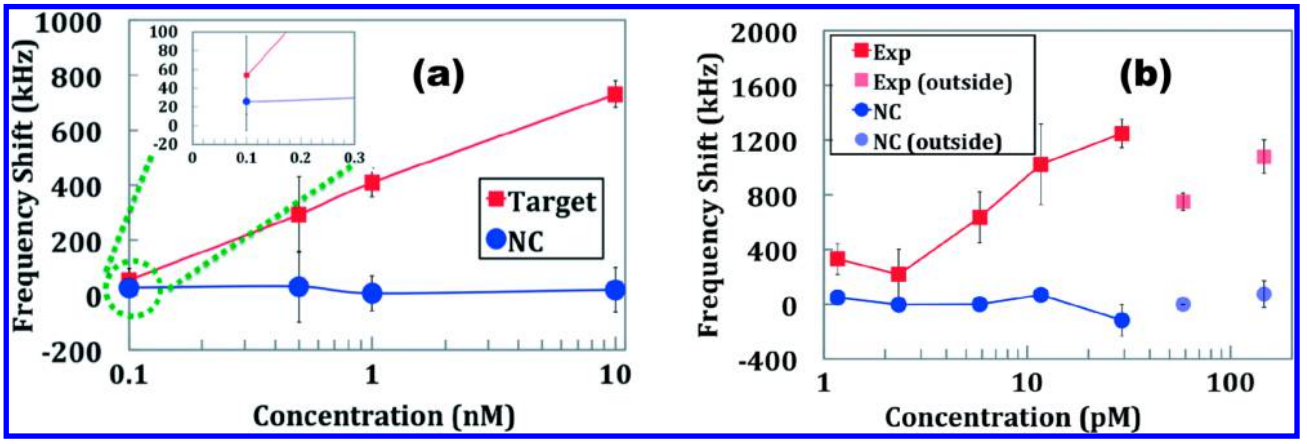

Figure 80. (a) DNA concentration response. (b) Immunoassay concentration response. NC = negative control. Reprinted with permission from ref 109. Copyright 2014 The Royal Society of Chemistry.

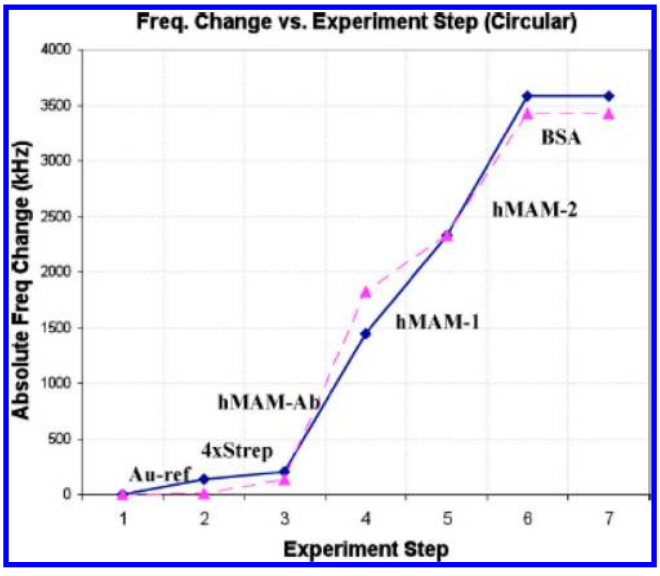

Figure 81. Overall frequency change response of circular CMOS-SAW devices. The dashed line represents the first access point readings, and the solid line shows the data collected from the second access point on the same chip. Reprinted with permission from ref 27. Copyright 2008 IEEE.

system showed linearity up to 10 mM for cholesterol and 20 mM for glucose. Figure 82 shows system response for wireless glucose monitoring in real time.[115]

5.11. Other Biosensors

Using the 0.18 μm CMOS process, Lee et al. described CNT-based biosensors for glutamate, a neurotransmitter, sensing. Modulation in conductance signals by generated ammonia

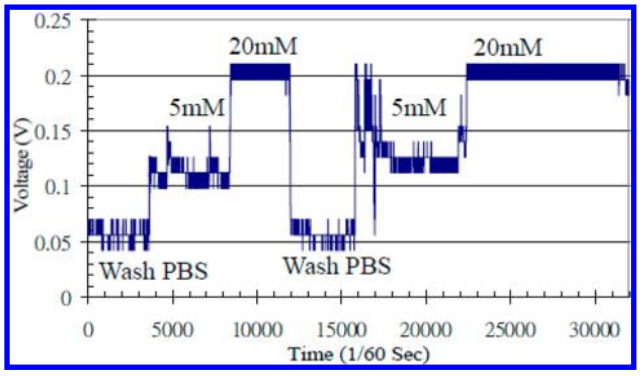

Figure 82. Real-time wireless continuous monitoring of the glucose reaction. Reprinted with permission from ref 115. Copyright 2005 IEEE.

DOI: 10.1021/cr500554n
Chem. Rev. XXXX, XXX, XXX−XXX

during the enzymatic reaction was successfully utilized for glutamate sensing.[116] Sun et al. described CMOS-based RF transceiver development for a portable, low-cost NMR system with a noise of 0.7 dB. The system showed the capability of detecting avidin up to 20 fmol or 1.4 ng in a 5 μL sample (Figure 83).[44]

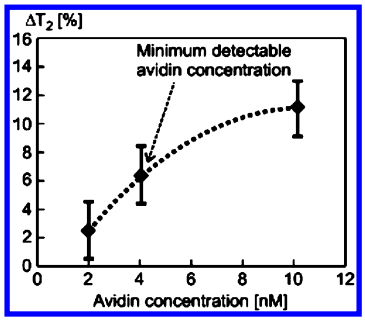

Figure 83. Measured ΔT_2 for various avidin concentrations. Reprinted with permission from ref 44. Copyright 2009 IEEE.

6. COMMERCIAL CMOS BIOSENSORS

In the past few years, some CMOS-based devices have made their transition to the market for biosensing application.

Among such devices, *Life Technologies* has developed and commercialized a CMOS-based nonoptical DNA sequencing technology called Ion Torrent. The device comprises tantalum oxide as the ion-sensitive-layer-based 1.2×10^6 FET sensor for simultaneous and parallel sensing of sequencing events. The device uses "template-directed DNA polymerase synthesis" on sensors, and generated ions for every inserted nucleotide were sensed via an in-built ISFET connected with an individual floating gate for recording the sequence data.[117]

Silicon Biosystems has developed a CMOS-based dielectrophoresis (DEP) array to individually identify, manipulate, and sort specific cells within a heterogeneous population. The device embeds more than 30 0000, 20 μm × 20 μm electrodes and results in 76 800 DEP cages in 11 μL of solution. Their system utilizes μDEP cages generated in 3-D space just above the sensor via an electric field from the CMOS circuit to confine, lift, and move single particles/cells from one microchamber location to another. The cells have been found to maintain viability with completely intact DNA and unmodified proliferation capability.[118]

Table 1. Present Status and Challenges in CMOS-Based Biosensor Technologies

Present status of CMOS based biosensors	Challenges in CMOS based biosensor
Many of the individual building blocks of CMOS based biosensor are existing today, which can be utilized in future for the advancement in this field. ❖ Fabrication process of various CMOS based array system is available. ❖ Various post processing technologies have been developed for lab level research. ❖ Various packaging technologies have been demonstrated. ❖ Various CMOS based circuits are now known for electrochemical, optical, piezoelectric, magnetic and other transducers development. ❖ Various CMOS based circuits are now known for lower power consumption and improvement in the sensitivity of the overall device. ❖ Various proofs of concepts have been reported. ❖ CMOS based DNA sensors have shown the promise in the practical applications and have been commercialized. ❖ Over the last decades, tremendous efforts have been invested in improving yield and reliability, while minimizing the size parameters and fabrication cost.	Though various proofs of concepts have been shown and some have been commercialized, there are various challenges, which should be looked in more details for wider applications. ❖ Newer and universally applicable post processing technologies are required to solve the issue of exposed aluminum on CMOS based systems. ❖ Novel and innovative methods are required to generate biomolecules modified surfaces that can interact with the CMOS electronics without affecting the CMOS circuit and device reliability. ❖ New technologies are required for the packaging of CMOS circuitry to be used within a liquid environment without damaging underneath circuits. ❖ Novel and unified approaches are required for the seamless integration of existing building blocks of CMOS technology and components of fluidics for the development of complex bio-electronic systems. ❖ Newer technologies especially for upcoming nanometer CMOS developments are required to counter issues of uniform power distribution, lower noise architecture, improved component matching, invulnerability to parameter variations and surface temperature distribution etc. ❖ For broader commercialization new technologies are required to bring down the cost of CMOS fabrication, post processing and packaging. ❖ More studies of sensitivity, specificity, environmental conditions etc are still needed for the development and commercialization of CMOS based systems.

DOI: 10.1021/cr500554n
Chem. Rev. XXXX, XXX, XXX−XXX

CombiMatrix has invested a lot of effort into the development of a CMOS-based electrochemical MEA,[119] and commercialized a multiplexed CMOS microarray, the "CombiMatrix ElectraSenseH microarray", for electrochemical immunoassay. The CombiMatrix ElectraSenseH microarray consists of individually addressable 12 544 Pt electrodes (44 μm in diameter). The device utilizes a capture antibody modified polypyrrole layer on the electrodes for measuring the generated current during enzyme-enhanced electrochemical reaction and shows 1 order of improvement in response when compared to the "conventional enzyme-linked immunosorbant assay (ELISA)".[120]

Recently, *Anitoa* has developed a CMOS image sensor built on the 0.18 μm CMOS technology, which exhibits a detection sensitivity of 3×10^{-6} lx with the capability to detect a very low number of molecules labeled with fluorescence reporter probes. Anitoa is also working on the development of a miniaturized "quantitative polymerase chain reaction" (qPCR) system using its CMOS imager.[121]

Other than these, there are other companies such as Nanogen, Affymetrix, Infineon Bioscience, CustomArray Inc., etc. intensely working on a CMOS-based array for bioapplications, and it is expected that in the next few years a lot more work and product will hit the market for better health care.

7. CHALLENGES AND PROSPECTS OF CMOS IN BIOSENSORS

CMOS-based biosensor arrays utilize direct interaction between the biosensing transducer and in-built circuits to measure the desired analyte. Incorporation of a sensing part enables high compactness, lower power consumption, and improvement in the sensitivity of the overall device. Therefore, opportunities for CMOS-based sensing devices are gaining popularity for biosensing applications. However, the major challenge in CMOS-based biosensor fabrication is the presence of exposed aluminum in the CMOS-based systems, which is not stable in a liquid environment and results in generation of toxic compounds during cell culturing on it. For CMOS-based biosensor development, another issue is to create a biomodified interface that can interact with the in-built electronics without interfering with microelectronic processing.[122] Furthermore, the CMOS circuit packaging for its application in liquids without damaging the circuits underneath is an open challenge.[31] The high investment cost to set up a production line has delayed extensive adoption of the CMOS biosensor despite these devices offering greater detection sensitivity and multiplex capability. Numerous methods have been reported in the literature, including the most prominent devices such as Ion Torrent, the Affimetric gene chip, and the Silicon Biosystems μDEP array. Unfortunately, the approaches vary considerably and raise the question of how they can be unified for commercial packaging and adopted by low-volume foundries. Also, the upcoming nanometer CMOS technology is raising issues of power and surface temperature distribution, noise, and component matching, along with resistance to variation in the sensing parameter. See Table 1 for a description of the status and challenges of CMOS-based sensor technologies.

In recent years, where systems are proposed only for research purposes, solutions to the above problems have been found partially via postprocessing-based modification of CMOS chips in clean room facilities. However, for wider acceptance of CMOS for commercial biosensor fabrication, issues related to the cost of CMOS fabrication and its postprocessing must be looked at in detail, while keeping the future of the ever-changing semiconductor technology in mind so that they can be applied to upcoming CMOS technology.[15] To date, biosensor arrays using CMOS technology have largely focused on circuits to achieve high speed and performance; however, the effect of using nanoscale technologies in generating a system with ultralow power and working with lower operating frequencies needs further investigations.[45] Although CMOS DNA sensors have shown promise, their working principles involving measurement of electrical or electrochemical secondary signals are very sensitive to the electrolyte properties. Thus, assay solutions in DNA electrical sensors require more careful control than those in optical DNA microarrays. In general, the sensitivity and specificity of label-free sensors under a wide range of environmental conditions have still not been fully investigated, and additional research is needed.[7] In microfluidic-based biosensor arrays, integration of a CMOS-based sensor into a microfluidic environment poses several more challenges, e.g., spatial separation of fluidic and electric interfaces, fluidic rigidity, low-resistance electrical contacts, and an approach to functionalize the sensing area. Existing solutions often use serial processes and glues or underfiller to seal and fluidically connect the sensing area, requiring additional dispensing steps and structures to avoid clogging of the fluidic channels.[34] Thus, we are not even near a complete system comprising a unified interface to connect a biological system to the microelectronic world. Though various building blocks required for a complete system have been described and shown promise, selection and integration of such blocks to generate complex, reliable, and commercially acceptable bioelectronic systems needs many more studies.[123] Once these challenges are solved, one can expect that CMOS-based microsystems will control the biomedical field, including "neuroscience and artificial intelligence research".

Moreover, the future of a new generation biosensor lies in the flexible electronics with possibilities to make good contact even on a nonuniform surface comprising electrodes, microelectronic circuits, etc. The success of such a flexible system with integrated sensors, electronics, and micro/nanofluidics holds a promising future for biosensing systems to realize in vivo and wearable devices to monitor biological markers in a continuous manner. Recently, some flexible systems have been proposed and have shown promise for the future, but still much more effort and research is required for CMOS-based systems to accomplish crucial parameters of power usage, performance, scalability, integration capability, and cost. Also new and advanced biocompatible packaging technologies with high flexibility are required to integrate microfluidic systems with a CMOS system.[35]

8. CONCLUSION

In development of a small-size, hand-held biosensor array for sensitive, faster, and multiplexed detection, CMOS-based biosensor arrays have shown promise for the highest degree of integration and cost efficiency. CMOS facilitates monolithic integration with circuitry and provides an unmatched yield, cost efficiency, a large integration capability, and low power consumption. Using CMOS-based systems with integrated electrodes and circuits for multiplexed biosensing/sensing, massive parallel optical and electrochemical imaging arrays have been realized. These arrays are capable of performing a wide field of optical imaging and electrochemical analysis. This

DOI: 10.1021/cr500554n
Chem. Rev. XXXX, XXX, XXX−XXX

review attempts to bridge the understanding between cross-disciplinary teams of biologists and engineers who work together to develop such biosensors. It is a sincere attempt by the authors to encourage more multidisciplinary collaboration between these groups by sharing already published modules/data/information and by presenting challenges and opportunities which exist in each area. The review covers the basics of CMOS design, fabrication, postprocessing, and packaging steps. Functioning of various biochemical sensors and circuitry designed to obtain signals with minimal signal loss are also reviewed. We are happy to state that CMOS-based biosensing technologies are starting to make a transition from research to the real world market. However, there are still many challenges in CMOS-based biosensor technology development before it can take over the conventional system presently dominating the market.

AUTHOR INFORMATION

Corresponding Author

*E-mail: sunilarya333@gmail.com. Phone: +65 67705621. Fax: +65 64640517.

Notes

The authors declare no competing financial interest.

Biographies

Sunil K. Arya received his M.Sc. in organic chemistry in 2004 and Ph.D. in chemistry biosensors in 2008 from the University of Delhi, India. He is currently a scientist at the Institute of Microelectronics, A*STAR, Singapore. He completed postdoctoral research at the University of South Florida, Tampa, FL, and at the National Institute of Nanotechnology at the University of Alberta, Edmonton, Alberta, Canada. His primary interests are in the synthesis and applications of nanomaterials, monolayers, and MEMSs for electrochemical biosensors.

Chee Chung Wong received his Bachelor of Engineering (mechanical) and Ph.D. degree in bioengineering from Nanyang Technological University (NTU), Singapore, in 2005 and 2011, respectively. In 2010, he joined the Bioelectronics Program at the Institute of Microelectronics (IME), A*STAR, Singapore, as a research scientist. The focus of his research activities is on the development and integration of a semiconductor-based cell diagnostic and analysis biochip. He has lead numerous research and project teams in the development of an automated fetal cell isolation platform, translating the rare cell isolation platform from prototype to benchtop in a clinical setting. Chee Chung is currently the lead investigator for the A*Star Joint Council Office Development Program, which focuses on the development of a 3D-integrated-circuit-based microfluidics cell analysis platform.

Yong Joon Jeon received B.S. and M.S. degrees in electronic and electrical engineering from the Pohang Institute of Science and Technology (POSTECH), Pohang, Korea, in 1993 and 1995, respectively. He received his Ph.D. degree in electrical engineering at the Korea Advanced Institute of Science and Technology (KAIST), Daejeon, Korea, on the design of flat panel display drivers for active-matrix liquid-crystal displays (AMLCDs) and active-matrix organic light-emitting diode (AMOLED) displays. From 1995 to 2005, he was with the LG Electronics Institute of Technology and worked on deep submicrometer MOSFET physics and modeling and RF linear power amplifiers for code division multiple-access (CDMA) applications in both GaAs and InGaP heterojunction bipolar transistor (HBT) technologies. From 2009 to early 2012, he was with LG Display, where he contributed to the development of a 3.8 in. AMOLED display for smart phones and several mobile low-temperature polysilicon (LTPS) liquid-crystal displays (LCDs). Since late 2013, he has been with the Institute of Microelectronics (IME), Singapore, following his postdoctoral research on energy-harvesting power ICs at KAIST. His research area includes RF front-end circuits, including low-noise amplifiers (LNAs), mixers, and RF power amplifiers for CDMA/

DOI: 10.1021/cr500554n
Chem. Rev. XXXX, XXX, XXX−XXX

wideband CDMA (WCDMA) applications in GaAs and InGaP HBT technologies and data driver ICs for flat panel displays such as LCDs and AMOLED displays. His current research interests are readout interfaces for biosensor arrays and their driving scheme.

Tushar Bansal received his M.Sc. and Ph.D. in electrical engineering in 2006 and 2009, respectively, from the University of Michigan, Ann Arbor. He is currently a Scientist and Manager (ID) at the Institute of Microelectronics, A*STAR, Singapore. His research interests include microfluidic device application.

Mi Kyoung Park received her B.Eng. and M.Eng. degrees in chemical engineering from Hong-Ik University, Seoul, Korea, in 1996 and 1998, respectively. She received her Ph.D. degree in chemistry from the Department of Chemistry, University of Houston, Houston, TX, in 2003. She is currently the Principal Investigator of the Bioelectronics Programme, Institute of Microelectronics, A*STAR, Singapore. Her main research areas are label-free immunosensors such as silicon biophotonics sensors, FET sensors, surface plasmon resonance (SPR) sensors, and electrochemical sensors for biomedical applications.

ACKNOWLEDGMENTS

This work was supported by A*STAR (Agency for Science, Technology and Research), Singapore, and Grants JCO-DP 1334i00052 and IME/13-519402.

GLOSSARY

ADC	analog-to-digital converter
Al_2O_3	aluminum oxide
AP	action potential
APS	active pixel sensor
ASK	amplitude shift keying
AuNPs	gold nanoparticles
BDD	boron-doped diamond
CBCM	charge-based capacitance measurement
CDS	correlated double sampling
C_{dl}	double-layer capacitance
CIS	CMOS image sensor
CMOS	complementary metal−oxide−semiconductor
DA	dopamine
DEP	dielectrophoresis
EGP	electroless gold plating
EIS	electrochemical impedance spectroscopy
EOC	ELISA-on-a-chip
FDC	frequency-to-digital converter
FET	field-effect transistor
FG FET	floating gate field-effect transistor
GMR	giant magnetoresistive
ICMR	input common-mode range
IDC	impedance-to-digital converter
ISFETs	ion-sensitive field-effect transistor
LOD	limit of detection
MEA	microelectrode array
MEMS	microelectromechanical system
MOSFETs	metal−oxide−semiconductor field-effect transistors
OGFET	open-gate field-effect transistor
OTA	operational transconductance amplifier
PCB	printed circuit board
PDMS	poly(dimethylsiloxane)
PSD	position-sensing detector
RF	radio frequency
SAW	surface acoustic wave
SC	switched capacitor
SEM	scanning electron microscopy
Si_3N_4	silicon nitride
SiO_2	silicon dioxide
SNR	signal-to-noise ratio
SoC	system on chip
TEM	transmission electron microscopy
TEOS	tetraethyl orthosilicate
TIA	transimpedance amplifier
TSMC	Taiwan Semiconductor Manufacturing Co.
TSV	through-silicon-via
ULCA	ultra-low-current amplifier

REFERENCES

(1) (a) Jang, B.; Hassibi, A. *IEEE Trans. Ind. Electron.* **2009**, *56*, 979−985. (b) Hasegawa, J.; Uno, S.; Nakazato, K. *Jpn. J. Appl. Phys.* **2011**, *50*, 04DL03−04DL03−09.

(2) Heer, F.; Franks, W.; Blau, A.; Taschini, S.; Ziegler, C.; Hierlemann, A.; Baltes, H. *Biosens. Bioelectron.* **2004**, *20*, 358−366.

(3) Nakazato, K. In *State of the Art in Biosensors—General Aspects*; Rinken, T., Ed.; InTech: Rijeka, Croatia, 2013; pp 163−177.

(4) Meyburg, S.; Stockmann, R.; Moers, J.; Offenhäusser, A.; Ingebrandt, S. *Sens. Actuators, B* **2007**, *128*, 208−217.

(5) Chang, A.-Y.; Lu, M. S. C. *Biosens. Bioelectron.* **2013**, *45*, 6−12.

(6) (a) Ghafar-Zadeh, E.; Sawan, M.; Therriault, D. *Sens. Actuators, A* **2008**, *141*, 454−462. (b) Widdershoven, F.; Van Steenwinckel, D.; Überfeld, J.; Merelle, T.; Suy, H.; Jedema, F.; Hoofman, R.; Tak, C.; Sedzin, A.; Cobelens, B.; Sterckx, E.; Van der Werf, R.; Verheyden, K.; Kengen, M.; Swartjes, F.; Frederix, F. *Proceedings of the 2010 IEEE International Electron Devices Meeting (IEDM)*, San Francisco, CA; IEEE: New York, 2010; pp 36.31.31−36.31.34. (c) Yu-Wei, C.; Yu-Ting, T.; Yang-Tung, H.; Yuh-Shyong, Y. *Proceedings of the 3rd International Conference on Sensing Technology*, Tainan, Taiwan; IEEE: New York, 2008; pp 82−85.

(7) Benini, L.; Guiducci, C.; Paulus, C. *IEEE Des. Test Comput.* **2007**, *24*, 38−48.

DOI: 10.1021/cr500554n
Chem. Rev. XXXX, XXX, XXX−XXX

(8) Graham, A. H. D.; Surguy, S. M.; Langlois, P.; Bowen, C. R.; Taylor, J.; Robbins, J. *Biosens. Bioelectron.* **2012**, *31*, 458−462.
(9) Esch, J. *Proc. IEEE* **2011**, *99*, 249−251.
(10) Lee, K.-H.; Lee, J.-O.; Sohn, M.-J.; Lee, B.; Choi, S.-H.; Kim, S. K.; Yoon, J.-B.; Cho, G.-H. *Biosens. Bioelectron.* **2010**, *26*, 1373−1379.
(11) Levine, P. M.; Gong, P.; Levicky, R.; Shepard, K. L. *IEEE J. Solid-State Circuits* **2008**, *43*, 1859−1871.
(12) (a) Yang, S. M.; Chang, C.; Yin, T. I.; Kuo, P. L. *Sens. Actuators, B* **2008**, *130*, 674−681. (b) DeBusschere, B. D.; Kovacs, G. T. A. *Biosens. Bioelectron.* **2001**, *16*, 543−556. (c) Schienle, M.; Paulus, C.; Frey, A.; Hofmann, F.; Holzapfl, B.; Schindler-Bauer, P.; Thewes, R. *IEEE J. Solid-State Circuits* **2004**, *39*, 2438−2445.
(13) Yang, S. M.; Yin, T. I.; Chang, C. *Sens. Actuators, B* **2007**, *123*, 707−714.
(14) Nah, J.; Fang, H.; Wang, C.; Takei, K.; Lee, M. H.; Plis, E.; Krishna, S.; Javey, A. *Nano Lett.* **2012**, *12*, 3592−3595.
(15) Graham, A. H. D.; Robbins, J.; Bowen, C. R.; Taylor, J. *Sensors* **2011**, *11*, 4943−4971.
(16) Chai, K. T. C.; Hammond, P. A.; Cumming, D. R. S. *Sens. Actuators, B* **2005**, *111*−*112*, 305−309.
(17) (a) Stagni, C.; Guiducci, C.; Benini, L.; Ricco, B.; Carrara, S.; Paulus, C.; Schienle, M.; Thewes, R. *IEEE Sens. J.* **2007**, *7*, 577−585. (b) Tigli, O.; Zaghloul, M. E. *Proceedings of IEEE Sensors 2005*, Irvine, CA; IEEE: New York, 2005; pp 137−140. (c) Yusof, Y.; Sugimoto, K.; Ozawa, H.; Uno, S.; Nakazato, K. *Jpn. J. Appl. Phys.* **2010**, *49* (01AG05), 01−06.
(18) Berggren, C.; Stalhandske, P.; Brundell, J.; Johansson, G. *Electroanalysis* **1999**, *11*, 156−160.
(19) Pui, T. S.; Chen, Y.; Wong, C. C.; Nadipalli, R.; Weerasekera, R.; Arya, S. K.; Yu, H.; Rahman, A. R. A. *Sens. Actuators, B* **2013**, *181*, 842−849.
(20) Watanabe, T.; Yoshida, Y. *Solid State Technol.* **1984**, *26*, 263−266.
(21) (a) Manickam, A.; Chevalier, A.; McDermott, M.; Ellington, A. D.; Hassibi, A. *IEEE Trans. Biomed. Circuits Syst.* **2010**, *4*, 379−390. (b) Hwang, S.; LaFratta, C. N.; Agarwal, V.; Xin, Y.; Walt, D. R.; Sonkusale, S. *IEEE Sens. J.* **2009**, *9*, 609−615.
(22) Manickam, A.; Johnson, C. A.; Kavusi, S.; Hassibi, A. *Sensors* **2012**, *12*, 14467−14488.
(23) Shu-Jen, H.; Liang, X.; Heng, Y.; Wilson, R. J.; White, R. L.; Pourmand, N.; Wang, S. X. *Proceedings of the 2006 IEEE International Electron Devices Meeting (IEDM)*, San Francisco, CA; IEEE: New York, 2006; pp 1−4.
(24) Fiscella, M.; Farrow, K.; Jones, I. L.; Jackel, D.; Muller, J.; Frey, U.; Bakkum, D. J.; Hantz, P.; Roska, B.; Hierlemann, A. *J. Neurosci. Methods* **2012**, *211*, 103−113.
(25) Schindler, M.; Kim, S. K.; Hwang, C. S.; Schindler, C.; Offenhausser, A.; Ingebrandt, S. *Phys. Status Solidi RRL* **2008**, *2*, 4−6.
(26) Huang, T.-c. D.; Paul, S.; Gong, P.; Levicky, R.; Kymissis, J.; Amundson, S. A.; Shepard, K. L. *Biosens. Bioelectron.* **2011**, *26*, 2660−2665.
(27) (a) Tigli, O.; Bivona, L.; Berg, P.; Zaghloul, M. E. *IEEE Trans. Biomed. Circuits Syst.* **2010**, *4*, 62−73. (b) Tigli, O.; Bivona, L.; Chaterjee, C.; Zaghloul, M. E.; Berg, P. *Proceedings of IEEE Sensors 2008*, Lecce, Italy; IEEE: New York, 2008; pp 1452−1455.
(28) Hayasaka, T.; Yoshida, S.; Inoue, K. Y.; Nakano, M.; Ishikawa, T.; Matsue, T.; Esashi, M.; Tanaka, S. *Proceedings of the 2014 IEEE 27th International Conference on Micro Electro Mechanical Systems (MEMS)*, San Francisco, CA; IEEE: New York, 2014; pp 322−325.
(29) Chang, S. R.; Chang, C. H.; Lin, J. S.; Lu, S. C.; Lee, Y. T.; Yeh, S. R.; Chen, H. J. *Micromech. Microeng.* **2008**, *18*, 115032.
(30) Chen, Y.; Wong, C. C.; Pui, T. S.; Nadipalli, R.; Weerasekera, R.; Chandran, J.; Yu, H.; Rahman, A. R. A. *Sens. Actuators, B* **2012**, *173*, 903−907.
(31) Li, L.; Mason, A. J. *Proceedings of IEEE Sensors 2010*, Waikoloa, HI; IEEE: New York, 2010; pp 1613−1616.
(32) Yang, H. S.; Ravindran, R.; Bakir, M. S.; Meindl, J. D. *Proceedings of the 2010 IEEE International Interconnect Technology Conference*, Burlingame, CA; IEEE: New York, 2010; pp 1−3.
(33) Li, L.; Liu, X.; Qureshi, W. A.; Mason, A. J. *IEEE Trans. Biomed. Circuits Syst.* **2011**, *5*, 439−448.
(34) Brettschneider, T.; Dorrer, C.; Suy, H.; Braun, T.; Jung, E.; Hoofman, R.; Brundel, M.; Zengerle, R.; Larmer, F. *Int. J. Electr., Electron. Sci. Eng.* **2013**, *7*, 81−85.
(35) Zhang, B.; Dong, Q.; Korman, C. E.; Li, Z.; Zaghloul, M. E. *Sci. Rep.* **2013**, 3, No. 1098.
(36) Rothe, J.; Frey, O.; Stettler, A.; Yihui, C.; Hierlemann, A. *Proceedings of IEEE Sensors 2012*, Taipei, Taiwan; IEEE: New York, 2012; pp 1−4.
(37) Tsai, H.-H.; Lin, C.-F.; Juang, Y.-Z.; Wang, I. L.; Lin, Y.-C.; Wang, R.-L.; Lin, H.-Y. *Sens. Actuators, B* **2010**, *144*, 407−412.
(38) Kirstein, K.-U.; Li, Y.; Zimmermann, M.; Vancura, C.; Volden, T.; Song, W. H.; Lichtenberg, J.; Hierlemannn, A. *Proceedings of the Design, Automation and Test in Europe Conference and Exhibition—DATE 2005*, Munich, Germany; IEEE Computer Society: Los Alamitos, CA, 2005; Vol. 2.
(39) Manickam, A.; Chevalier, A.; McDermott, M.; Ellington, A. D.; Hassibi, A. *2010 IEEE International Solid-State Circuits Conference Digest of Technical Papers*, San Francisco, CA; IEEE: New York, 2010; pp 130−131.
(40) Simpson, M. L.; Sayler, G. S.; Patterson, G.; Nivens, D. E.; Bolton, E. K.; Rochelle, J. M.; Arnott, J. C.; Applegate, B. M.; Ripp, S.; Guillorn, M. A. *Sens. Actuators, B* **2001**, *72*, 134−140.
(41) Yang, C.; Yue, H.; Hassler, B. L.; Worden, R. M.; Mason, A. J. *IEEE Trans. Biomed. Circuits Syst.* **2009**, *3*, 160−168.
(42) Yang, C.; Rairigh, D.; Mason, A. *Proceedings of IEEE Sensors 2006*, Daegu, Korea; IEEE: New York, 2006; pp 93−96.
(43) Hassibi, A.; Lee, T. H. *IEEE Sens. J.* **2006**, *6*, 1380−1388.
(44) Sun, N.; Liu, Y.; Lee, H.; Weissleder, R.; Ham, D. *IEEE J. Solid-State Circuits* **2009**, *44*, 1629−1643.
(45) Tajalli, A.; Leblebici, Y. *IEEE Trans. Circuits Syst.—I: Regular Pap.* **2011**, *58*, 2189−2200.
(46) Hosseini, Y.; Kaler, K. V. I. S. *Sens. Actuators, A* **2010**, *157*, 1−8.
(47) Patounakis, G.; Shepard, K. L.; Levicky, R. *IEEE J. Solid-State Circuits* **2006**, *41*, 2521−2530.
(48) Erarslan, R. B.; Adiyan, U.; Lulec, S. Z.; Olcer, S.; Temiz, Y.; Leblebici, Y.; Torun, H.; Urey, H. *Sens. Actuators, A* **2014**, *215*, 44−50.
(49) Nakajima, A.; Kimura, H.; Sawadsaringkarn, Y.; Maezawa, Y.; Kobayashi, T.; Noda, T.; Sasagawa, K.; Tokuda, T.; Ishikawa, Y.; Shiosaka, S.; Ohta, J. *Opt. Express* **2012**, *20*, 6097−6108.
(50) Anderson, E.; Daniels, J.; Yu, H.; Lee, T.; Pourmand, N. *2008 IEEE International Instrumentaion and Measurement Technology Conference Proceedings*, Victoria, BC, Canada; IEEE: New York, 2008; pp 1631−1636.
(51) Zhang, J.; Trombly, N.; Mason, A. *Proceedings of IEEE Sensors 2004*, Vienna, Austria; IEEE: New York, 2004; pp 36−39.
(52) Zhang, M.; Haider, M. R.; Huque, M. A.; Adeeb, M. A.; Rahman, S.; Islam, S. K. *Smart Mater. Struct.* **2007**, *16*, 525.
(53) Huang, Y.; Mason, A. J. *Proceedings of the 2009 IEEE Biomedical Circuits and Systems Conference (BioCAS 2009)*, Beijing; IEEE: New York, 2009; pp 29−32.
(54) Zhang, L.; Xiangqing, H.; Yan, W.; Zhiping, Y. *Proceedings of the 2011 IEEE Custom Integrated Circuits Conference (CICC)*, San Jose, CA; IEEE: New York, 2011; pp 1−4.
(55) Kruppa, P.; Frey, A.; Kuehne, I.; Schienle, M.; Persike, N.; Kratzmueller, T.; Hartwich, G.; Schmitt-Landsiedel, D. *Biosens. Bioelectron.* **2010**, *26*, 1414−1419.
(56) Levine, P. M.; Gong, P.; Shepard, K. L.; Levicky, R. *Proceedings of the 2007 IEEE Custom Integrated Circuits Conference (CICC)*, San Jose, CA; IEEE: New York, 2007; pp 825−828.
(57) Yang, S. M.; Chang, C.; Yin, T. I. *Sens. Actuators, B* **2008**, *129*, 678−684.
(58) Stagni, C.; Guiducci, C.; Benini, L.; Ricco, B.; Carrara, S.; Samori, B.; Paulus, C.; Schienle, M.; Augustyniak, M.; Thewes, R. *IEEE J. Solid-State Circuits* **2006**, *41*, 2956−2964.
(59) Hu, J.; Kim, Y.-B.; Ayers, J. *Proceedings of the 53rd IEEE International Midwest Symposium on Circuits and Systems*, Seattle, WA; IEEE: New York, 2010; pp 541−544.

DOI: 10.1021/cr500554n
Chem. Rev. XXXX, XXX, XXX−XXX

(60) Eversmann, B.; Jenkner, M.; Hofmann, F.; Paulus, C.; Brederlow, R.; Holzapfl, B.; Fromherz, P.; Merz, M.; Brenner, M.; Schreiter, M.; Gabl, R.; Plehnert, K.; Steinhauser, M.; Eckstein, G.; Schmitt-Landsiedel, D.; Thewes, R. *IEEE J. Solid-State Circuits* **2003**, *38*, 2306−2317.
(61) Xin, Z.; Wai Man, W.; Yulong, Z.; Yandong, Z.; Fei, G.; Nelson, R. D.; LaRue, J. C. *Proceedings of the Annual International Conference of the IEEE Engineering in Medicine and Biology Society (EMBC 2009)*, Minneapolis, MN; IEEE: New York, 2009; pp 3814−3817.
(62) Lie, D. Y. C.; Das, V.; HU, W.; Liu, Y.; Nguyen, T. *Open J. Appl. Biosens.* **2013**, *2*, 104−111.
(63) Ballini, M.; Muller, J.; Livi, P.; Chen, Y.; Frey, U.; Shadmani, A.; Jones, I. L.; Gong, W.; Fiscella, M.; Radivojevic, M.; Bakkum, D.; Stettler, A.; Heer, F.; Hierlemann, A. *Proceedings of the 2013 Symposium on VLSI Circuits (VLSIC)*, Kyoto, Japan; IEEE: New York, 2013; pp C54−C55.
(64) Kagohashi, Y.; Ozawa, H.; Uno, S.; Nakazato, K.; Ohdaira, K.; Matsumura, H. *Jpn. J. Appl. Phys.* **2010**, *49*, 01AG06.
(65) Im, M.; Ahn, J. H.; Choi, Y.-K. *Proceedings of the 2008 International SoC Design Conference*, Busan, South Korea; IEEE: New York, 2008; pp III-66−III-67.
(66) Lu, M. S. C.; Chen, Y.-C.; Huang, P.-C. *Biosens. Bioelectron.* **2010**, *26*, 1093−1097.
(67) Yang, M.-Z.; Dai, C.-L.; Hung, C.-B. *Microelectron. Eng.* **2012**, *97*, 353−356.
(68) Xin, Z.; Daly, J. C.; Yong, C. *Proceedings of the 2nd International IEEE EMBS Conference on Neural Engineering, Arlington, VA*; IEEE: New York, 2005; pp 660−663.
(69) Yufera, A.; Rueda, A. *Microelectron. J.* **2010**, *41*, 231−239.
(70) (a) Yang, C.; Jadhav, S. R.; Worden, R. M.; Mason, A. J. *IEEE J. Solid-State Circuits* **2009**, *44*, 2844−2855. (b) Yang, C.; Mason, A. J. *Proceedings of IEEE Sensors 2008*, Lecce, Italy; IEEE: New York, 2008; pp 642−645.
(71) Huang, C.-W.; Hsueh, H.-T.; Huang, Y.-J.; Liao, H.-H.; Tsai, H.-H.; Juang, Y.-Z.; Lin, T.-H.; Lu, S.-S.; Lin, C.-T. *Sens. Actuators, B* **2013**, *181*, 867−873.
(72) Lechuga, L. M.; Tamayo, J.; Álvarez, M.; Carrascosa, L. G.; Yufera, A.; Doldán, R.; Peralías, E.; Rueda, A.; Plaza, J. A.; Zinoviev, K.; Domínguez, C.; Zaballos, A.; Moreno, M.; Martínez-A, C.; Wenn, D.; Harris, N.; Bringer, C.; Bardinal, V.; Camps, T.; Vergnenègre, C.; Fontaine, C.; Díaz, V.; Bernad, A. *Sens. Actuators, B* **2006**, *118*, 2−10.
(73) Hua, W.; Sideris, C.; Hajimiri, A. *Proceedings of the 2010 IEEE Custom Integrated Circuits Conference (CICC)*, San Jose, CA; IEEE: New York, 2010; pp 1−4.
(74) Rezaul Hasan, S. M. *Circuits Syst. Signal Process.* **2008**, *27*, 351−366.
(75) Al-Dirini, F.; Mohammed, M.; Mohammad, M.; Shahroury, F. *Proceedings of the 2011 IEEE International Conference on RFID-Technologies and Applications (RFID-TA)*, Sitges, Spain; IEEE: New York, 2011; pp 56−63.
(76) Crepaldi, P. C.; Pimenta, T. C.; Moreno, R. L.; Rodriguez, E. C. *IEEE Trans. Instrum. Meas.* **2012**, *61*, 729−739.
(77) Paglinawan, A. C.; Chung, W.-Y.; Wang, Y.-H.; Cheng, S.-C.; Lee, W.-H.; Albason, A.; Chuang, C.-C.; Lou, S.-L. *J. Med. Biol. Eng.* **2011**, *31*, 321−329.
(78) (a) Berdondini, L.; van der Wal, P. D.; Guenat, O.; de Rooij, N. F.; Koudelka-Hep, M.; Seitz, P.; Kaufmann, R.; Metzler, P.; Blanc, N.; Rohr, S. *Biosens. Bioelectron.* **2005**, *21*, 167−174. (b) Franks, W.; Tosatti, S.; Heer, F.; Seif, P.; Textor, M.; Hierlemann, A. *Biosens. Bioelectron.* **2007**, *22*, 1426−1433. (c) Hassibi, A.; Lee, T. H. *2005 IEEE International Solid-State Circuits Conference Digest of Technical Papers*, San Francisco, CA; IEEE: New York, 2005; pp 564−617. (d) Liu, Y.; Smela, E.; Nelson, N. M.; Abshire, P. *Proceedings of the 26th Annual International Conference of the IEEE Engineering in Medicine and Biology Society (EMBC 2004)*, San Francisco, CA; IEEE: New York, 2004; pp 2534−2537. (e) Thewes, R.; Hofmann, F.; Frey, A.; Schienle, M.; Paulus, C.; Schindler-Bauer, P.; Holzapfl, B.; Brederlow, R. In *Advanced Micro and Nanosystems*; Baltes, H., Brand, O., Fedder, G. K., Hierold, C., Korvink, J., Tabata, O., Eds.; Wiley-VCH Verlag GmbH & Co. KGaA: Weinheim, Germany, 2004; Vol. *1*, pp 383−414. (f) Barbaro, M.; Bonfiglio, A.; Raffo, L. *IEEE Trans. Electron Devices* **2006**, *53*, 158−166.
(79) Levine, P. M.; Gong, P.; Levicky, R.; Shepard, K. L. *Biosens. Bioelectron.* **2009**, *24*, 1995−2001.
(80) Anan, H.; Kamahori, M.; Ishige, Y.; Nakazato, K. *Sens. Actuators, B* **2013**, *187*, 254−261.
(81) Chang, S. R.; Chang, C. H.; Lin, J. S.; Lu, S. C.; Lee, Y. T.; Yeh, S. R.; Chen, H. *J. Micromech. Microeng.* **2008**, *18*, 115032.
(82) Maruyama, Y.; Terao, S.; Sawada, K. *Biosens. Bioelectron.* **2009**, *24*, 3108−3112.
(83) (a) Barbaro, M.; Bonfiglio, A.; Raffo, L.; Alessandrini, A.; Facci, P.; Barák, I. *Sens. Actuators, B* **2006**, *118*, 41−46. (b) Barbaro, M.; Bonfiglio, A.; Raffo, L.; Alessandrini, A.; Facci, P.; BarakBarak, I. *IEEE Electron Device Lett.* **2006**, *27*, 595−597.
(84) Xue, Q.; Bian, C.; Tong, J.; Sun, J.; Zhang, H.; Xia, S. *Sens. Actuators, A* **2011**, *169*, 282−287.
(85) Lee, K.-H.; Lee, J. O.; Choi, S.; Yoon, J.-B.; Cho, G.-H. *Biosens. Bioelectron.* **2012**, *31*, 343−348.
(86) Welch, D.; Christen, J. B. *Proceedings of the 34th Annual International Conference of the IEEE Engineering in Medicine and Biology Society (EMBC 2012)*, San Diego, CA; IEEE: New York, 2012; pp 4990−4993.
(87) Pancrazio, J. J.; Bey, J. P. P.; Loloee, A.; SubbaRao, M.; Chao, H.-C.; L. Howard, L.; Milton Gosney, W.; Borkholder, D. A.; T.A. Kovacs, G.; Manos, P.; Cuttino, D. S.; A. Stenger, D. *Biosens. Bioelectron.* **1998**, *13*, 971−979.
(88) Frey, U.; Sedivy, J.; Heer, F.; Pedron, R.; Ballini, M.; Mueller, J.; Bakkum, D.; Hafizovic, S.; Faraci, F. D.; Greve, F.; Kirstein, K. U.; Hierlemann, A. *IEEE J. Solid-State Circuits* **2010**, *45*, 467−482.
(89) Hafizovic, S.; Heer, F.; Franks, W.; Greve, F.; Blau, A.; Ziegler, C.; Hierlemann, A. *Proceedings of the 2006 IEEE 19th International Conference on Micro Electro Mechanical Systems (MEMS)*, Istanbul, Turkey; IEEE: New York, 2006; pp 4−7.
(90) Cheng, Y.-T.; Tsai, C.-Y.; Chen, P.-H. *Sens. Actuators, B* **2007**, *120*, 758−765.
(91) Kim, B. N.; Herbst, A. D.; Kim, S. J.; Minch, B. A.; Lindau, M. *Biosens. Bioelectron.* **2013**, *41*, 736−744.
(92) Ma, H.; Wallbank, R. W. R.; Chaji, R.; Li, J.; Suzuki, Y.; Jiggins, C.; Nathan, A. *Sci. Rep.* **2013**, *3*, No. 2730.
(93) Lee, K.-H.; Choi, S.-H.; Lee, J.-O.; Sohn, M.-J.; Yoon, J.-B.; Cho, G.-H. *Biosens. Bioelectron.* **2011**, *26*, 4591−4595.
(94) Lai, W.-A.; Lin, C.-H.; Yang, Y.-S.; Lu, M. S. C. *Biosens. Bioelectron.* **2012**, *35*, 456−460.
(95) (a) Prakash, S. B.; Abshire, P.; Urdaneta, M.; Smela, E. *Proceedings of the 2005 IEEE International Symposium on Circuits and Systems*, Kobe, Japan; IEEE: New York, 2005; pp 3495−3498. (b) Prakash, S. B.; Abshire, P. *Proceedings of IEEE Sensors 2005*, Irvine, CA; IEEE: New York, 2005; pp 1177−1180.
(96) Yang, S. M.; Chang, C. *Sens. Actuators, B* **2010**, *145*, 405−410.
(97) Song, J. M.; Culha, M.; Kasili, P. M.; Griffin, G. D.; Vo-Dinh, T. *Biosens. Bioelectron.* **2005**, *20*, 2203−2209.
(98) Ji, H.; Abshire, P. A.; Urdaneta, M.; Smela, E. *Proceedings of the 2005 IEEE International Symposium on Circuits and Systems*, Kobe, Japan; IEEE: New York, 2005; pp 3491−3494.
(99) Yan, R.; Mestas, S. P.; Yuan, G.; Safaisini, R.; Dandy, D. S.; Lear, K. L. *Lab Chip* **2009**, *9*, 2163−2168.
(100) Ho, W.-J.; Chen, J.-S.; Ker, M.-D.; Wu, T.-K.; Wu, C.-Y.; Yang, Y.-S.; Li, Y.-K.; Yuan, C.-J. *Biosens. Bioelectron.* **2007**, *22*, 3008−3013.
(101) Bolton, E. K.; Sayler, G. S.; Nivens, D. E.; Rochelle, J. M.; Ripp, S.; Simpson, M. L. *Sens. Actuators, B* **2002**, *85*, 179−185.
(102) Eltoukhy, H.; Salama, K.; El Gamal, A. *IEEE J. Solid-State Circuits* **2006**, *41*, 651−662.
(103) Jeon, J.-W.; Kim, J.-H.; Lee, J.-M.; Lee, W.-H.; Lee, D.-Y.; Paek, S.-H. *Biosens. Bioelectron.* **2014**, *52*, 384−390.
(104) Shepard, K. L.; Levicky, R.; Patounakis, G. (Columbia University). Active CMOS Biosensor Chip for Fluorescent-Based Detection. US7738086B2, 2010.

DOI: 10.1021/cr500554n
Chem. Rev. XXXX, XXX, XXX−XXX

(105) Yu-Wei, C.; Yen-Pei, L.; Ming-Yu, L.; Yang-Tung, H.; Yuh-Shyong, Y. *Proceedings of the 2009 IEEE 35th Annual Northeast Bioengineering Conference*, Boston, MA; IEEE: New York, 2009; pp 1−2.
(106) Tokuda, T.; Noda, T.; Sasagawa, K.; Ohta, J. *Materials* **2010**, *4*, 84−102.
(107) (a) Aytur, T.; Beatty, P. R.; Boser, B.; Anwar, M.; Ishikawa, T. *Proceedings of the Solid-State Sensors, Actuators and Microsystems Workshop*, Hilton Head Island, SC; IEEE: New York, 2002; pp 126−129. (b) Skucha, K.; Gambini, S.; Liu, P.; Megens, M.; Kim, J.; Boser, B. E. *J. Microelectromech. Syst.* **2013**, *22*, 1327−1313−1338.
(108) Wang, H.; Hajimiri, S. A. (California Institute of Technology). Frequency-Shift CMOS Magnetic Biosensor Array with Single Bead Sensitivity and No External Magnet. US8378669B2, 2013.
(109) Pai, A.; Khachaturian, A.; Chapman, S.; Hu, A.; Wang, H.; Hajimiri, A. *Analyst* **2014**, *139*, 1403−1411.
(110) Nirschl, M.; Rantala, A.; Tukkiniemi, K.; Auer, S.; Hellgren, A.-C.; Pitzer, D.; Schreiter, M.; Vikholm-Lundin, I. *Sensors* **2010**, *10*, 4180−4193.
(111) Ohta, J.; Tokuda, T.; Sasagawa, K.; Noda, T. *Sensors* **2009**, *9*, 9073−9093.
(112) Anwar, M. M.; Matsudaira, P. (Whitehead Biomedical Institute). Implantable Wireless CMOS Biosensor. WO2009008932A2, 2009.
(113) Poustinchi, M.; Musallam, S. *Proceedings of the 5th International IEEE EMBS Conference on Neural Engineering*, Cancun, Mexico; IEEE: New York, 2011; pp 695−699.
(114) O'Sullivan, T. D.; Heitz, R. T.; Parashurama, N.; Barkin, D. B.; Wooley, B. A.; Gambhir, S. S.; Harris, J. S.; Levi, O. *Biomed. Opt. Express* **2013**, *4*, 1332−1341.
(115) Nan-Fu, C.; Jmin-Min, W.; Cheng-Wei, L.; Chun-Hao, C.; Hsiao-Chin, C.; Lung-Jieh, Y.; Shey-Shi, L.; Chii-Wann, L. *Proceedings of the 27th Annual International Conference of the IEEE Engineering in Medicine and Biology Society (EMBC 2005)*, Shanghai, China; IEEE: New York, 2005; pp 1933−1936.
(116) Lee, B. Y.; Seo, S. M.; Lee, D. J.; Lee, M.; Lee, J.; Cheon, J.-H.; Cho, E.; Lee, H.; Chung, I.-Y.; Park, Y. J.; Kim, S.; Hong, S. *Lab Chip* **2010**, *10*, 894−898.
(117) Rothberg, J. M.; Hinz, W.; Rearick, T. M.; Schultz, J.; Mileski, W.; Davey, M.; Leamon, J. H.; Johnson, K.; Milgrew, M. J.; Edwards, M.; Hoon, J.; Simons, J. F.; Marran, D.; Myers, J. W.; Davidson, J. F.; Branting, A.; Nobile, J. R.; Puc, B. P.; Light, D.; Clark, T. A.; Huber, M.; Branciforte, J. T.; Stoner, I. B.; Cawley, S. E.; Lyons, M.; Fu, Y.; Homer, N.; Sedova, M.; Miao, X.; Reed, B.; Sabina, J.; Feierstein, E.; Schorn, M.; Alanjary, M.; Dimalanta, E.; Dressman, D.; Kasinskas, R.; Sokolsky, T.; Fidanza, J. A.; Namsaraev, E.; McKernan, K. J.; Williams, A.; Roth, G. T.; Bustillo, J. *Nature* **2011**, *475*, 348−352.
(118) Silicon Biosystems Inc. The DEPArray System. http://www.siliconbiosystems.com/deparray-system (accessed June 2012).
(119) (a) Dill, K.; Montgomery, D. D.; Ghindilis, A. L.; Schwarzkopf, K. R. *J. Biochem. Biophys. Methods* **2004**, *59*, 181−187. (b) Dill, K.; Montgomery, D. D.; Ghindilis, A. L.; Schwarzkopf, K. R.; Ragsdale, S. R.; Oleinikov, A. V. *Biosens. Bioelectron.* **2004**, *20*, 736−742. (c) Dill, K.; Montgomery, D. D.; Wang, W.; Tsai, J. C. *Anal. Chim. Acta* **2001**, *444*, 69−78.
(120) Cooper, J.; Yazvenko, N.; Peyvan, K.; Maurer, K.; Taitt, C. R.; Lyon, W.; Danley, D. L. *PLoS One* **2010**, *5*, e9781.
(121) CMOS biosensor breakthrough enables portable diagnostics solution. Ding, Z., Anitoa Systems, LLC. http://www.anitoa.com/products.html (accessed August 2014).
(122) Lenci, S.; Tedeschi, L.; Pieri, F.; Domenici, C. *Appl. Surf. Sci.* **2011**, *257*, 8413−8419.
(123) Guiducci, C.; Schmid, A.; Gurkaynak, F. K.; Leblebici, Y. *Proceedings of the Design, Automation and Test in Europe Conference and Exhibition—DATE 2008*, Munich, Germany; IEEE Computer Society: Los Alamitos, CA, 2008; pp 1328−1333.

DOI: 10.1021/cr500554n
Chem. Rev. XXXX, XXX, XXX−XXX